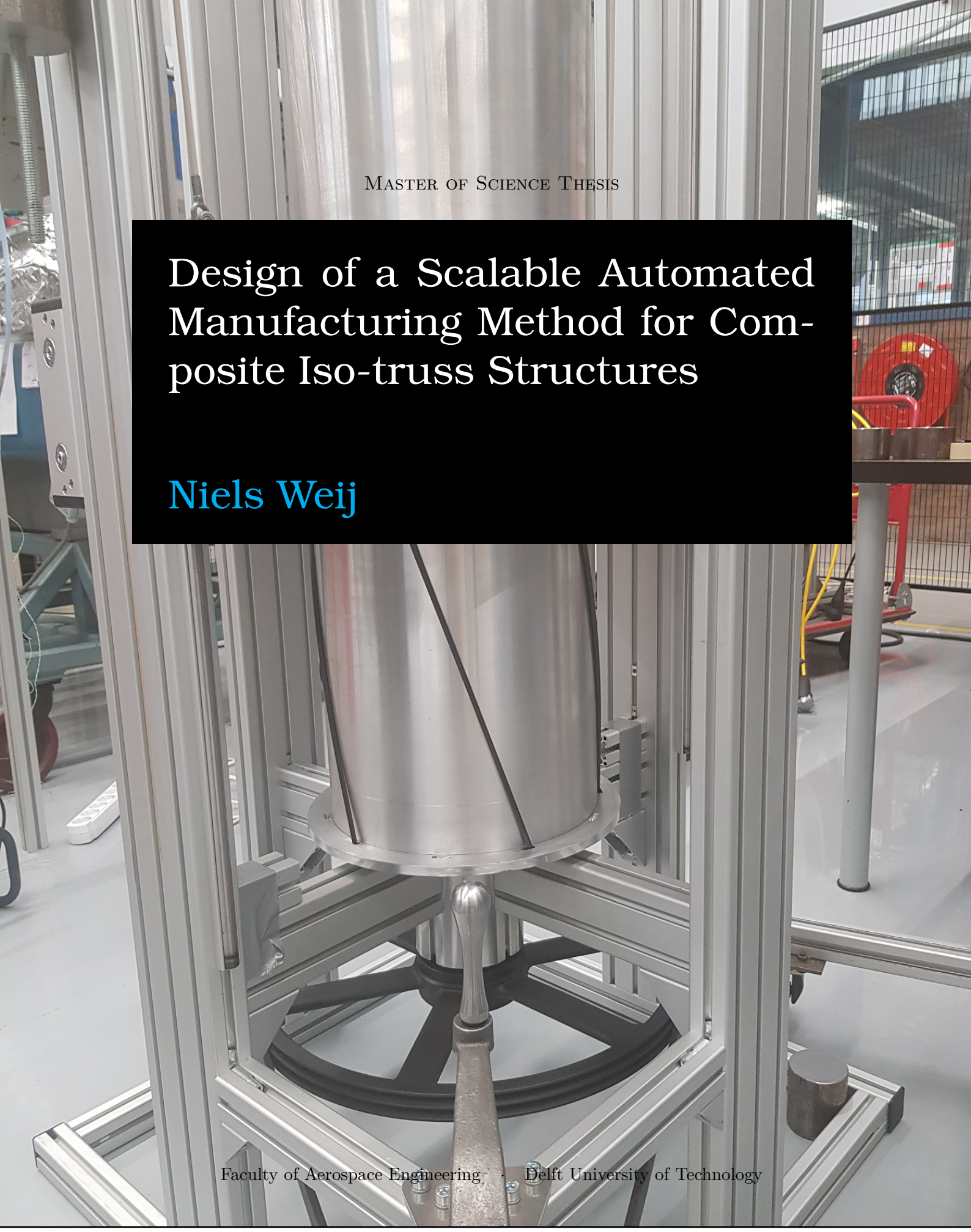

Master of Science Thesis

Design of a Scalable Automated Manufacturing Method for Composite Iso-truss Structures

Niels Weij

Faculty of Aerospace Engineering · Delft University of Technology

TU Delft Delft University of Technology

Design of a Scalable Automated Manufacturing Method for Composite Iso-truss Structures

Master of Science Thesis

For obtaining the degree of Master of Science in Aerospace Engineering
at Delft University of Technology

Niels Weij

May 21, 2021

Faculty of Aerospace Engineering · Delft University of Technology

The work in this thesis was supported by Arkema and vDijk Pultrusion Products. Their cooperation is gratefully acknowledged.

Delft University of Technology
Faculty of Aerospace Engineering
Department of Aerospace Structures and Materials

GRADUATION COMMITTEE

Dated: May 21, 2021

Chair holder:

Dr.ir. R.C. Alderliesten

Committee members:

Dr.ir. O.K. Bergsma

Dr.ir. I. Fernandez Villegas

Dr.ir. J. Sinke

Abstract

The IsoTruss® is an interesting continuous fibre reinforced polymer composite design which is closely related to open lattice composite structures, although it is currently aimed mostly at civil applications. While it currently lacks applicability to the aerospace sector, its production process is easier to automate (or change the shape input parameters on the fly) than open lattice structures, which rely on a fixed mandrel. Although automated compaction of these structures is a challenging problem, the structure can be optimised for any (static) load case if their production process could be automated, providing a range of applications where aerodynamic contour is not a requirement. To bridge the gap between the IsoTruss and other composite lattice structures, a conceptual design for an IsoTruss derivative, termed the "iso-truss", was envisioned. This raised the following research question:

Can composite continuous fibre reinforced iso-truss structures be produced using a scalable and cost-effective automated manufacturing method?

Through this thesis project, an affirmative answer to this question was sought. The focus of this thesis was on the investigation of all the aspects necessary for a production of this iso-truss structure, focusing on a process suited for later automation.

Initial concepts using thermoset composites like the original IsoTruss could not solve the issue of automated compaction, as these would always rely on vacuum bagging to minimise the void content within the composite members. Automated vacuum bagging of the finished iso-truss structure was considered to be an infeasible solution due to the product's complexity. Through the use of thermoplastic composite materials however, the process steps could be split up and compaction could be moved to the very beginning of the process in the form of pultrusions. The shape of the resulting iso-truss was designed to make use of this process, providing a parameterised structure which could easily be optimised. The structure would make use of straight pultrusion rods, acting as the longitudinal members in the truss, and curved pultrusion rods, which would act as helical members. The iso-truss structure would be created by joining these members together at intersections by means of thermoplastic welding, forming a continuously produced open lattice tubular structure.

With this, conceptual production of an iso-truss was based on three key steps: pultrusion, forming, and intersection welding. The pultrusion process was outsourced to an outside

company, vDijk Pultrusion Products (DPP), due to its high required equipment cost. It was not the aim of this thesis to re-invent this process, as it has already reached a sufficient state of maturity. Nevertheless, the process has not yet been optimised for thermoplastic based composites, leaving room for improvement in this area. Materials for the concept were based on availability. Elium® resin (a PMMA based thermoplastic polymer developed by Arkema) was chosen for its similarity to existing process materials and its direct availability from DPP. As reinforcement, a Toray T700SC type carbon fibre was used.

By taking pultrusion out of the research scope, forming and welding were left as processes to demonstrate. A separate welding test was isolated to provide a way to perform standardisable tests. Simultaneously, a forming process demonstrator was designed, as well as a welding jig to demonstrate assembly of the iso-truss.

For the execution of the welding and forming experiments, a single batch of material was ordered from DPP. The batch was the result of a first successful attempt to make rods of this diameter with this combination of materials. Upon arrival of the samples, several tests including SEM, TGA and DSC were performed to estimate important composite material parameters. From these tests, the fibre volume fraction could be estimated to be around 70%, while the onset of T_g was estimated to be 95 °C by definition of maximum loss modulus. Additionally, several interesting phenomena were observed at elevated temperatures in the form of fibre kinking when bent and circumferential decompaction when twisted, indicative of a weak fibre-matrix interface. More indications of this limited fibre-matrix interface were obtained from SEM images, some of which showed small voids around fibres. DMA tests showed a steady decline of the material's (shear) stiffness over a large temperature range, including before the onset of glass transition. This could likely be attributed to the amorphous nature of the polymer.

For the execution of joining experiments, a standard intersection layout was established, after which several joining techniques were considered to create these intersections. From these techniques, heated mould welding was selected as the best currently feasible option. After performing numerous experiments to fine-tune the method of heated mould welding, a standard setup could be designed around this technique. This setup addressed methods for heating, alignment of members to be welded, a compaction mechanism, physical test preparation and physical testing.

Simultaneously, a detailed design of a helical winder demonstrator was made, which was prepared for production by DEMO. The design focused on the demonstration of the mechanical aspect, leaving heating as a secondary concern. Similarly, a more detailed concept of an assembly demonstrator was discussed and designed, although a production-ready design did not prove feasible within the time frame of this project.

The main goal of the intersection welding experiments was to optimise the joint strength by optimising the processing conditions. Due to the limited resin volume content, PMMA foil and epoxy adhesive were used to locally increase resin volume, greatly improving the bond strength compared to initial samples. Using mould temperatures in between 180 °C to 200 °C, a large degree of deformation could be achieved to maximise the joint area, creating mostly consistent intersection samples.

Physical tests proved that the PMMA-based joints were very fragile, while epoxy based joints performed significantly better. Estimated shear strengths for the samples varied from 3 MPa

for some of the lower performing PMMA-based intersections which were believed to have sustained prior damage, to as high as 13 MPa for the epoxy based intersections. For the buckling tests, maximum loads in between 2.1 kN to 3.2 kN were observed. In the final buckling test setup, diagonal members did not increase the buckling load by forcing higher-mode buckling. Instead, they offered some support in post-buckling by resisting out-of-plane deformation. Failure modes in both shear and buckling tests were within the adherend, occurring as a combination of fibre break-out, member kinking and member splitting, more indications of a poor fibre-matrix interface. In summary, the experiments proved that the investigated welding method is feasible if the base material can be improved. As of writing, such improvements have already been reported by DPP through increased process stability and (likely) better fibre sizing.

For the helical winding experiments, the main goal was to demonstrate the production process of heated forming of initially straight pultrusion samples into helices. The physical test setup was designed to offer continuous support of the members over their full length, realise a gradual increase in radius of curvature and allow torsional and axial forces to be introduced independently. For the resulting setup, heating of the central cylinder and introduction of heat through both contact and a heated air chamber proved most feasible within the time frame of this project. It did not prove feasible to produce carbon-Elium composite helices due to the current material limitations, that is the fibre kinking observed in previous tests. Instead, the process was demonstrated using pure PMMA rods at forming temperatures of around 90 °C, which proved highly effective. The process showed the potential to create constant curvature helices with controllable helical angle, although more testing should be performed to achieve accurate and repeatable results.

It is concluded that it is theoretically possible to produce continuous fibre reinforced iso-truss structures using a scalable and cost-effective automated manufacturing method. The process would rely on existing production capabilities which can easily be scaled up or down, without greatly affecting the cost of equipment. The pultrusion, helical shaping and intersection welding processes can all be easily automated using existing techniques to be able to produce an iso-truss tube of indefinite length. The only limitation of this manufacturing method would be the variation of process parameters within the same iso-truss sample. While it is theoretically possible to vary the radius of curvature of pultrusion dies during the pultrusion process, enabling the possibility of varying the outer diameter and the intersection node-to-node distance along the length of a tube, the current state-of-the-art does not accommodate such a design. While it would also be possible to vary the cross-sectional area of each member along their length, it is considered undesirable as it would negatively affect the fibre volume content for a pultrusion-based process. Instead, it is recommended to construct an iso-truss structure in stages, being connected by a structure that is to be envisioned and produced in future research.

Preface

Before you lies the final report summarising my thesis project, fulfilling in partial the requirements for the MSc program in Aerospace Engineering. This document summarises my research into an automated manufacturing method for iso-truss structures.

I would like to be perfectly honest by saying that it was not easy for me to get to this final document. Even though I chose the topic and my supervisor early on, I found myself making little progress in the beginning, partly due to other obligations, but also partly because the scope of this research project continuously seemed too large with the goal I had in mind. Because of this, I thought to give up on this thesis topic many times and choose something more manageable. However, after thoroughly going through the state of the art of composite manufacturing processes, I found a new path that, while it had many obstacles, finally makes the objective of my thesis project seem feasible. This is why I am proud to present this final report, as it proves that through dedication and perseverance, anything is possible.

I would like to thank everyone for their patience with me. I would like to thank my supervisor Otto for his guidance and for not giving up on me, my girlfriend Andreea for supporting me through these difficult times and my colleagues for keeping me sane during all the times I was blankly staring at my computer screen. I would like to note that it would not have been possible to complete this thesis to this extent without the help of everyone in the lab. I would like to personally thank Fred, Victor and Gertjan for all the brainstorming sessions for the design of my test setups. I would also like to thank the DEMO crew, that is Rob, Peter and Ed, because without them my design would have been no more than just an idea.

Everyone, thank you for your patience.

Delft, University of Technology — Niels Weij
May 21, 2021

Table of Contents

List of Figures

List of Tables

Nomenclature

List of Acronyms

ASM	Aerospace Structures and Materials
CFRP	Continuous Fibre Reinforced Polymer
DASML	Delft Aerospace Structures & Materials Laboratory
DSC	Differential Scanning Calorimetry
DEMO	Dienst Elektronische en Mechanische Ontwikkeling
DMA	Dynamic Mechanical Analysis
POM	Polyoxymethylene
PETG	Polyethylene terephthalate glycol
PMMA	Poly(methyl methacrylate)
SEM	Scanning Electron Microscope
TGA	Thermogravimetric Analysis
TU Delft	Delft University of Technology

Chapter 1

Introduction

Truss structures have long dominated the world of lightweight design, with applications in bridges, early aircraft and nowadays still in satellites. The idea behind them is simple: to divide a structure into beams that connect at nodes, where the load in a beam is mainly in the axial direction of that beam. If all the loads inside a truss structure are evenly distributed over each member, the structure is called an iso-truss. However, for this thesis topic, the term iso-truss has a more specific meaning: A tubular open lattice structure, where loads are introduced only at the ends of the tube. The result is a structure that consists of longitudinal and helical members, both with different functions, as shown in Figure 1.1.

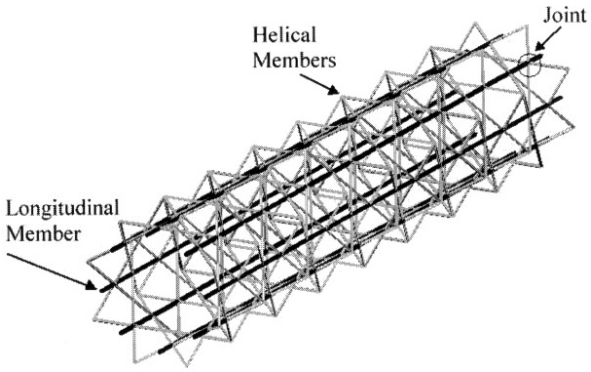

Figure 1.1: Overview of an iso-truss structure [1]

Composite materials like fibre reinforced polymers combine the high tensile strength of synthetic fibres with the high shear strength of polymers. Combining these qualities, they can outperform metals in terms of their mechanical properties, leading to lighter structures. However, these properties can only be realised if the fibres are of reasonable length (i.e. continuous), so the load in a composite structure does not have to be transferred from one set of fibres to the next. Additionally, the fibres should lie as much as possible in the direction of loading, otherwise they are not as effective. This also means that designers should avoid sharp bends and kinks in thin fibre bundles, for example at node locations of a truss, as the

fibres themselves cannot support the outwards load that is necessary for equilibrium. This presents a problem for the application of composite materials to iso-truss structures, as the presented design with its many kinks is likely not the optimal solution.

If iso-trusses could take advantage of the continuous nature of the fibres in a continuous fibre reinforced polymer (CFRP), a structure could be obtained that is far lighter than any closed tubular counterpart. If designed correctly, it can support tension and torsion, as well as bending and compression.

To bring composite iso-truss structures to current composite industry and to allow them to compete on the market, it should be investigated how to manufacture them in such a way that their cost is minimised. This usually implies the availability of a single manufacturing process to produce iso-truss structures in a variety of sizes and other characteristics with as little alterations to the process as possible. The main goal of this thesis topic is therefore to investigate this manufacturing process and prove that it exists, and can be automated to further cut down on production cost. If this is achieved, composite iso-trusses may soon offer better mechanical characteristics than other materials and designs, leading to lighter structures and opening new possibilities.

Chapter 2

Literature Review Summary

The state of the art of research on the topic of iso-truss structures can be divided into three different categories, relating to the Trinity approach in engineering design. These three categories are:

1. **Design:** Detailed descriptions of the umbrella term composite lattice structures, with elaborations on member intersection design, applications of composite lattice structures and existing designs
2. **Materials:** The state of the art of current (composite) materials
3. **Manufacturing:** The main research direction for this topic, specifying the state of current automated manufacturing methods for composite parts, shape control methods for iso-trusses, laminate compaction methods and scalability of current production methods

2.1 Iso-truss Design

Looking at their characteristics, iso-trusses fall in the category of composite lattice structures: Structures characterised by continuous thin-walled ribs, consisting of fibre reinforced polymers, running in both the longitudinal and circumferential direction of a usually cylindrical shape (defined by Barynin et al. [7]). Within this group, there exist several examples, that each provide their own challenges in manufacturing. Products that are considered part of this group are grid-stiffened panels, open lattice panels (as well as cylindrical (open) lattices), and the existing IsoTruss® design. In grid-stiffened panels, the lattice is integral with the skin, which is also load carrying. This is similar to currently employed stiffened skin configurations, as shown in Figure 2.1.

Grid-stiffened panels are defined by several configurations and parameters. In terms of configuration, they can be defined as orthogrids, triangular grids, offset triangular grids, also

Figure 2.1: Difference between a conventional composite semi-monocoque structure (left [2]) and a grid stiffened structure (right [3])

known as anisogrids, and other grid types, like the one investigated by Wang et al. [8]. The (offset) triangular grid is most similar to the IsoTruss design. Other parameters that define the grid structure are the spacing between the longitudinal members, the spacing between the lateral members and the pitch angle of the lateral members, in the case of non-orthogrids. As grid members are often rectangular in cross-section, they can be defined by their width and height. The parameters of a triangular grid are visualised in Figure 2.2.

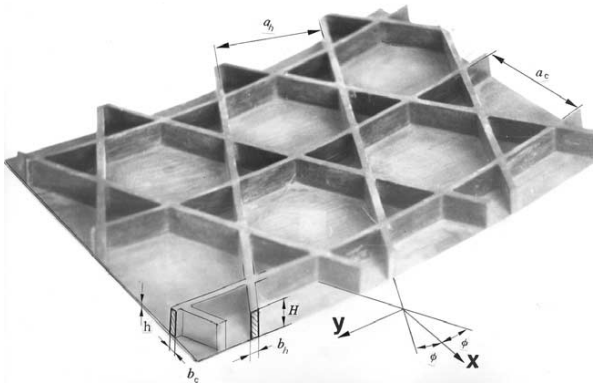

Figure 2.2: Lattice parameters of a grid-stiffened panel [4]

The production of grid stiffened panels is not as straight-forward as conventional composite shell elements, due to the lack of a single surface to consolidate the entire structure against. To counter this, core elements are usually included in most tooling designs to fit in between the grid elements, like in the design of Bellini et al. [9]. However, this kind of tooling does not allow for any adaptability in the layout of the grid pattern. Another challenge is the continuity of fibres in intersections. Because the amount of fibres in intersections is at least two times as high when compared to a single grid member, it is hard to ensure the same fibre volume fraction throughout the entire structure. ATG Europe has tried to overcome this problem, as shown by Pavlov et al. [3], by using prepreg tows, expansion tooling and limiting each intersection to only two grid members at a time.

Grid stiffened panels are currently widely used in space applications, where they are used in a cylindrical or conical form for interstages, intertanks, payload adaptors and fairings of launch vehicles. In the aircraft industry, they may be used for any structural element, like the

fuselage or the wingbox structure, though current use is limited. In fact, they could be used for any lightweight cylindrical composite structure, like helicopter tail beams, space telescope bodies, submarine bodies and many civil engineering structures like masts, columns and pipes (summarised by Barynin et al. [7]).

When aerodynamic considerations are not important for a structure, an open lattice structure may be used instead. While it is defined by the same parameters as grid-stiffened panels, an open lattice is a true truss, as its members mostly support loads in their own direction, while loads can only be transferred from member to member at nodes. Unlike grid-stiffened panels, open lattices can be manufactured in one production step, making the process simpler to automate. Cylindrical lattices are usually filament-wound around either a flexible silicon coating of a mandrel, where the core can be retracted after cure (as shown by Wu et al., Vasiliev et al., Totaro et al. and Barynin et al. [2, 4, 7, 10, 11]) or a disposable foam core, where the foam can be either dissolved or left inside the structure (for example as presented by Vasiliev et al., Barynin et al. and Buragohain et al. [4,7,12]). Applications of open lattices are currently more restricted to civil use, due to the lack of an integrated aerodynamic surface.

The original IsoTruss® is a design by US Ph.D. David W. Jensen [13]. While it shares many characteristics with other open lattice structures, it is a category of its own. The design is visualised in Figure 1.1.

The current design uses a braiding technique to produce unidirectionally reinforced members with a braided sleeve as the outer layer. The IsoTruss is defined by parameters that are similar to the ones used to describe cylindrical open lattice structures, as described by Weaver et al. [14]. External hooks are used to realise the shape of the IsoTruss, which can be adjusted by computer input. Because of this, internal support that is usually offered in the form of a mould is not needed according to Jensen et al. [1]. This manufacturing technique is visualised in Figure 2.3

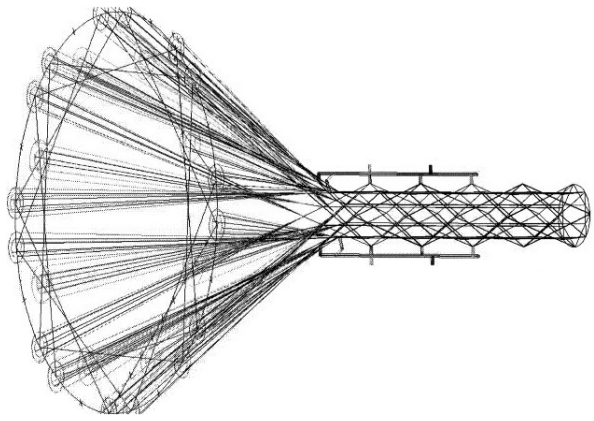

Figure 2.3: Overview of the IsoTruss continuous manufacturing process [5]

A derivative of the IsoTruss has been developed for more specific applications in certain structures, as demonstrated by Asay et al. [6]. This design has been dubbed the IsoBeam and incorporates a more rectangular shape. As the structure is closely related to the IsoTruss, it is worth including its design and manufacturing approach in the research scope of this thesis. The manufacturing method for IsoBeam structures is currently different than for the IsoTruss in the sense that it does in fact use a module-like inner mandrel to hold the beam

in shape, as can be seen in Figure 2.4. Furthermore, the importance of composite quality was emphasised in its design, as evident through the incorporation of shrink tape to better consolidate individual members.

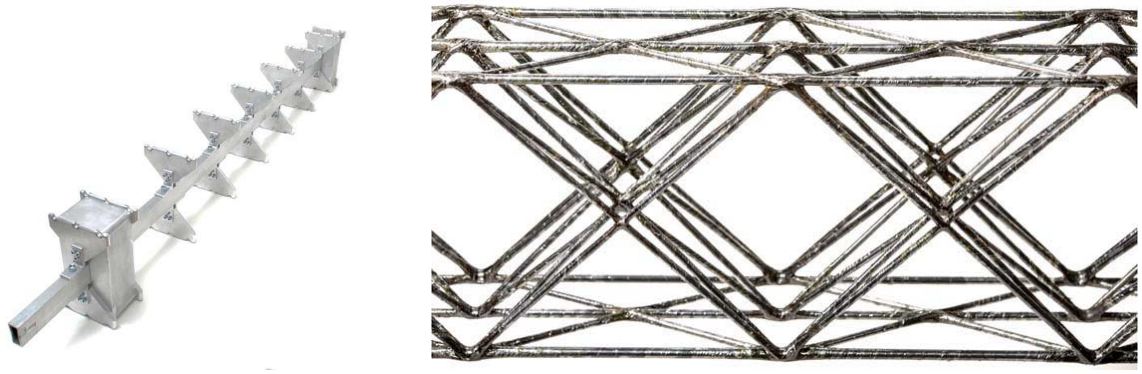

(a) Overview of the mandrel [6] **(b)** View of the beam showing shape quality and consistency

Figure 2.4: Manufacturing process for the IsoBeam structure [6]

2.2 Composite materials

Different materials have different restrictions on available processing methods, so it is crucial to include material selection in the design process for this thesis topic. The materials considered in this thesis are conventional polymer composite materials, consisting of either a thermoset or thermoplastic polymer matrix, and a reinforcing continuous fibre material. For the latter, glass, carbon, aramid and Dyneema® (UHMWPE) fibres have been considered, of which glass and carbon fibres seem to offer the most advantages for use in iso-trusses. The more impacting consideration however is whether to use a thermoset or thermoplastic based matrix system, as this drastically influences the available range of production processes. To be able to weigh different options against each other, information is collected from the 'Composite Materials Handbook Volume 3' [15] and the book 'Thermoplastics and Thermoplastic Composites' [16].

The thermoset matrix types that have been considered are epoxies and esters. Polyesters offer the advantage of fast curing and a low cost, while epoxies offer superior mechanical properties. Vinyl-esters offer an option in between by combining the curing benefits of polyesters with mechanical properties similar to epoxies.

From the available range of thermoplastic materials, polymers that show some degree of crystallinity were preferred due to their superior mechanical properties and chemical resistance. The thermoplastic polymers that exhibit these kind of characteristics are polyphenylene sulfide (PPS), polyketones (PEEK, PEKK, PAEK), Nylon (PA) and some commodity polymers like polypropylene and polyethylene. While PPS and PEEK offer higher mechanical properties, Nylon and commodity plastics are far easier to process. For this reason, within the scope of this thesis, the latter options (Nylon, PP and PE) are considered the better alternative, with the recommendation to continue research with higher grade thermoplastics once a proof of concept has been demonstrated. Alternatively, some amorphous polymers like poly(methyl methacrylate) PMMA could also be considered purely for demonstration of the process.

For composite materials, it is crucial to consider in which form they should be supplied. For example, a composite can either be consolidated during the process, or it can be supplied in an already consolidated state, like in the case of thermoset pultrusion parts. In the former case, there is much more freedom in shape-ability of the composite, while the process itself is more complicated, thus harder to automate. However, thermoset materials offer very little advantages for use in iso-trusses if supplied as already-consolidated pultrusions. Thermoplastic matrix composites on the other hand offer the advantages of both processes: They can be pre-consolidated to make further processing easier, while still allowing for reshaping and joining of components when sufficiently heated. Of course, thermoplastic resins can also be supplied as a non-cured mixture, as in the case of for example the Elium® resin from Arkema [17].

2.3 Manufacturing Processes

A focus is placed on the state of the art of current manufacturing methods that could be considered for implementation in this thesis. The aim is to provide an overview of available options for each manufacturing step in the production of composite structures. First the combination of the matrix and reinforcement (or wetting) has to be considered, followed by compaction and curing (for thermosets) or welding (for thermoplastic composites). Additionally, an overview of current automated production techniques for composite lattice-like structures is given.

For the combination of matrix and reinforcement, three options are considered: ordering material where the two components are already combined (also known as prepreg), combining matrix and reinforcement just before compaction (referred to as manual wetting), and infusing the matrix after the reinforcement has already been compacted. The latter option is discarded due to clashes between the requirements for the process and available production methods for iso-trusses.

Several compaction methods are considered for use in iso-truss structures. These include an environmental pressure difference to generate the compaction force (making use of vacuum bagging), shrink tapes around the circumference of individual members (like the ones supplied by Dunstone [18]) and the use of industrial presses. The former two options both come with challenges that make automation of the process very difficult. Presses on the other hand require complicated and thus expensive adaptable tooling in order to be of use for iso-truss structures.

To cure a thermoset based matrix, the two most viable methods include the use of environmental heat, like in an industrial oven, and UV light to selectively cure portions of the structure, as shown by Decker et al., Bird et al. and Park et al. [19–21]. Of these two options, UV curing is the most suitable to incorporate in an automated process. Additionally, the incorporation of both methods to accurately control the degree of cure of a thermoset has also been shown by Okamoto et al. [22]. Another option for curing using induction heating was considered, as investigated by Apostolidis et al. and Severijns et al. [23, 24], though this option was quickly discarded for lack of applicability to iso-truss composite structures.

For thermoplastics, the consolidation process refers to (selectively) melting the matrix material to fuse different parts together. Options that are available for use in iso-truss structures

include the use of hot plates, ultrasonics, infrared light and induction. Of these processes, hot plate pressing is the simplest and cheapest to incorporate, though it takes relatively long to heat up the material to its melt temperature, even longer if adaptable flexible tooling is used to compress the material with (an example is a silicone gasket by Intertronics [25]). Ultrasonic welding is far faster, but has a small area of influence due to the limited physical size of the welding device. However, methods have been shown to adapt the process for use in a continuous line by Jongbloed et al. [26]. Yet, it does suffer from the same applicability problems if the generated waves need to pass through flexible tooling. Infra-red welding seems to offer better advantages for incorporation in the manufacturing process, as it is as fast and direct as ultrasonic welding, while also being able to heat the material through flexible tooling.

Several automated manufacturing approaches exist that could be adapted for use in the production of iso-truss structures. One of these methods is (Maypole) braiding, as explained by Kyosev et al. [27] and incorporated in the manufacturing of landing gear components at NLR [28]. It has also been adapted for use in the production of the current IsoTruss®. Additionally, filament winding shows promise for incorporation in an automated manufacturing process, as shown by Minsch et al. and Shen et al. [29–31]. Furthermore, the use of 3D printing, as shown by Driezen [32], and assembling of both composite and metallic based parts of an iso-truss, like shown by DiCaprio et al. [33], have both been considered.

2.4 Summary

To conclude, iso-truss structures aim to bridge the gap between open lattice composite designs, which lack a high degree of adaptability in processing, and the existing IsoTruss®, which currently lacks applicability to the aerospace sector. By closing the gap between these two sectors, the author aims to introduce the iso-truss design to lightweight industry, as it is expected that this structure can provide significant weight savings over existing designs. To do this, a new manufacturing approach is likely required, using a combination of processes that have already been demonstrated for the aerospace industry. This approach is influenced by the shape design of the iso-truss, as well as the materials it comprises.

Chapter 3

Problem Description

The literature presented so far shows a clear gap between the current state-of-the-art and demonstration of a fully automated iso-truss manufacturing process for aerospace applications. This scientific gap can be used to define the main research goal for this thesis, which will be presented in this chapter.

The main desired outcome of this thesis is the proof that an automated manufacturing method for iso-trusses can be developed. Other requirements for this thesis include the use of continuous fibre reinforcement as the base material and economic feasibility of the design (limiting cost of the production method to a finite amount). With these requirements in mind, the main research question for this thesis can be formulated as follows:

Can composite continuous fibre reinforced iso-truss structures be produced using a scalable and cost-effective automated manufacturing method?

To answer this question, a set of sub-questions that relate back to the different research categories and important design pillars discussed in Chapter 2 can be formulated. These questions are thought to address the main challenges that would present themselves in answering the main research question.

- Design:
    1. What is the definition of an iso-truss structure for this thesis project?
    2. How can iso-truss bundle intersections be designed to fulfill as many of the automation requirements as possible?
    3. What are the applications of high-production-volume iso-truss structures?
    4. How does the final design of this thesis compare to existing designs of tubular open lattice manufacturing methods, considering all the requirements?
- Material:
    5. What is the best combination of materials to use for the iso-truss structure, considering their possible degree of automation?

- Manufacturing:

    6. How can a production method be designed to offer the highest degree of automation?
    7. How can the shape of the iso-truss structure be accurately controlled during the manufacturing process?
    8. How can the quality of the members of the iso-truss structure be maximised, similar to the quality benefits of conventional vacuum bagging and autoclave procedures for composite plates?
    9. How can the manufacturing process of the iso-truss structure be made independent of the desired length of the structure?

It can be seen that most of these questions address the boundary conditions of the problem, in other words top level decisions that have to be addressed before the start of experiments. These questions, namely question 1, 2, 5, 6 and 7, require a research direction, which is chosen in Chapter 4 as the most likely path to successful demonstration of the production process. Execution of the experiments in turn aims to provide a definitive answer to these questions. On the other hand, questions 3 and 4 relate more to validation and economic feasibility of the production method, and should be addressed before a definitive answer to the main research question can be given. This leaves questions 7 and 8 as the main concerns for experimentation.

Another important aspect in describing the main problem, is the development of a main research objective. This objective can be formulated by considering the main research direction, which is to assess the possibility of designing an automated manufacturing process for composite iso-truss structures. The goal is then to prove that this process can be realised. This proof is delivered by (simulated and/or idealised) demonstration of the process: making several test samples that address different difficulties in the manufacturing process. Taking these expected difficulties into account, the objective can be formulated as:

Prove that a scalable and cost-effective manufacturing method for composite iso-truss structures can be realised, by making several high-quality test samples with a fixed length, that show different diameters and different helical patterns using the same automated manufacturing method.

Here it can be seen that it was decided to fix the length of the iso-truss in the scope of this project. This was done under the assumption that it is of little influence to demonstration of the process, instead relating more to scalability of the solution. Although the boundary condition still holds that it should be possible to use the same production process for an iso-truss of indefinite length, it is assumed that demonstrating the production of a section of an iso-truss is able to prove its feasibility as well. Recommendations will then be made on how to scale the solution, relating back to research question 9. Instead, research will focus on how to vary other product parameters like the main diameter of the structure and pitch between intersection. If these variations can not be demonstrated, it should be possible to provide proof that it is already possible to vary these parameters using current production capabilities which can be readily incorporation into the production line.

Chapter 4

Top Level Design

With an accurate definition of the problem, this chapter elaborates on the top level design choices for this thesis project. Design choices include the selection of materials for the iso-truss and definition of the iso-truss by one set of parameters as the boundary conditions to the problem, addressed in this chapter. Furthermore, this chapter elaborates on the design of the different (isolated) production aspects for an iso-truss. These include an intersection production and testing setup, the design of a demonstrator for shaping of the members and the design of a final shape consolidation demonstrator.

4.1 Design Choices

In this section, the top level design choices are established, taking into account the knowledge obtained from literature and the problem definition discussed in the previous chapter. These design choices address research question 5 (material combination) and question 1 (shape definition of an iso-truss), each in their respective subsection.

4.1.1 Material Selection

As a first design choice, the selection of continuous fibre-reinforced polymer materials, most notably the choice between thermoset or thermoplastic based polymers, greatly influenced the design of the production process. For thermoset based matrix materials for example, shaping of the members of an iso-truss would only be possible before curing and consolidation of the matrix. Due to the complexity of the iso-truss shape however, it was not possible to envision an automatable consolidation solution which could satisfy the requirement imposed by research question 8. Conventional vacuum bagging and autoclave solutions could not be used to ensure proper compaction and minimisation of voids due to the shape complexity of the structure, while other solutions like dedicated mandrels and shrink tape impaired adaptability of the process.

To circumvent these clashing requirements, thermoplastic materials were believed to offer a better solution, as they allowed for separation of the different process steps: by heating the material, it would still be possible to reshape members after initial consolidation. Using this benefit, a solution was envisioned where straight already-consolidated members would be shaped and joined into an iso-truss tubular structure. To produce these straight members, pultrusion was believed to offer the most flexibility in automation of the design.

Regretfully, pultrusion of thermoplastic based composites is still a relatively novel technology compared to thermoset based pultrusion, making the selection of an optimal combination of materials currently limited. The selection of the thermoplastic for use in the iso-truss structure was therefore solely based on availability. Using an existing relation with the pultrusion company vDijk Pultrusion Products (DPP) [34], the acrylic based Elium® resin developed by Arkema [17] was selected. The main advantage of this resin system is its process-ability in a pultrusion setup, which is similar to a typical thermoset resin system in terms of solution viscosity and and curing rate, even though the final matrix is thermoplastic in nature. The resin formulation for use in pultrusion was discussed between Arkema and DPP, resulting in the selection of Elium 591 as the matrix component in the composite.

While not as critical for the production process, fibre type selection was based on wettability, availability, limit to the influence on process-ability and some mechanical characteristics (compressive and fibre-matrix interface). Carbon, glass, aramid and basalt fibres were all considered, though carbon fibre was selected due to its immediate availability for the pultrusion process performed at DPP. The fibre type used was a mid-range, high-strength Toray T700SC carbon fibre with a tensile strength of 4900 MPa, tensile modulus of 230 GPa and a density of $1.8\,\mathrm{g\,cm^{-3}}$ [35].

These materials were ordered at the start of the thesis in the form of straight, unidirectionally reinforced thermoplastic pultruded rods, taking into account the lead time for their production (around a month). Due to the novelty of this material, it had to be characterised to be able to assess its general feasibility and optimise its use.

4.1.2 Iso-truss Shape Definition

Before an iso-truss sample could be made, a detailed definition of its shape was required, based on manufacturing and mechanical performance considerations. The members in the axial direction of the iso-truss structure (the longitudinal members) were defined as straight for structural and processing reasons. Structurally, this would make the members less likely to buckle when loaded in compression. For the production of these members, this shape would eliminate the need for further manipulation of the member after the pultrusion step, spare for the joining of these members to circumferential members. For these circumferential (or helical) members, it was decided that a true-helical shape would offer the most benefit. Comparing this solution to the helical members in the Isotruss®, true helical members would distribute the non axial load component (resulting from the curvature of the members) over their entire length, instead of focusing this component at sharp bends in an intersection. Processing-wise, this solution would allow for the incorporation of a winding process to shape the members, which was believed to be the simplest solution to automate.

Based on these considerations, the iso-truss was defined as a tubular open lattice structure composed of circular cross-section longitudinal and true-helical members, with either a fixed

length or a fixed number of repeating units. A true helix is defined solely by a pitch and a diameter, the latter of which is directly related to the major diameter of the tube. Helices are wound both clockwise and counter-clockwise, and are defined as symmetric, though a small offset could be incorporated to prevent the intersection of three members at the exact same location. The shape of the truss is fully defined by inclusion of separate thicknesses (cross-sectional diameter) and a total number of helical and longitudinal members. This set of parameters fully defines the shape of the iso-truss. A CAD representation visualising these parameters can be seen in Figure 4.1. This representation used the set of parameters above as easily variable input. Finally, a flattening parameter was used to account for the change in shape of members at an intersection in order to maximise their contact area. Initial parameter values were based on availability and manageability within the scope of this thesis, tabulated in Table 4.1.

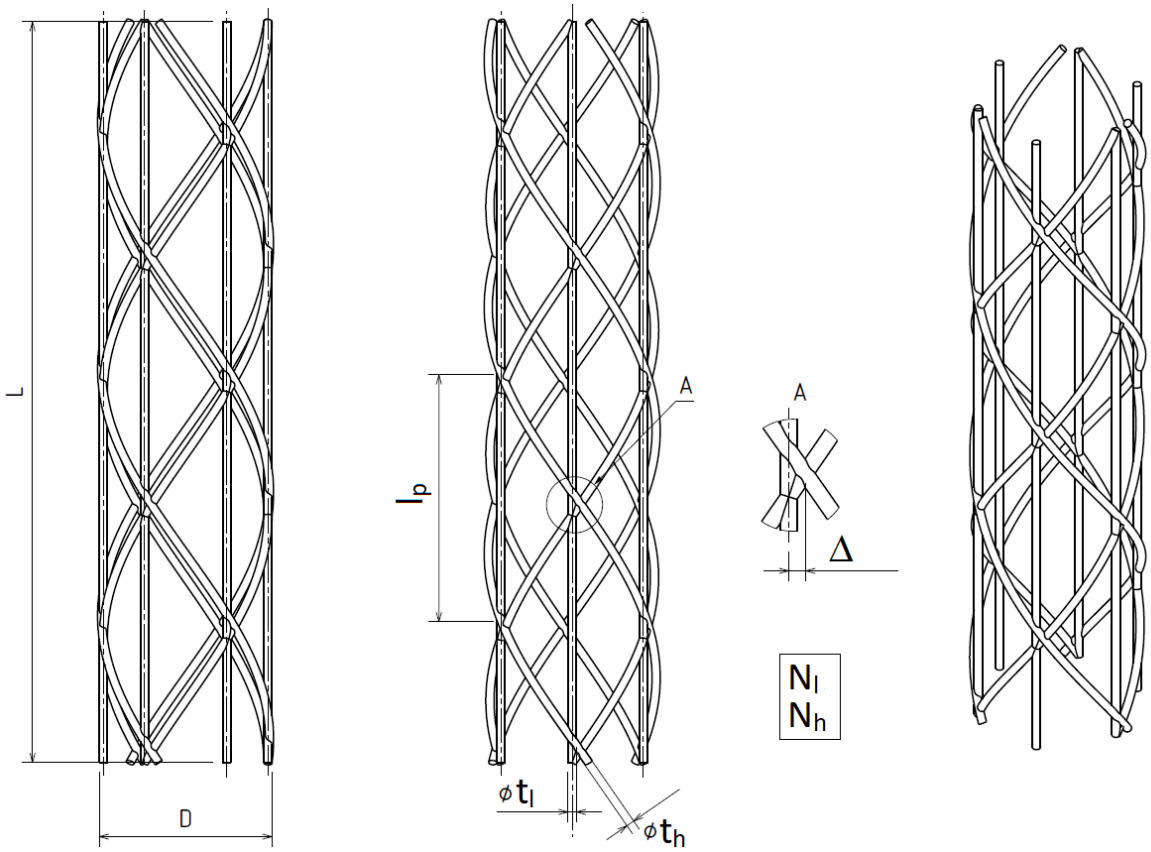

Figure 4.1: Visualisation of all the parameters that define the shape of the iso-truss

In the final application of this structure, all these parameters should be variable. However, to limit the scope of this thesis, only the major diameter and helical pitch were made adaptable, as these present the main challenges for the design of a suitable manufacturing method. Recommendations will be made at the end of this thesis, on how to include variability of the other parameters in the design.

Parameter	Meaning	Estimated value
L	Total tube length	1 m
D	Total tube (outer) diameter	200 mm to 300 mm
l_p	Helical pitch (between intersections)	100 mm to 200 mm
Δ	Helical intersection offset	10 mm
t_l	Longitudinal member thickness	5 mm
t_h	Helical member thickness	5 mm
N_l	Number of longitudinal members	10
N_h	Number of helical members	$5 + 5$

Table 4.1: Details of the parameters that define the iso-truss

4.2 Methodology

With the design of the iso-truss fully defined in terms of shape and materials, focus can be shifted to demonstration of the processes required to produce the structure. With the use of thermoplastic based composite materials, the process steps can be split up into wetting and consolidation, helical member shaping and intersection joining. While wetting and (initial) consolidation is outsourced as part of the pultrusion step, the joining of intersections is believed to be a problem that should first be isolated. The steps to be executed can therefore be defined as testing of intersection production methods, shaping of helical members and final assembly of the structure. This section aims to define the methodology for these steps. Additionally, methods for physical testing of an iso-truss can be considered, as part of formulation of an answer to research question 4: comparing the final design to existing tubular open lattice manufacturing methods.

4.2.1 Intersection Production & Testing

As one of the main concerns in the production of an iso-truss structure, a setup to successfully join together longitudinal and helical members had to be designed. Before this could be integrated in the final assembly setup, a dedicated joining setup was to be designed for the production of separate intersections to isolate the problem. This setup would consist of both a mould and a welding device. Optimal manufacturing conditions like temperature and applied pressure were to be determined through limited testing.

Furthermore, a mechanical test was to be designed, assessing the strength between members that have been joined together. This testing would be used to obtain some basic characteristics of the joint. Further optimisation of the test conditions and the development of a reasonable test base would be left as recommendation for further research. It was determined that, within the scope of this thesis, about 20 samples for mechanical testing could be produced in total.

4.2.2 Helical Member Production

Another technology to be demonstrated was the shaping of helical members. The two most important aspects of this process would be to ensure a controlled shaping movement as input,

as well as a heating mechanism to soften the material to allow straight members to be reshaped. The setup was to be designed in a CAD program and individual components were to be selected as soon as possible, to account for lead times of items like electric motors or parts that require custom manufacturing. Demonstration would include assembly of the design and extensive testing on the available material. Parameters of influence were believed to be the required temperature for successful shaping as well as maximum possible helix curvatures. It was expected that length and curvature could be controllable inputs, while modifications to the setup would allow for the production of at least two different helix diameters.

4.2.3 Iso-truss Assembly

With separate setups to assess the shaping of helical members and joining of different members, a final setup would be designed and manufactured for the assembly of iso-truss structures. It would consist of an adaptable mandrel and a fixing method for all individual members. With all members in place, the integrated joining method would allow for the fixation of intersections between all individual members, after which the completed iso-truss sample could be released from the fixture. This setup would be designed to be adaptable to different tube diameters and helical patterns.

4.2.4 Full-scale Testing

If time permits, one of the iso-truss structures produced was to undergo a compression test to determine its mechanical characteristics. Design of this test would include a simple clamping device for the tube ends. The test would be meant to provide a comparison of the design against a sample of the existing IsoTruss design. Performance would be expressed normalised to the weight of the structure, allowing for a comparison of the design to different open lattice structures of similar shape and size.

4.3 Experimental Setup

After establishing the methodology for demonstration of the different process aspects for production of an iso-truss, the experimental setup for each of these aspects could be developed. These different setups could be divided into characterisation of the composite material, production and testing of intersections, helical member production demonstration, assembly demonstration and full-scale testing of the produced structures. It should be noted that a certain budget was made available for this project. While limited, it was expected to allow for sufficient material ordering and for equipment manufacture and component cost.

4.3.1 Material Ordering and Characterisation

The first critical phase for this project was the ordering of materials to test with. As already mentioned, vDijk Pultrusion Products was selected as the company to produce Elium based carbon fibre reinforced pultruded composite rods. A rod diameter (or thickness) of 5 mm was thought to be a reasonable representation for an iso-truss on the scale of about 1 m. The

thickness of these rods would not be varied as part of this thesis, first of all to allow for easier comparison between different tests and secondly to limit the material cost. A standard rod length of 2.5 m was chosen so that the rods could remain straight, while not making shipping of the rods too difficult. If this length would be smaller, it would be limiting on the longest single-piece element within the structure: a helix for the iso-truss with the largest outer diameter. The rods were ordered with this length in mind under the assumption that they could be cut to any length using available facilities. The material was meant to be used for the production of intersection test samples and helical members, as well as for longitudinal members.

A material inventory was established in order to keep track of the amount of material used and to be able to identify samples cut from the same rod. This was done under the assumption that the process conditions could have varied during the pultrusion process, leading to slight differences between the rods. Before any physical test could be done, some basic information like fibre (volume) distribution and the influence of temperature on the material's behaviour was to be obtained. This would be accomplished through the use of microscopy, degradation analysis, heat flow analysis, and temperature-dependent mechanical behaviour analysis.

4.3.2 Intersection Test Setup

For individual intersection testing, a separate setup would be designed. Samples from the main material batch would be used in this setup, albeit in short lengths. The setup was defined to consist of a tool to compress the members against, likely made of aluminium or steel, and a welding device to consolidate the members by means of heat and pressure, as visualised in Figure 4.2a.

After making these samples, they would be physically tested to determine the strength of the joint. This would be accomplished by clamping one of the members (representing a longitudinal iso-truss member) in a load applicator, while a clamp was to be designed and produced to support the other members (representing helical members), as visualised in Figure 4.2b.

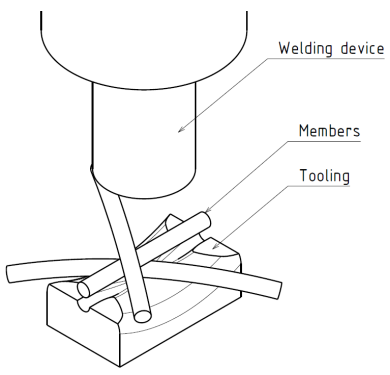

(a) Production of separate intersections

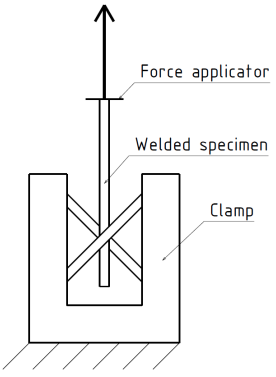

(b) Example intersection testing method

Figure 4.2: Overview of the intersection test setup

4.3.3 Helical Member Production Demonstrator

The production demonstrator for helical members would prove to be the most complex aspect of physical design in this thesis. Not much was known about its detailed design at this point, other than that it would be of cylindrical shape, with supports on either end of a collection of initially straight members to hold them in place, as shown in Figure 4.3. The idea for this demonstrator was to heat up the members to allow them to be reshaped, but not too much as to disturb the shape of their cross-section. This placed requirements on the temperature regime of the plastic in which they would easily form. The support on one side of the members would be twisted in a controlled manner, requiring both supports to move closer to each other to account for the height change of the members as they would be twisted around the cylinder. The setup should be used twice for each iso-truss sample: once to produce all clockwise-wound helical members, and once to produce all counter-clockwise-wound members.

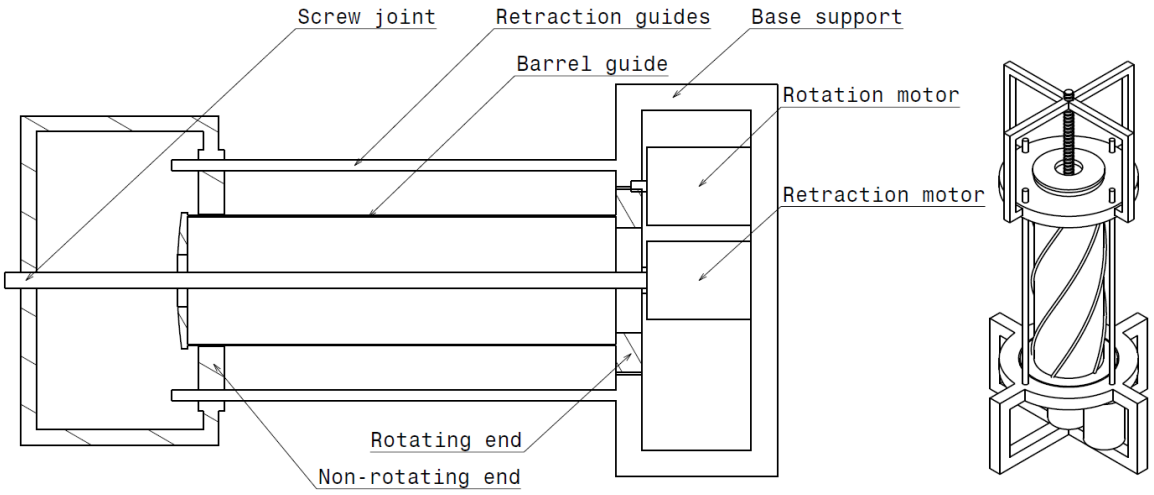

Figure 4.3: Conceptual design for the helical member production demonstrator

4.3.4 Iso-Truss Assembly Demonstrator

In parallel with the design of a helical member production setup, a jig was designed for the assembly of different members into an iso-truss. This assembly demonstrator was meant to integrate the intersection welding setup by providing (removable) support from within the tube at every intersection, while allowing access from the outside to join them. The inside support would be responsible for the final shape of the structure, should of course be easily removable without damaging either the structure or the support itself, and should be adaptable to allow for different design parameters. A preliminary design of this support was based on literature concerning the production of the IsoBeam, as presented in Section 2.1. It features metal tooling consisting of a core beam and repositionable support modules, as seen in Figure 4.4. Another feature of the assembly jig is the use of rotary bearings on either side of the support to allow easy access to any location of the sample during its production (in case the welding setup itself is not movable for example).

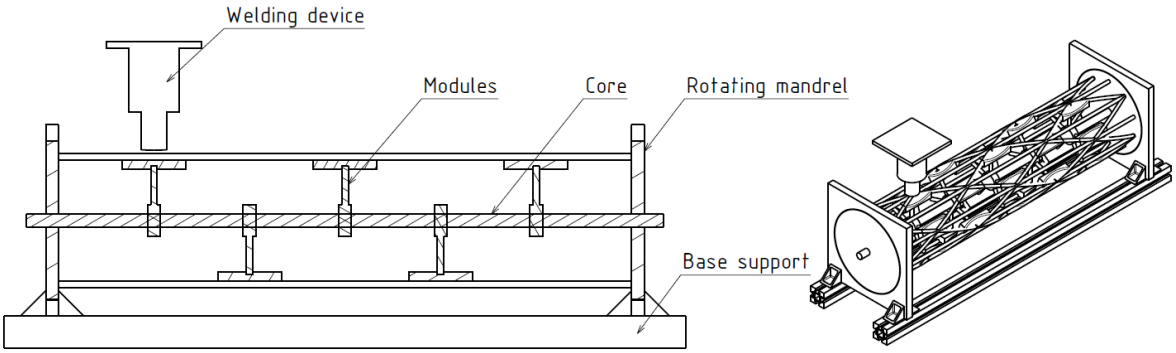

Figure 4.4: Conceptual design for the iso-truss assembly demonstrator

4.3.5 Iso-truss Test Setup

For full-scale physical testing of a completed iso-truss sample, the main consideration was on how to introduce loads into the structure, as load introduction design is not within the scope of this thesis. Because it was not a primary concern of this research, a simple workaround could be used to still be able to test a sample. Similar to how IsoTruss tests have been described in literature, a low-melting-temperature metal, like Wood's metal or the non-toxic but more expensive Field's metal, could be used to create a solid disc on both ends of the tube, through which load can be introduced into each member. Alternatively, a disc can also be created from a low-temperature curing thermoset polymer. After clamping these ends in a compression loading test bench, the structure could be loaded until failure. From this test, several important characteristics like the structure stiffness, failure load and failure mode could be extracted.

As elaborated on later in this report, it was not possible to produce a physical representation of a full-scale iso-truss as part of this project. The test setup described above is therefore left as a recommendation for continued research after such a sample has been successfully produced.

Chapter 5

Material Characterisation

As the Elium-carbon pultrusion composite used for this thesis topic is a relatively novel material, there is no extensive database on its mechanical and thermal behaviour. This information is crucial in order to narrow down the processing condition range before production testing. Additionally, a crucially important parameter for successful welding and forming of the composite (both matrix dependent processes) is the matrix volume content. This chapter presents an overview of the tests performed on the Elium-carbon composite material in order to assess the viability of its use for this project. The tests performed can be divided into Scanning Electron Microscopy (SEM) to provide a close-up look at the composite, Thermogravimetric Analysis (TGA) to provide an indication of the fibre volume content, Differential Scanning Calorimetry (DSC) to identify interesting temperature ranges for the composite, and deformation tests to give a crude indication of the material's mechanical behaviour at elevated temperatures. Finally, externally supplied DSC and Dynamic Mechanical Analysis (DMA) data is discussed. This data was supplied by Arkema, the company developing the Elium resin.

5.1 Scanning Electron Microscope (SEM)

In any composite material, close observation of the cross-sectional surface provides incredibly useful initial data. Through the use of SEM, resolutions of up to 1 nm are possible, allowing for a maximum magnification far greater than light microscopes. This way, individual fibre bundles can be visualised, as well as microscopic voids and resin distribution, to name a few.

5.1.1 Methodology

Samples used for the SEM analysis, performed on a Jeol JSM-7500F field emission scanning electron microscope, were prepared by cutting off small pieces of the test material of a few cm long. These pieces were then encased in a standard cylindrical epoxy sample in different orientations (see Figure 5.1). This way, cross-sections across and along the fibre direction could

both be visualised. After casting, the surface to be inspected was polished and then coated in gold powder to make it conductive and easily ground-able, as non-conductive specimens collect charge, negatively affecting the image quality.

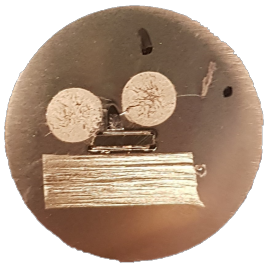

Figure 5.1: Close-up of the sample

5.1.2 Results

Several pictures were taken at different locations and magnifications, the most notable of which are presented in Figures 5.2, 5.3 and 5.4. Other images can be found in Appendix B.1.

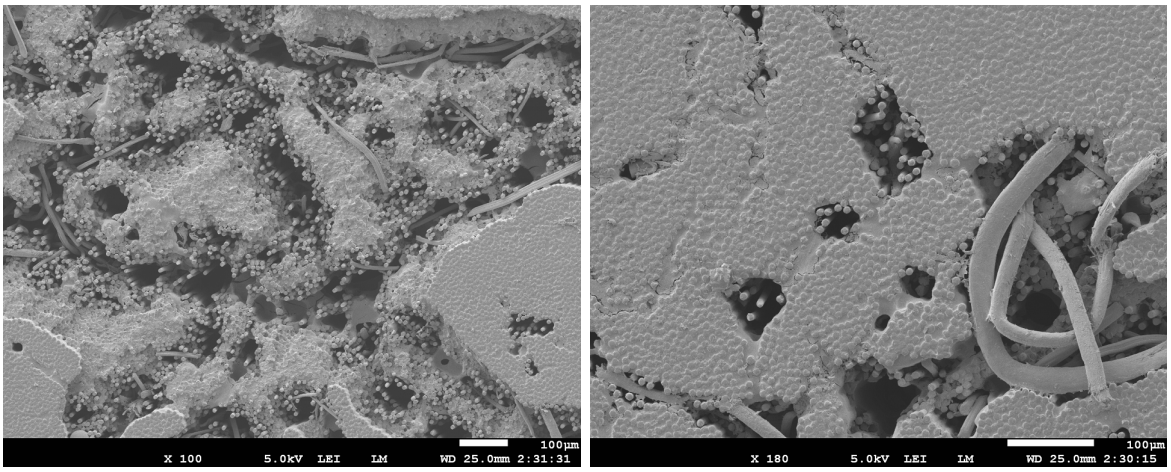

(a) Region showing several composite 'clusters' **(b)** Close-up of an individual cluster

Figure 5.2: Low magnification of the composite cross-sectional surface across the fibre direction

In the low magnification images of the composite cross-section across the fibre direction (Figure 5.2a), several clusters can be seen, with pockets in between. In a close-up of one of these clusters (Figure 5.2b), the individual fibre bundles can be easily distinguished, and a small crack can be seen on the left side of the picture. In Figure 5.3, showing a cross-section along the fibre direction, the fibre bundles can again be easily distinguished. Notable to observe is the straightness of these bundles, and the termination of some of them within the picture. Figure 5.4 shows a higher magnification of the across-fibre cross-section within one of the clusters. Here, the general density and distribution of fibres can be clearly observed, as well as their interaction with the matrix material in between.

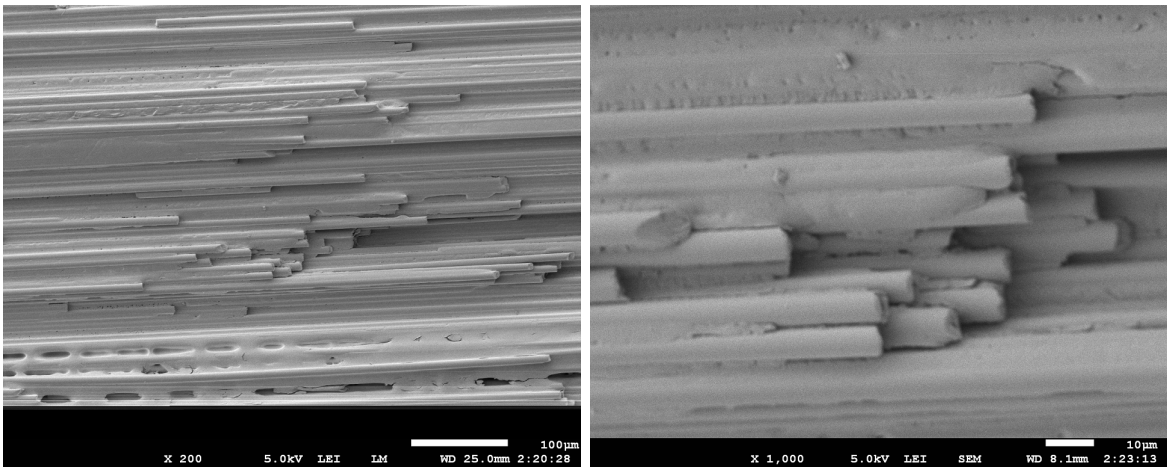

(a) Region showing both fibres and resin **(b)** Close-up of the fibre ends

Figure 5.3: Magnification of the composite cross-sectional surface along the fibre direction

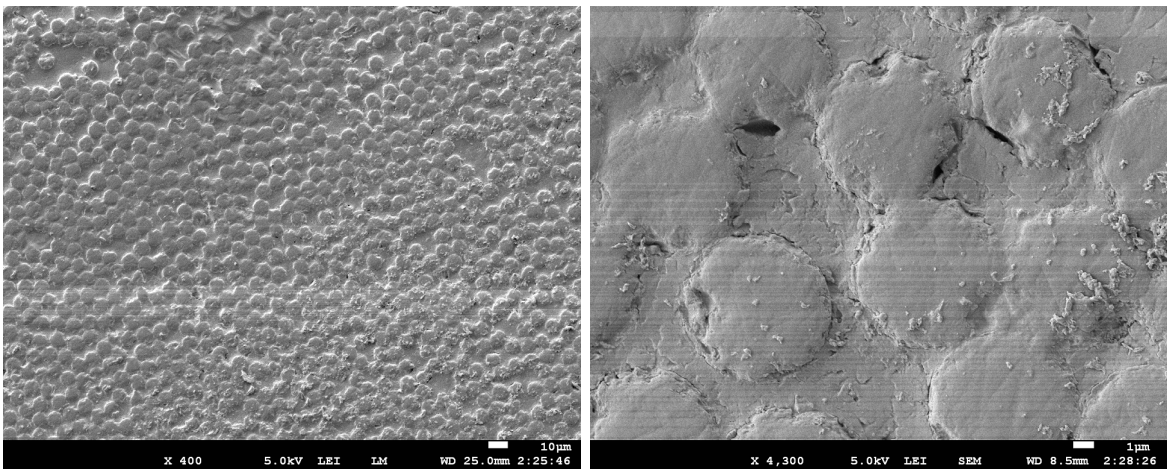

(a) A cluster of fibres **(b)** Close-up on the fibre-matrix interface

Figure 5.4: High magnification of the composite cross-sectional surface across the fibre direction

5.1.3 Discussion

As one of the very first experiments performed as part of this thesis, viewing the material through a Scanning Electron Microscope provided several important initial results. It allowed for a close-up view of the composite material, showing a clear distinction between fibres and matrix.

From the low magnification images showing a cross-section across the fibre direction, the composite was observed to consist of several clusters, with voids seemingly appearing in between. Whether this is due to the processing used to prepare the samples is unknown, but it seems in line with initial inspection of the material cross-section, which showed several cracks in the centre region of the 5 mm rod which were visible with the naked eye. It is hypothesised that this is due to the way in which the composite pultrusion was formed. As the process was not yet optimised for this relatively new material, there may have been unaccounted shrinkage effects during curing of the resin within the pultrusion die. As the die is usually heated, it is hypothesised that the resin in the outside of the cross-section in contact with the die could have cured slightly faster than the centre region, preventing the cross-section from shrinking as a whole, causing cracking as the material in the centre region shrank.

A crucially important property in fibre reinforced polymer composites is the fibre volume content, denoted as V_f and given as a ratio between 0 and 1. Similarly, the matrix volume content V_m is an indication of the composite's performance, and is given as $1 - V_f$. While generally, a higher fibre volume content implies higher specific properties like tensile strength and stiffness, there is an optimum fibre content above which the material becomes 'too dry'. This is characterised by a reduction in shear and impact strength, as there is not enough resin to transfer load between fibre bundles. The matrix volume content is also especially important for thermoplastic composite manipulations like forming and welding, as both rely on thermoplastic matrix-related properties. From the close-up pictures presented in Figure 5.4, an initial estimation of the fibre volume content could be given. As the fibres with their circular cross-section are clearly distinguishable from the matrix material in between, and the cross-sectional area can be assumed to be a representation of the volume of the composite, the fibre volume can be estimated by dividing the number of pixels representing fibres by the total number of pixels in the image. As tools would have to be used in order to distinguish between pixels representing fibres and pixels representing the matrix, determination of the fibre volume fraction using the image in Figure 5.4a is considered out of scope of this thesis project. However, for the image in Figure 5.4b, the contour of the fibres could be drawn by hand relatively easily. By doing this, it was possible to separate the pixels representing fibres from the image. The amount of pixels that were left within the image (excluding the ones corresponding to the legend) could then be counted and divided by the total amount of pixels, yielding a percentage of around 35%. This percentage was the first indication that could be given with regards to the matrix volume content, with the fibre volume assumed as the remainder (65%). It should be noted however that the matrix volume in this image may not be a very good representation of the total fibre volume fraction, especially by comparing this image to Figure 5.4a, in which the fibre volume content is clearly higher (i.e. closer to 0.75 or 0.8). The method also did not take into account voids which, by looking at Figure 5.2, apparently make up a significant portion of the total volume.

While not many other conclusions are drawn from the SEM images in the scope of this thesis

project, one other observation is made: Figure 5.4b shows the presence of small pockets around some of the fibres (seen as dark spots in the image). It is believed that these may be an indication of fibre-matrix interface limitations.

5.2 Thermogravimetric Analysis (TGA)

For a more accurate estimation of the fibre volume fraction, it was believed that a Thermogravimetric Analysis (TGA) would provide valuable information. The analysis relies on the weighing of a small sample (about 5 mg) through a heat cycle (in this case employing a steady increase in temperature). For most fibre reinforced polymer composite materials, as the temperature increases, the matrix material starts degrading and evaporating before the fibres do, causing a reduction in weight. As most fibre materials are stable up to far higher temperatures than most matrix materials, this leads to the formation of a plateau in a graph plotting weight over temperature. This plateau would be a direct indication of the fibre weight content of the material and, with the knowledge of the densities of both composite constituents, an indication of the fibre volume content. Furthermore, TGA provides an indication of the degradation behaviour of the matrix material, with which a maximum processing temperature limit can be established.

5.2.1 Methodology

Due to the size limit of the samples, small sections (around 2 mm to 3 mm wide) of the carbon-Elium composite were cut of from the 5 mm rod pultrusions using a hacksaw to provide a first indication. Because of this processing method, sections broke up into smaller chunks that were collected in a sample bag. Because the automatic sampling function of the TGA device (a PerkinElmer TGA 4000) was not working correctly, samples had to be manually put inside the test chamber. Due to the length of the test, this only allowed for the conduction of two tests, mostly because this test was not seen as the focus of this thesis. Both tests were conducted in a pure nitrogen environment and heated up using a constant heating rate of $5\,^{\circ}\mathrm{C}\,\mathrm{min}^{-1}$ until a final temperature of 900 °C. The first test was unfortunately aborted at a temperature of around 180 °C, then resumed with the new weight at 200 °C until a final temperature of around 900 °C. Because of this, there is some discontinuity in the data. The second test however was run successfully until 900 °C. Both of these tests are visualised in a graph presented in Figure 5.5.

5.2.2 Results

From the graph, it can be seen that both samples show a very similar behaviour to an increase in temperature. A total of four different degradation phases can be seen: The first between roughly 160 °C to 260 °C (although the first test failed to fully capture this region), the second between 260 °C to 340 °C, the third between 340 °C to 440 °C, and finally the fourth initiating after around 720 °C. Very interesting to observe here is the plateau at a weight fraction of around 77%, where the weight of both samples remained constant until the final degradation phase.

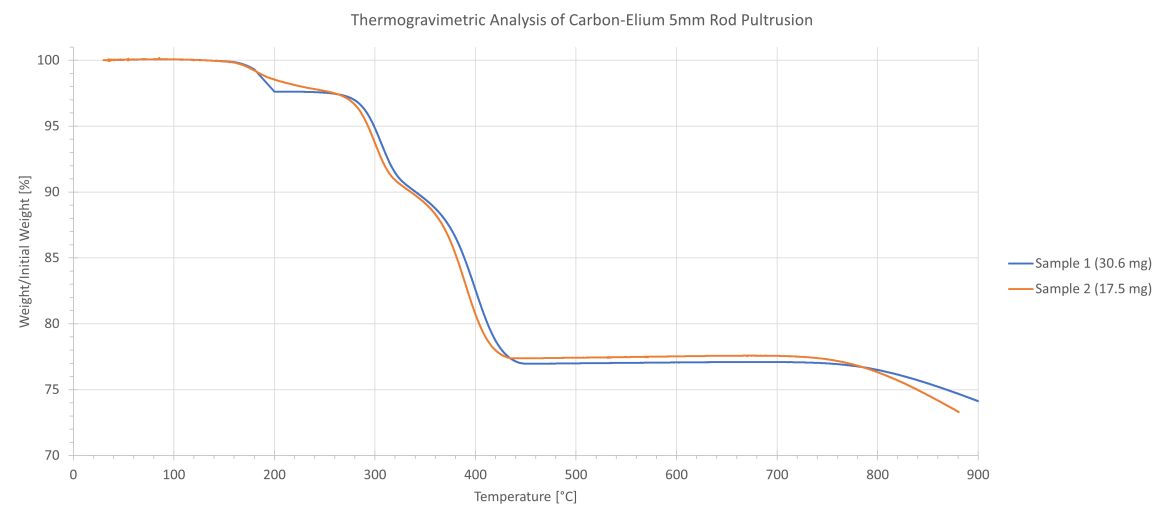

Figure 5.5: Thermogravimetric analysis of two Elium-carbon composite sample

5.2.3 Discussion

Although only two TGA tests could be performed as part of this thesis, several conclusions can still be drawn. Most importantly, the experiments provided a simple way to determine the fibre content of the composite due to the presence of the clear plateau in the graph of Figure 5.5. As carbon fibre is more temperature stable than most resin systems, it would only start degrading long after the last of the Elium resin had evaporated. The graph clearly shows this as the weight fraction which remained constant between a temperature of 440 °C and 720 °C. It can therefore be assumed that this weight fraction (about 0.77 as read from the graph), is the fibre weight fraction (W_f) of the composite. Using the densities of both resin systems, this fibre weight fraction could be used to compute the fibre volume fraction. For the Toray T700SC fibre used in the composite, the density (ρ_f) was known to be $1.8\,\mathrm{g\,cm^{-3}}$ [35]. Assuming a cured density of the Elium 591E resin system (ρ_m) of $1.19\,\mathrm{g\,cm^{-3}}$ [17], the fibre volume fraction can be computed using the following formula:

$$V_f = \frac{W_f}{W_f + (1 - W_f)\dfrac{\rho_f}{\rho_m}} = \frac{0.77}{0.77 + (1 - 0.77)\dfrac{1.8}{1.19}} \approx 69\% \tag{5.1}$$

This is mostly in line with the fibre volume fraction estimated from the SEM images (65%). Compared to most fibre reinforced polymer composites, this computed value is near the upper limit of commonly used fibre volume fractions (which are usually in between 40% and 70% [36]). For the envisioned applications of this material however, that is welding and forming of the composite, this value is sub-optimal, as both processes rely on resin-related properties.

Another interesting phenomenon to observe is the step-wise degradation of the Elium resin. These degradation steps are in line with the conclusions of a paper describing the degradation of PMMA [37]. After consulting Arkema for welding processing conditions, they recommended

a processing temperature between 180 °C to 200 °C. However, it can be seen that the material is already slightly evaporating in this temperature regime.

5.3 Differential Scanning Calorimetry (DSC)

While a Thermogravimetric Analysis provides insight into the degradation of composite materials, Differential Scanning Calorimetry (DSC) can be used to identify (reversible) phase transitions of the material, like the glass-transition temperature (T_g) and, in the case of some thermoplastic materials, the melting temperature (T_m). Like TGA, DSC measures the response of a material to a change in temperature. However, in the case of DSC this response is measured as the amount of energy that is required (or heat flow) to increase the temperature of the sample as compared to a reference sample, in this case an empty sample pan subjected to the same heat cycle. Depending on the heat-up rate, one would expect a linear relation between heat flow and temperature for materials that are temperature stable. However, polymers above T_g show a slightly different reaction to this heat flow, which can usually be seen as a shift in the linear relation above this temperature. Additionally, crystalline thermoplastic polymers have two additional transitions: The transition above which they de-crystallise (known as the crystallisation temperature T_c) and the transition above which they melt (known as the melting temperature T_m). As these transitions are exothermic and endothermic, respectively, they show up as peaks in the heat flow graph: De-crystallisation releases energy (exothermic), making it require less heat flow to go through, while melting and other phase transitions require energy (endothermic), requiring more heat flow to go through. The presence of these peaks is a strong indication that the tested thermoplastic polymer is crystalline in nature. However, as Elium resin mostly consists of Poly(methyl methacrylate) (PMMA), which is known to be highly amorphous due to its transparent properties, these peaks are not expected.

5.3.1 Methodology

For the DSC test, a total of six different samples were prepared. Three of these used pieces of the 5 mm composite rod, prepared similarly to the samples for TGA. Two samples were cut from pultrusions made for another thesis project for which the same composite was used, although in the form of thin strips of 3 mm × 0.13 mm. The last sample used a combination of the two materials. The weight of all samples was in between 3 mg to 10 mg. The device used for testing was a TA Instruments DSC 250. The samples would be collected in measuring pans which would be closed using a lid. While a hermetically sealed lid was used for samples 2 and 3, only a normal (non-sealed) lid could be used for the other samples. All samples were subjected to the same heat cycle: First, a sample would be kept at room temperature for 10 min, after which it would be heated up to a maximum temperature of 200 °C at a rate of 10 °C min^{-1}. It would be kept at this temperature for another 10 min, after which it would be cooled down at a rate of 10 °C min^{-1}. This cycle would then be repeated once again (as is common in DSC analysis). In Figure 5.6, the heat flow of one of the samples is plotted over temperature. For the other samples, the reader is referred to Appendix B.2. In addition to the DSC performed in DASML, DSC data was also supplied by Arkema, the company developing the Elium resin. This data can be found in Appendix B.2 as well. It should be noted that the

thermal history of the samples, which is of large influence to the transitions discussed before, was unknown. On top of this, it was unknown what effect the sample preparation method had on the results of the test.

5.3.2 Results

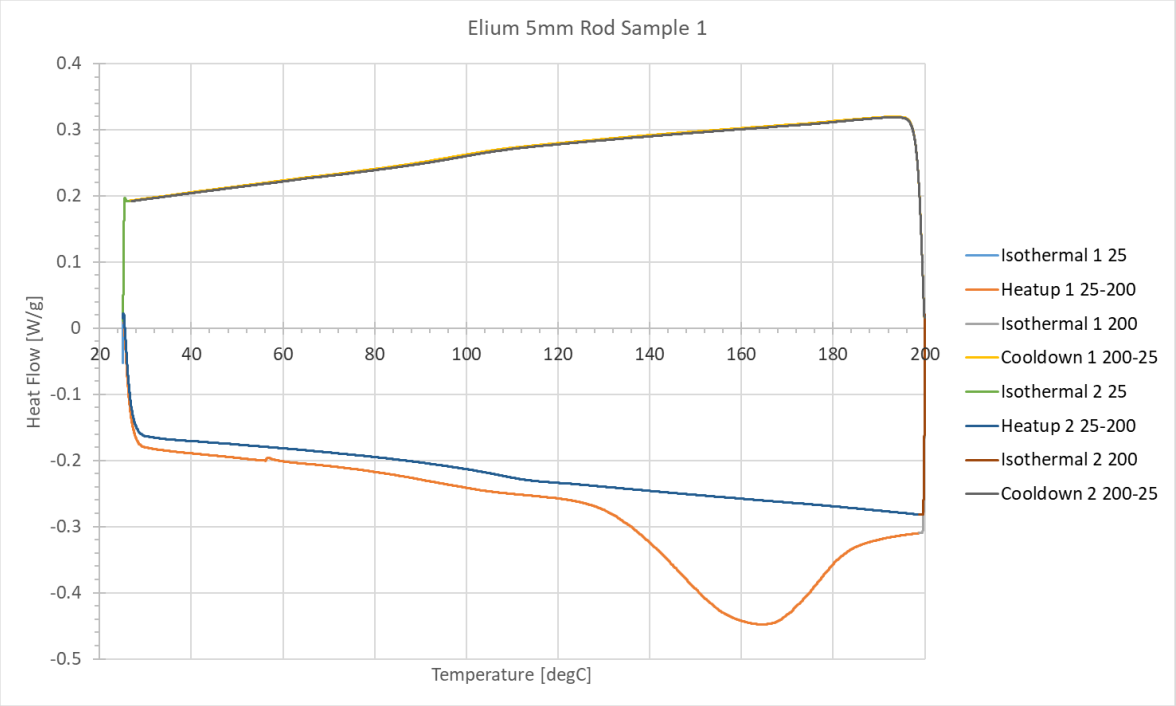

Figure 5.6: Different Scanning Calorimetry of one of the Elium-carbon composite samples

From these graphs, several interesting phenomena can be observed. First of all, a generally linear relationship between heat flow and temperature can be seen, with the sample requiring more heat flow to heat up at higher temperatures, and less heat flow at lower temperatures. However, there is a noticeable shift in this linear relationship between 80 °C to 100 °C in both the heat-up and the cool-down phase. Additionally, while the two cooling phases overlap to a large extent, there is a noticeable shift in heat flow between the two heating phases, with the second heating phase requiring generally less heat flow to warm up the sample. The most striking phenomenon to observe in these graphs is the endothermic peak during the first heat-up phase occurring in the temperature range of 130 °C to 200 °C. Notably, this phenomenon is not observed in the cooling phase, nor during the second heating phase.

5.3.3 Discussion

With a total of six experiments performed on the carbon-Elium composite, combined with the data of one sample supplied by Arkema, a small test-base could be established which showed a variety of phenomena. First of all, the glass transition could be observed in all experiments as a very slight shift in the heat flow curve, mostly in a temperature range of 80 °C to 100 °C.

For the samples showing the endothermic peak in the first heating phase, the glass transition slightly shifted to the right for the second heating phase. This shift was seen as part of a general shift of the curve: Samples showing an endothermic peak would require slightly less heat flow to warm up on the subsequent heating phase, while samples showing an exothermic peak would require slightly more heat flow to reach the same temperature as before. Whether the peaks and these shifts are related or not is unknown.

Interestingly, samples showed either an endothermic, an exothermic, or no process occurring in the temperature range between 130 °C to 200 °C. The samples that did not show this peak were the thin carbon-Elium pultruded strips which were intended for another thesis topic, while the carbon-Elium rods were sometimes observed to show an exothermic process instead of an endothermic process. While it is known that evaporation (of volatile gases produced from degradation for example) is an endothermic process, it is unknown what causes this process to be exothermic (to release energy). There are also two small endothermic peaks observed in the strips at low temperatures (the first one at around 50 °C and the second at 70 °C). While this could also be due to surface contamination, another hypothesis is that the peaks result from the evaporation of products within the material. With the strips having a far larger surface-to-volume ratio than the 5 mm rods, this would explain why the volatiles would be able to escape from the material at lower temperatures. Softening of the matrix within the rods at elevated temperatures might be how volatiles are still able to escape, albeit at higher temperatures than for the strips. The possibility of a crystallisation process occurring in the higher temperature region is ruled out for two reasons: Firstly, the process is only observed during the first heating cycle and not during cooling or the second heating cycle. Secondly, PMMA (the base component in the Elium resin) is known to be highly amorphous due to its asymmetric molecular structure. Another interesting observation that was made was that the endothermic peaks occurred in samples that had a regular lid on the sample container, while the samples with exothermic peaks were hermetically sealed. This supports the theory that the endothermic peaks are caused by evaporation, as this is not possible for the hermetically sealed samples. The exothermic peaks might in turn be useful in determining what the substance is. With the volatiles unable to escape, perhaps they are forced to react within the sample container, releasing energy. With this information, the hypothesis is formed that the volatile gas actually consists of leftover peroxides that are used for curing the polymer. Still, more testing should be done to confirm this, and to determine if this process impacts the material properties.

Finally, an observation is made with regards to the DSC data presented by Arkema. While the graph generally shows similar results, with the T_g distinguishable in between 80 °C and 100 °C and a similar endothermic peak occurring between 170 °C and 220 °C during the first heating cycle, a slightly exothermic peak can also be observed at temperatures slightly above the glass-transition temperature. As the test conditions were not known for this sample, no conclusions can be drawn with regards to the nature of this peak.

5.4 (Externally Supplied) Dynamic Mechanical Analysis (DMA)

Although TGA and DSC tests provide useful data with regards to the influence of temperature on the state of a material, they provide little information on the mechanical properties of a material under different temperature conditions. For the envisioned forming and welding

tests however, this data is of crucial importance, as they both rely on different degrees of softening of the thermoplastic resin. A test that can be used to obtain such information is Dynamic Mechanical Analysis (DMA). This testing method subjects a sample to a dynamic (usually sinusoidal) load while the temperature of the sample is slowly increased. For viscoelastic materials like polymers, which exhibit both viscous (i.e. stress relaxation) and elastic (i.e. stress storage) properties, DMA can be used to study the ratio between these two properties, which is dependent on temperature. As thermoplastic polymers become softer at higher temperatures, the material becomes more viscous than elastic. This leads to easier deformation of the material, with less springback (where the material tends to return to its original shape). As both helical winding and welding rely heavily on permanent deformation of the material, this test would provide useful information.

5.4.1 Methodology

The DMA data presented in this section was supplied by Arkema, who performed tests with another composite material using the same Elium resin system. The test was performed under a torsional sinusoidal load with a frequency of 1 Hz using a rectangular sample. Three different samples were tested in total, each using a different fibre orientation (0°, 45° and 90°). They were each subjected to two temperature cycles between room temperature and 180 °C. During the test, four properties were recorded: The temperature of the sample (T), the bulk/storage shear modulus (G'), the loss modulus (G") and the ratio G"/G', also known as the loss angle $\tan\delta$. Using this data, the glass-transition temperature of the material could be confirmed, as it is usually defined as the peak in loss modulus. More importantly however, the data offered an accurate representation of the material's stiffness (or bulk shear modulus) over a large temperature range. This data is presented in Figure 5.7, where the bulk modulus, loss modulus and loss angle are plotted on a logarithmic scale against temperature.

5.4.2 Results

The graphs show a large influence of temperature on the (shear) stiffness of the composite, even at low temperatures: While the (shear) bulk modulus is measured to be around 4 GPa at room temperature, it steadily decreases with increasing temperature to a value of around 3 GPa at a temperature of 60 °C and slightly more than 2 GPa at 80 °C. The loss in bulk modulus is highest at a temperature of around 115 °C, where the inflection point in the graph occurs and where the loss modulus is maximum. After this point, the bulk modulus continues to decrease until roughly 20 MPa at the maximum testing temperature of 180 °C.

5.4.3 Discussion

The Dynamic Mechanical Analysis performed on a carbon-Elium composite sample showed some interesting aspects about the mechanical behaviour of the material at elevated temperatures. First and foremost, the data showed a steady loss of bulk (shear) modulus over the full range of tested temperatures, even at relatively low temperatures. The modulus declined most rapidly between temperatures of 80 °C to 140 °C, somewhat stabilising again at higher temperatures. For helical winding, a temperature should be selected at which the material

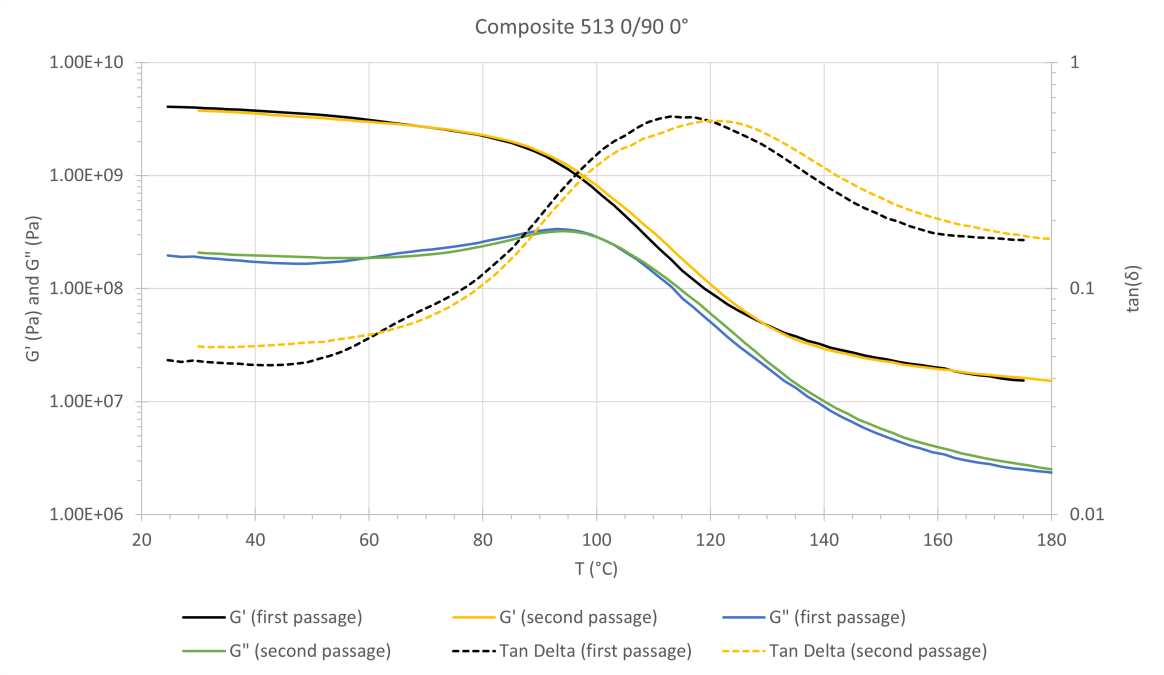

Figure 5.7: Dynamic Mechanical Analysis of a carbon-Elium composite sample. Data provided by Arkema

easily bends, while retaining a certain stiffness to prevent flattening of the cross-section and to hold the material together. Because this would rule out the higher temperatures, the remaining steady loss in bulk modulus implied a high sensitivity of the material to temperature changes in the forming process. While this would make the selection of an optimum forming temperature more difficult, it did allow for the investigation of a variety of forming results as discussed in Section 5.5.

In addition to an general insight into the stiffness of the material at different temperatures, the test allowed for an accurate definition of the glass-transition temperature (T_g). This was determined as the temperature corresponding to the maximum loss modulus, representing the onset of the glass transition ($T_{g_{onset}}$). While the peak in $\tan\delta$ could also be taken as the definition of the T_g, this peak corresponds to the inflection point in the bulk modulus, at which point the modulus has already reduced by more than a factor 20 when compared with its value at 25 °C. Although the onset peak also corresponds to a bulk modulus reduction of around a factor 3, it is usually taken as a safer estimate for the glass transition. From the loss modulus peaks, the T_g was found to range from 93 °C to 100 °C for the three presented samples, being slightly higher during the second passage for the same sample. The average $T_{g_{onset}}$ was found to be around 95 °C, compared to 115 °C if defined as the peak in $\tan\delta$.

5.5 Deformation (Oven) Tests

As a more intuitive and qualitative test of the temperature behaviour of the carbon-Elium composite samples, several samples were subjected to a variety of oven cycles. This provided an accessible method to assess the behaviour of the material at a variety of temperatures and

loading conditions. Although different aspects were tested for different samples, all samples subjected to some form of oven cycle were denoted with the prefix "O." to keep track of the tests performed.

5.5.1 Methodology and Results

Initial samples O.1-O.5, each around 300 mm long, were subjected to temperatures of around 160 °C, far above the glass-transition temperature but below the degradation phase observed in the TGA. At this temperature, they could be easily deformed by hand. When bending the samples, it was observed that they would tend to 'kink' instead of deflecting with a constant bending radius. This kinking was observed as fibre bundles on the inner bending radius buckling away from or into the composite. Once this weakness had formed, bending the sample would simply cause this kink to hinge. A similar phenomenon was observed when twisting the samples: Instead of a constant angle of twist over the length of a sample, decompaction 'knots' would form at regular distances over the sample's length. One of the samples was deformed by simultaneously pulling on and twisting the ends, after which it could be bent with a somewhat constant bending radius.

For samples O.6 to O.12, the bending behaviour was assessed in more detail at different temperatures around the glass-transition temperature, with a temperature ranging between 90 °C to 140 °C. The samples were put on a single aluminium plate and fixed on one end using a piece of polyester tape. At a temperature of 90 °C, it was attempted to bend one of these samples. While it was possible to deflect the sample, it would immediately spring back to its original shape upon release. The same was observed for the subsequent sample at a temperature of 95 °C. However, the third sample showed the same kinking behaviour as was observed before, at a temperature of 100 °C. The fourth sample showed the same response at a temperature of 110 °C. To confirm that this phenomenon was present at all temperatures above glass-transition, the last sample was bent at a temperature of 140 °C, during which it was observed that the composite rod would kink even more easily.

To attempt to combat this issue and to provide a more consistent loading condition for the samples, a small setup was constructed with which samples O.13 to O.21 could be pre-bent outside the oven. As a goal for this test, it was attempted to deform samples below the glass-transition temperature using creep (or stress relaxation over time). Deformation of the 300 mm samples was measured as vertical deflection of the middle. The sample temperature would be measured using a thermocouple positioned just outside the middle of each sample. Sample O.13, put in the oven with a deflection of around 30 mm, buckled before it could reach its target temperature of 90 °C, at a temperature slightly below 70 °C. Sample O.14, deflected to roughly 15 mm, kinked at around 90 °C, as did a repetition sample O.15. While sample O.16 did appear to be stable at a temperature of 80 °C and a deflection of around 11 mm, it kinked after being left in this state for around an hour. Sample O.17, left overnight in the oven at a deflection of 11 mm and a temperature of 60 °C was the first stable sample which did not kink. When taken out of the oven the next day, around 15 hours later, it did spring back to mostly its original shape, although some permanent deflection (around 1 mm) remained. Sample O.18 however buckled again after being left in he oven at the same temperature but at a higher deflection of around 16 mm. Similar attempts with sample O.19 (70 °C with 11 mm deflection) and sample O.20 (70 °C with 15 mm deflection) again showed

the same kinking behaviour. As a final attempt, sample O.17 was put in the oven again together with sample O.21 at a temperature of 60 °C and deflection of 11 mm and 12 mm respectively, then left overnight. Both samples showed some degree of permanent deflection without kinking, though only a few mm.

(a) Initial forming (O.1-O.5) **(b)** Temp. influence (O.6-O.12) **(c)** Creep forming (O.13-O.21)

Figure 5.8: Overview of the different oven experiment samples

5.5.2 Discussion

Although more of a qualitative approach, the oven experiments provided some interesting information with regards to the final application of the carbon-Elium material. Most importantly, they provided insight into the interpretation of the DMA experiment, as they confirmed just how sensitive the material was to elevated temperatures.

From the initial deformation experiments, it was seen that softening of the matrix close to the T_g lead to undesirable phenomena, most notably decompaction of the material in the form of kinking when bent and the formation of knots when twisted. This was a strong indication of the material's reduced ability in stabilising fibre bundles. In the case of bending, fibre bundles in the inner radius of the bend (which would be in compression) were not held in place by the matrix enough to prevent them from buckling. This phenomenon was observed to occur whenever the material was heated to close to its T_g, not necessarily above. This kinking prevented the rest of the rod from adapting any form of curvature when bent further, instead hinging around this newly created weakness. Elevated temperatures only accentuated this problem. Twisting the sample was thought to improve this behaviour by creating an alternating pattern in the role that fibre bundles had to perform: A twisted fibre bundle would alternate between lying on the inner and outer bending radius of the sample with a frequency depending on the degree of twist. Depending on the softness of the matrix and the degree of twist, it was thought that a fibre bundle would be able to shift to compensate for stretch in the upper bending radius with the tendency to contract in the inner bending radius. However, attempting to twist the material led to the second observed phenomenon, which was decompaction of the material at regular intervals along the length of the sample. Still, through a combination of twisting and bending while keeping tension on a sample, it was possible to bend the sample with a somewhat constant curvature. Because of this, the method of pre-twisting a sample to aid in bending was to be considered later, as discussed in

Chapter 7.

With the stiffness reduction of the matrix at elevated temperatures seemingly complicating the material's application for forming experiments, low temperature experiments were thought to help circumvent this issue. This was because they relied on a retention of the matrix's stiffness while permanently deforming the material through a process known as creep. Due to the molecular nature of thermoplastic resins, the individual polymer chains within the material are able to slide when subjected to a constant load for a prolonged period of time, especially at higher temperatures. Although slow, this process leads to stress relaxation by permanent deformation of the material. The tests performed were somewhat able to capture this phenomenon. Although the possible initial deformation was limited, with kinking still occurring at temperatures of 70 °C and above, some samples could be created with some degree of permanent curvature and no observed kinking. Although the concept was abandoned due to the apparent limitations of the method (that is required time, possible maximum deformation and the degree of springback after release of the load) it may still be worth considering in the future with combined loading of the sample (like bending of the sample under pre-tension).

5.6 Recommendations

The initial experiments described in this chapter aided in characterising the carbon-Elium composite material and providing valuable information for the welding and forming experiments that were to be performed. As these experiments, like the selected base material, were used as a means to an end, they were not the main focus of research. Still, these kind of experiments would provide valuable information when performed on other selections of materials for use in the iso-truss as well, so it is important to discuss recommendations for these tests.

First of all, in order to establish a better test base and to obtain a more thorough understanding of the material, all tests should be repeated with different test conditions. This way, it can be investigated if the phenomena observed are actually consistent throughout the experiments, while new phenomena may also present themselves. Secondly, samples for the experiments should be better prepared so that this process does not influence the test significantly. Other process-specific recommendations are discussed in the following paragraphs.

For the SEM pictures, the process of test repetition is relatively straightforward: Simply investigate more samples under a variety of cross-sectional angles and magnifications, to obtain a clear understanding of the material distribution within the composite. From this, it should also be possible to estimate the fibre, matrix and void volume fractions of the composite by post-processing of the pictures. Furthermore, a clear map should be created to indicate where exactly the material is being inspected within the cross-section. When preparing the samples, care should be taken to clean the samples properly to prevent contamination and to cut without disturbing the material inside the composite. The preparation process should not lead to a significant increase in temperature within the sample, as this might allow for deformation and perhaps even evaporation on a microscopic scale.

For the TGA, repetition is key in determining the characteristics of the material, especially the fibre fraction, as only two tests could be performed in the scope of this thesis. In addition to this, preparing the samples should be done by taking the same precautions as for the SEM

pictures, as a significant temperature increase may influence the results. More importantly however, it would be interesting to perform the TGA under a normal atmosphere instead of the nitrogen environment that was used for the experiments. Some papers report that the degradation of this particular resin is different in oxygen-rich environments as compared to a nitrogen environment, so it would be important to provide a side-by-side comparison.

While the DSC experiments provided several interesting insights into the characteristics of the material, more tests should be performed in order to obtain a clear understanding of all the different phenomena that were observed. Before these tests are to be conducted however, the preparation of the samples would have to be improved in order to prevent contamination and influence to the thermal history of the material. After this improvement, the experiments should be repeated in their current form to see if this process affected the results. It is expected however that the endothermic and exothermic peaks would still be observed. As it was observed during the TGA analysis that weight loss occurred at these temperatures, the samples should be re-weighed before the second heating cycle. This is because the heat flow for this cycle was normalised with respect to the original weight, leading to the observed shift as explained by a troubleshooting guide released by TA Instruments [38].

For the DMA experiments, different loading cycles could be assessed. Again, repetition is key, although it would also be interesting to continue the same tests to higher temperatures as these temperatures were recommended for welding.

Finally, more oven tests can be performed under a variety of loading conditions to try to find ways to prevent the observed phenomena from occurring. The key principles that are believed to help accomplish this are outside support and (fibre) pre-tension. An outer support over the length of a composite sample like a (flexible) tube is thought to help prevent fibre bundles from kinking outwards and from decompacting during twisting, while pre-tension could prevent fibre bundles from being loaded in compression during bending. It would be interesting to pursue the design of a test setup to investigate these methods. Additionally, more experiments to assess the feasibility of employing creep to form the samples should also be investigated.

Chapter 6

Welding Demonstration

This chapter focuses on the design process for the demonstration of joining techniques for iso-truss representative intersections. This demonstration can be divided into several phases: First, the welding test presented in Section 4.3.2 was designed in more detail, focusing on sample configuration and welding setup, as discussed in Section 6.1. Section 6.2 focuses on the production of welding samples for physical testing, while Section 6.3 presents the results of these physical tests. Finally, these results are discussed in Section 6.4, together with recommendations for future research.

6.1 Welding Test Design

With several welding options being considered as part of the scope of this thesis, different setups were designed for the most likely suitable techniques. The first most likely suitable welding method considered was ultrasonic welding. After this failed to provide promising results, heated moulds were considered the next best alternative. While other welding options would likely have been suitable as well, it was decided to focus on the use of heated moulds as it provided the most versatility. This section focuses on the test approach for both welding methods considered, and why one was chosen over the other.

6.1.1 Sample Configuration Design

Before designing the welding setups, a standard sample shape and configuration(s) had to be established to be able to easily compare different samples. With a sample consisting of one straight vertical member (representative of a longitudinal member in the iso-truss) and two straight diagonal members (representative of two helical members intersecting the longitudinal one), there are several parameters that define the node-to-node distance, as can be seen in Figure 6.1. These parameters are the helical pitch (l_p) and the circumferential node-to-node distance (l_c), the latter of which can be calculated from the outer diameter of the iso-truss and the number of longitudinal members through $l_c = \frac{\pi D}{N_l}$.

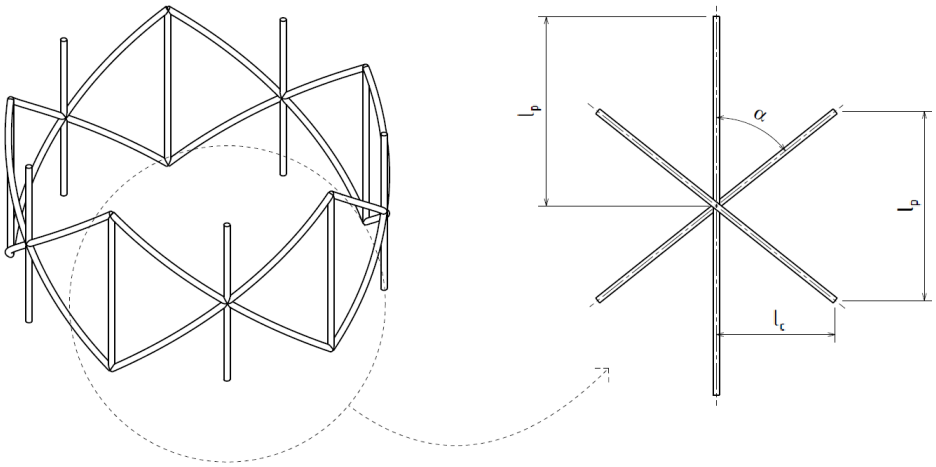

Figure 6.1: Left: a unit section of an iso-truss, right: an unfolded unit node

With both the helical pitch and the outer diameter being considered 'variable' within the scope of this thesis, the larger value for both was taken. With this, a standard sample is defined by the lengths of the different members, and the angle that the helical members make with the longitudinal member:

$$L_l = 2l_p = 300mm \tag{6.1a}$$

$$\alpha = \tan^{-1}\left(\frac{2\pi D}{N_l l_p}\right) \approx 51.5° \tag{6.1b}$$

$$L_h = 2\frac{\pi D}{N_l \sin\alpha} \approx 241mm \tag{6.1c}$$

While the actual length of the members would depend on the type of physical test to be performed, the angle was kept fixed for the scope of the experiments. On top of these basic parameters, the previously discussed offset parameter, introduced to avoid three members intersecting at once, was set to zero. With this, different intersection configurations could be considered: One where a longitudinal member would be positioned in between two helical members, and one where two helical members would cross over (or under) a longitudinal member. The first configuration was considered under the assumption that it would provide better support in the buckling behaviour of a longitudinal member: the member would always have interference contact with one of the helical members regardless of the direction in which it would buckle. On the other hand, in case heating could only be provided on one side of the intersection, like in the case of ultrasonic welding, it was deemed interesting to consider the second configuration in which both helical members would be on the same side of the longitudinal member. This way, a more asymmetric heating distribution might be more effectively employed.

An additional parameter to be introduced is a compaction factor for the helical members. This is done under the assumption that, to maximise contact between the circular-shaped members, the members would have to be flattened. The compaction factor is defined as a number between 0 and 1 that is multiplied with the original thickness of a helical member.

This would be used later in determining the required travel of the ultrasonic welding device, as well as the shape of the moulds used for 'hot-plate' welding.

6.1.2 Ultrasonic Heating

In ultrasonic welding, constraining the parts to be welded properly is crucial. This is because the welding process needs to generate enough localised vibration between the parts to generate the heat required for the welding. The less constrained the parts are, the more energy is lost. Additionally, in order to be able to weld circular cross-sections on top of each other, alignment of the welding device and the members to be welded is crucial. The tendency for the welding device 'slipping' when trying to weld members ruled out the use of handheld welding devices. Instead, a welding setup was designed for use with an Aeson D3000 ultrasonic welding machine present in DASML. This allowed the use of controlled force application and ultrasonic vibration strength, as well as controlled travel of the welding device. What was left up for design was a fixture to hold the members in the correct orientation for welding, and a mould surface to consolidate against.

As a first test, a simple 3D printable fixture was designed, taking into account the established value for α in Equation 6.1b. This fixture would be printed on a Formlabs Form 2 stereolithography (SLA) printer, which left enough design freedom while it also allowed for relatively high-strength and tough parts. This fixture would then fit around an aluminium mould surface that could be fixed to the machine. This aluminium mould was left as a flat surface for the first iteration. The fixture was designed such that it would allow downwards travel of the members so they could be consolidated, while mostly constraining horizontal movement and vertical movement upwards. This test setup can be seen in Figure 6.2.

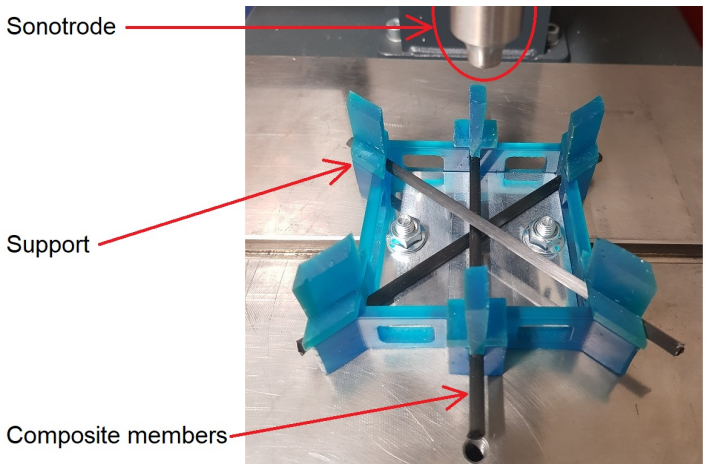

Figure 6.2: Overview of the ultrasonic welding test setup

After trying to create several samples with this method, it became clear that it had its limitations. First of all, it proved difficult to weld composite parts with a fibre volume content this high. This would not have been a definitive deal-breaker for this method, as this could be solved through the use of either a different material or energy directors in between the members (basically thermoplastic foils). However, other issues became clear which proved the limitations of this welding method for application in this setup. For example,

a certain force was needed to establish intimate contact between the welding sonotrode and the members, which would provide optimal vibrational energy transfer. However, because of the very limited initial contact area between members and the sonotrode due to the circular shape of the members, this force could not be carried by the members without them cracking or splitting. Additionally, while the area to be joined could have likely reached the temperature required for the matrix material to soften enough, the portion of the member just outside the sonotrode area could not. This area proved crucial however as it became a transition between the members flattened under the sonotrode and the undisturbed (circular) portion of the members outside the weld area. Since this deformation was not possible under the temperature conditions that could be reached, the material would always split just outside the weld area. While it was proposed that the use of a deliberate (vibrational) energy loss could lead to a better temperature distribution, it was determined that these conditions could not be reliably created, nor replicated. It was therefore concluded that ultrasonic welding could not be easily adapted for use in creating iso-truss intersections, or at least within the scope of this thesis.

6.1.3 Heated Moulds

With ultrasonic welding proving difficult for use in this thesis, hot-plate welding was considered as the next best alternative. Though not as time-efficient as ultrasonic welding, hot-plate welding is more versatile as the shape of the 'plates', heat generation and consolidation force application can all be independently changed. Instead of generating heat directly at the joint interface, heat is introduced into the members (and later at the joint interface) through contact with a hotter mould surface. Even though this process is slower, the additional time would allow a more throughout heat distribution within the members, allowing them to adapt their shape more easily, something which proved to be crucial for this kind of joint.

For the design of the heated moulds, aluminium was chosen for its ease in manufacturing and excellent heat conduction. However, with the temperature range for welding in mind (a maximum of 200 °C), the coefficient of linear expansion for aluminium had to be taken into account in the design, as it is relatively large (about 24×10^{-6} m/m°C as opposed to 10×10^{-6} m/m°C for steel for example). Two block-like mould halves were designed (one for above and one for below the sample) with a relatively small floor space of 60 mm × 60 mm. The mould halves were made thick enough to offer a reasonable heat capacity, as the temperature of the mould surface in contact with the samples should not drop significantly during welding. Of course, the more heat capacity the moulds would have, the longer it would take them to heat up, so a mould thickness of 20 mm was chosen as a compromise between temperature stability and heating time.

As for the shape of the moulds, grooves were made in both mould halves to dictate the shapes of the members. These grooves were designed in such a way that, by moving the moulds closer together, pressure (and heat) would be applied to the middle of the members only. This was done by elevating the bottom of the groove in the middle area of both helical members. The amount of local elevation was dictated by the compaction factor, which was chosen to be 0.75 as a first iteration (based on the expected possible degree of flattening of a helical member). To make sure that the moulds would be aligned during compaction, guiding pins were used. Finally, to allow for the use of wedges in case the moulds would get stuck together, some

openings were left on the outer perimeter of the blocks. The final design was sent to DEMO for production, the result of which can be seen in Figure 6.3.

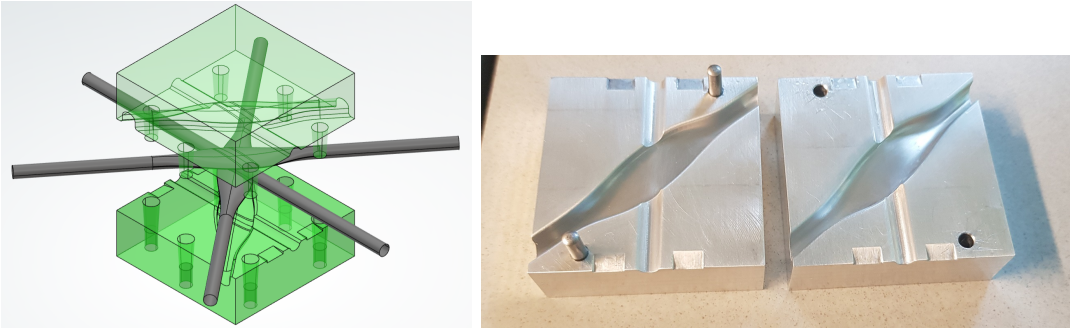

(a) Final design in CATIA **(b)** Moulds produced by DEMO

Figure 6.3: Overview of the moulds used for testing intersection welding

With the moulds complete, experimental samples could be made to get acquainted with the production process and its limitations. These samples were cut from the composite rods in lengths of about 150 mm to maximise material use. These experimental intersection samples were labelled as X.[sample number].

Initial samples (X.1-X.9) were made by heating up the mould halves in an oven, their temperature monitored by use of one thermocouple for each half. They were then taken out and, with the rods positioned by hand in between the moulds, were clamped together using a screw-driven glue clamp. In the first few samples it became clear that, while deformation of the helical members was significantly easier, the resulting joint was very fragile, with members separating easily. It was believed that this was due to the high fibre volume content of the material, so X.8 and X.9 were the first samples that made use of plastic foil in between the members to provide more thermoplastic resin for bonding. Due to its immediate availability, polyethylene terephthalate glycol (PETG) foil was used for this, even though its softening temperature was higher than that of the matrix material. Intersections made using this principle proved significantly stronger, though they were still relatively fragile.

For later samples, it was decided to make use of weights to consolidate the members, as the clamps proved difficult to operate: The clamps provided no real way of measuring the applied clamping force easily and the clamps often caused the moulds to align poorly, leading to damage in the alignment pins. Other than this improvement, a new alignment tool was made which would resist the temperature of the moulds. This alignment tool was made from a silicon resin, which was cast into a PLA 3D printed mould. This led to far better alignment of the members.

Another major improvement was the incorporation of a hot-plate heating station and soldering iron for heating the moulds, visualised in Figure 6.4. With this method, the lower mould half could be heated up in several minutes to the required testing temperature. The heating station featured a probe which could measure the temperature inside the mould block and use it to control the heating output. The upper mould half could be heated separately using a soldering iron which fit inside a hole in the block, heating it up through contact. While this process was slower and not directly controlled, testing temperatures in excess of 200 °C could still be reached this way. Using this setup, heating could be maintained and controlled

throughout the production of a sample.

Figure 6.4: Overview of the heating station used for producing intersection test samples

After continued testing and purely qualitative assessment of the bond strength, it was decided to replace the PETG foil by poly-methylmethacrylate (PMMA) foil from sample X.15 onwards. This was done because of its chemical similarity to the composite matrix and its similar softening temperature, both of which were thought to improve the bond strength. As this foil was not directly available, it was decided that a self-made foil would provide a decent first indication of the material's use. This piece of foil was made by compressing a scrap block of acrylic/PMMA in a thermoplastic press at 200 °C. The resulting foil, still transparent, was roughly 0.6 mm thick in the centre, tapering off towards the outside. Due to the way in which this foil was made, it was not stress-free, showing the tendency to thicken when heated far above T_g. While not necessarily a desired effect, it was hypothesised that this could be beneficial for the bond, as the foil would likely be pressed more into the members due to its own internal pressure.

Samples made using the PMMA foil proved significantly stronger than the ones made before. Compared to previous samples, separating the members of the intersection caused fibres to break out of the composite, a sign that they likely adhered well to the foil. Samples X.15 and X.16 were used for experimentation with this new foil, while sample X.17 was the first to make use of the new welding station setup. After this proved successful, sample X.18 was made as a first intersection that could be prepared for physical testing, with corresponding member lengths. During later production, sample X.19 was used to test a method of preforming the members for later adhesive bonding, while X.20 and X.21 assessed the possibility of replacing the middle member by a 5 mm thick steel rod.

After ordering pure PMMA rod samples for use in winding, as will be later elaborated on in Section 7.2.3, several experimental intersection samples were made to be able to compare these against pultrusion based intersection. Initial samples X.22 and X.23 used at the same processing temperatures as previous samples showed an interesting phenomenon: The otherwise transparent rods were filled with gas bubbles, in the case of X.22 creating a vastly expanded intersection joint which filled up the full mould cavity. Lowering the processing temperature to in between 150 °C to 160 °C eliminated this phenomenon, creating fully transparent intersections X.24 and X.25. As a comparison, sample X.26 was made with a mould

temperature of 160 °C as well, but was consolidated at this temperature for far longer, around 15 min. The resulting intersection looked identical to sample X.22. These samples raised the question whether a similar phenomenon could be occurring in the carbon-Elium pultrusions, as the Elium resin was chemically similar to the PMMA material. This would be supported by the results from the TGA and DSC analysis discussed in Chapter 5.

An overview of the testing details of all samples can be found in Appendix A.1.

6.2 Welding Sample Production

After conceptualising a feasible intersection production method, obtaining an understanding of the process conditions and tweaking the process to obtain acceptable and somewhat repeatable results, the next step was producing samples for physical testing. This section elaborates on the production conditions for 20 of these samples, produced in testing batches of 5. Sample production included two steps: welding of the sample members under repeatable conditions, and then casting an epoxy frame around the sample which would be used for compression testing. Both these aspects are elaborated on in their respective subsections.

6.2.1 Compression Jig Design

A challenge in the physical testing of these kind of samples, is the way in which load is introduced into the individual members. In a tensile test for example, gripping the members properly is of extreme importance: Too loose and the grips will slip, too tight and one would damage the sample, leading to failure near the clamping area. In contrast, compression tests are relatively easy to perform, as load introduction is a result of interference contact. Additionally, based on the way in which a standard test sample is configured, it is relatively easy to change between an in-plane shear test and a buckling test of a welded sample when using compressive loading. This is illustrated in Figure 6.5 as discussed in the top level design. If a vertical member is not connected to the bottom of the testing clamp or jig, a compression load is in equilibrium with tension in the two diagonal members, loading the bond area in shear. On the other hand, by extending the vertical member to the bottom, a compression load will be reacted almost purely by the vertical member itself, up until the point where it will buckle.

With this, the only remaining challenges were how to grip the member ends effectively, and how to provide a platform for the introduction of load. Gripping should preferably not be on the end of a member, as this creates a dependency on the way and the accuracy with which a member is cut to size. Additionally, a testing jig should be able to accommodate different intersection configurations and some degree of misalignment of the members. As a simple solution to these challenges, it was decided to encase member ends in a cast epoxy frame. This frame would consist of two parts: A U-profile which created a direct connection between the diagonal member ends and the loading platform, and a small block around the top part of the middle member to act as load introduction, as can be seen in Figure 6.7.

For the production of this epoxy compression jig, a mould was designed. Requirements for this mould were that it should be able to accommodate a standard sample to be encased, and should make the processes of casting the epoxy and releasing the finished sample as

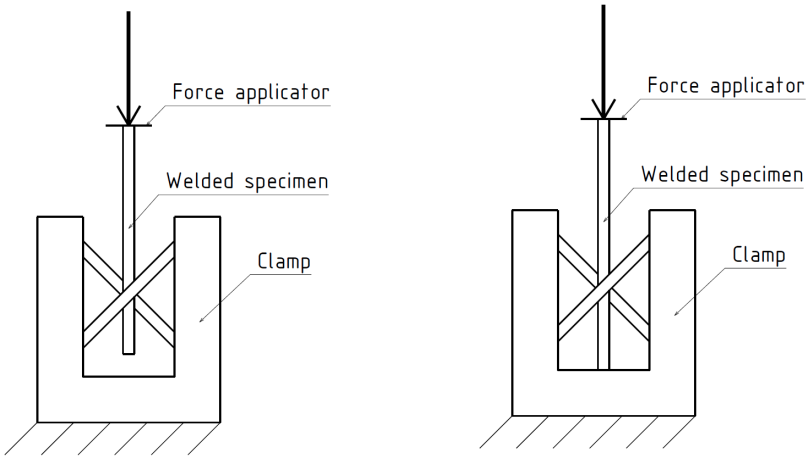

(a) Schematic representation of an in-plane shear test

(b) Schematic representation of a buckling test

Figure 6.5: Overview of the intersection test configurations

straightforward as possible, while allowing for multiple re-uses. The two most important surfaces of the mould were the ones defining the bottom and top of the sample jig. These two surfaces had to be parallel and at a defined distance with respect to each other.

The final design of this mould is shown in Figure 6.6. It features alignment for the sample, two Polyoxymethylene (POM) blocks with cavities for casting, removable aluminium back plates, draft angles for easier release of the final product and a releasing mechanism: After a sample would be cast, the back plate could be removed and screwed back with wooden strips between the epoxy product and the plate, pushing the finished product out of the mould without damaging the sample.

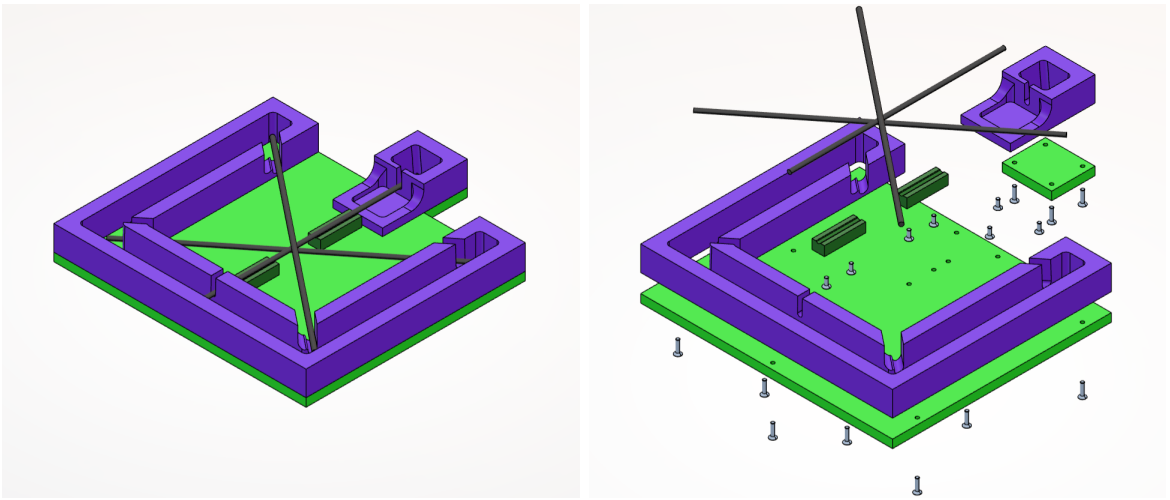

(a) Assembled

(b) Exploded view

Figure 6.6: Detailed design of the compression jig mould

6.2.2 Sample Parameters and Production

Based on the production of experimental test samples, several process conditions were hypothesised to be of influence to the bond strength of welded samples. These conditions were thought to be the temperature of the moulds during welding, the consolidation force, the consolidation time and dimension related aspects, like size and thickness of the PMMA foil in between the samples. Another aspect thought to be of influence, was whether the members to be welded were heated together with the moulds, or placed after heating up the moulds. With the process described in Section 6.1.3 and shown in Figure 6.4, it was shown that most of these process conditions could be accurately monitored and/or controlled.

It should be noted that, because of the limited sample size possible within the desired time frame, only a few different process combinations could be tested with a limited number of repetitions (2 or 3). By producing samples in batches of 5, test conditions could be tweaked based on the physical test results. For example, after it appeared that a foil size of 10 mm × 10 mm did not fully cover the contact area between members, it was decided to continue with a foil size of 15 mm × 15 mm for the remainder of the samples. Additionally, some samples made use of an epoxy adhesive (Araldite 2012) for creation of the joint, after pre-forming the members separately.

Two main types of samples were produced, denoted by A and B. Type A was used for in-plane shear testing of the weld strength, featuring a shorter longitudinal member that was not fixed at the bottom of the testing jig. The type B samples featured a longitudinal member that would be connected to both the top and bottom of the test fixture, creating a simple buckling test when loaded in compression. Additionally, one sample was produced using a metal rod as longitudinal member. This was thought to give additional insight in the buckling behaviour of a sample as it forced failure at a helical member. This test type was denoted by the letter C.

Table 6.1: Overview of intersection sample parameters (* = rewelded)

#	**Type**	T_W (°C)	F_W (N)	**Foil size** (mm)	**Pre-heated**
1	A	190	200	10x10	no
2	A	200	200	10x10	no
3	B	190	200	15x15	yes
4*	B	190	200	15x15	no
5	B	190	200	15x15	yes
6	A	190	200	15x15	yes
7	A	190	200	15x15	no
8	B	190	200	15x15	yes
9	B	190	200	15x15	no
10	B	190	200	Adhesive	yes
11	A	200	200	Adhesive	yes
12	A	200	200	Adhesive	no
13	B	200	200	15x15	yes
14	B	200	200	15x15	no
15	B	200	200	15x15	yes

16*	A	200	200	15x15	yes
17*	A	200	200	15x15	no
18	C	200	200	15x15	yes
19*	B	200	200	15x15	no
20	B	200	200	Adhesive	yes

6.2.3 Casting of Samples

After a sample had been produced, it was encased in an epoxy frame by using the previously discussed casting mould. Before the sample was placed, the mould parts would be cleaned, coated in release agent and assembled. The outside perimeter of the mould was then taped to eliminate leaks from in between the mould plate and the plastic (POM) block. In the meantime, the casting epoxy could be prepared (around 650 ml per sample, including a small margin for leaks). Since this casting epoxy is designed to be used in larger volumes, the curing time is relatively long when compared to film epoxies to limit the chance for thermal runaway. As well as being the most critical time limiter for the production of test samples, this aspect also meant that the resin would take longer to gel. This imposed a strict leak-tightness condition on the mould, as any significant leak would lead to a large loss of resin over a period of several hours. To meet this condition, gaps between the mould and the member ends were filled with hot glue, creating a solid barrier between the casting cavity and the outside, while allowing for differences in the alignment of diagonal members.

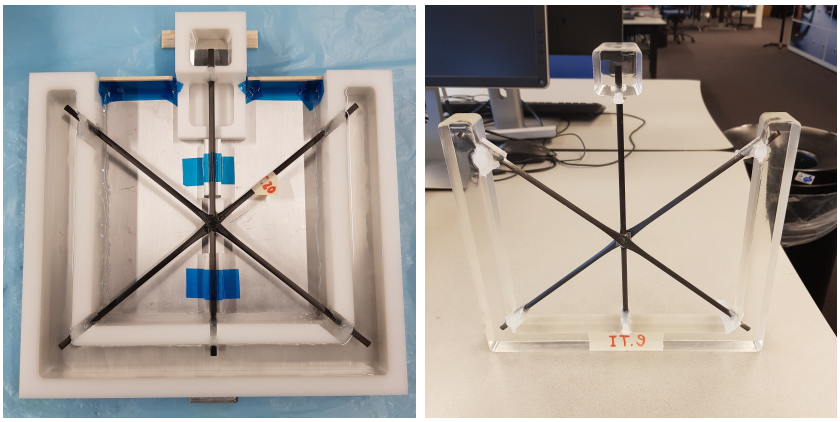

Figure 6.7: Two different samples during (left) and after casting (right)

With the sample prepared, the resin was gently poured inside the two cavities until a thickness of around 25 mm was reached. The epoxy was then left to gel and partially cure for at least 24 hours, after which final curing was achieved by placing the mould in an oven at 40 °C for at least 12 hours. This allowed 3 samples to be made in a single week, leaving the third sample to cure fully at room temperature over weekends.

After curing, the sample was carefully released from the mould, taking care not to load or peel the fragile bond. If member separation occurred, the members were rewelded by using the same moulds, consolidation weight and temperature as for the original process. The samples for which this had to be done are indicated in Table 6.1 by *.

6.3 Intersection Compression Testing

With every batch of samples produced, a physical test was set up for subsequent compression testing of the welded intersection. An overview of the methodology of these tests can be found in the next section. Subsequently, the results of these experiments are presented and discussed.

6.3.1 Methodology

All physical tests were conducted at DASML on displacement controlled ZwickRoell machines: A type Z010 with a maximum allowed load of 10 kN for most samples and a type Z020 (with a maximum load of 20 kN) for several samples where the maximum load was expected to be higher. In order to improve load measurement precision, a 1 kN load cell was used to measure the loads on most shear test samples, as the expected failure loads for these samples was considered to be relatively low. The standard load cell was used for the remainder of experiments. Samples would be secured to the lower base plate of the testing area using double-sided tape and a single large glue clamp to prevent samples from sliding within the plane of the base plate. All tests were displacement controlled: A maximum allowed displacement of 10 mm allowed for the capture of a variety of different failure modes in both the shear and buckling test samples. Although the initial deformation rate was set to $0.5\,\mathrm{mm\,min^{-1}}$, this rate was doubled after a sudden load reduction of 50% of the peak load was recorded. To provide visual information about the failure modes during the test, a recording phone held in place by a gimbal was positioned next to the sample. This would allow for better analysis of the failure modes in post-processing of the data. An initial separation of 295 mm between the base and the load cell would be established for every test. After initiating displacement of the base platform, the test would commence when a compressive pre-load of 10 N was reached on the sample.

To test the setup, experimental sample X.18 was used as a sacrificial intersection, similar to how it was used for demonstrating the casting process. As this was a buckling test sample, a Linear Variable Differential Transformer (LVDT) was used on this particular sample to record the out-of-plane deflection of the middle of the intersection during buckling. However, its use was omitted for subsequent samples, as it was determined that it did not provide any additional information on the failure behaviour in comparison to the effort required to set up and calibrate the device for every sample.

As intersections IT.1 and IT.2 were shear test samples (as defined in Figure 6.5a), where the failure load was considered relatively low, they were tested using the 1 kN load cell. The same was true for samples IT.6, IT.7, IT.11, IT.16 and IT.17. For sample IT.11, the maximum load exceeded the load cell safe rating slightly, so the standard 10 kN load cell was used for the similar sample IT.12. Samples IT.3, IT.4, IT.5, IT.8, IT.9, IT.10 and samples IT.12 up to IT.15 were all tested using the standard 10 kN load cell. As sample IT.18 was expected to be able to exceed this value, it was tested on the 20 kN Zwick together with IT.20, which was tested on the same day. Unfortunately, one of the intersecting members in sample IT.19 was observed to separate while clamping the sample, so it was rewelded later. As its production conditions were not notably different from other buckling samples, it was decided to leave this sample untested for presentation purposes.

6.3.2 Results

In-Plane Shear Tests

During the physical tests, a wide variety of maximum loads could be observed. These maximum loads varied between about 200 N for tests T.1 and T.2, to as much as 1.3 kN for test T.12. The load-displacement curve of a typical sample is shown in Figure 6.8, where different sharp peaks can be observed. For the other load-displacement graphs, the reader is referred to Appendix C.1. Interesting to observe was the sharp drop in load carrying capabilities after the first peak, usually the maximum load, which could be observed as separation from one of the diagonal supporting members. As can be seen from the sharpness of the peak, this failure occurred without any significant decrease in the stiffness slope beforehand. After this drop, the load would still increase for increasing displacement, although at a shallower slope, before slightly flattening and leading to the second sudden drop in load, observed as separation from the second diagonal member. Notably, the second peak was sometimes just as high or higher than the first, as was observed during tests T.6 and T.17. Some very slight load carrying capability could be observed beyond this second failure mode, sometimes leading to a third drop in the load. As an overview, the two peak loads for each shear test sample are presented in Table 6.2.

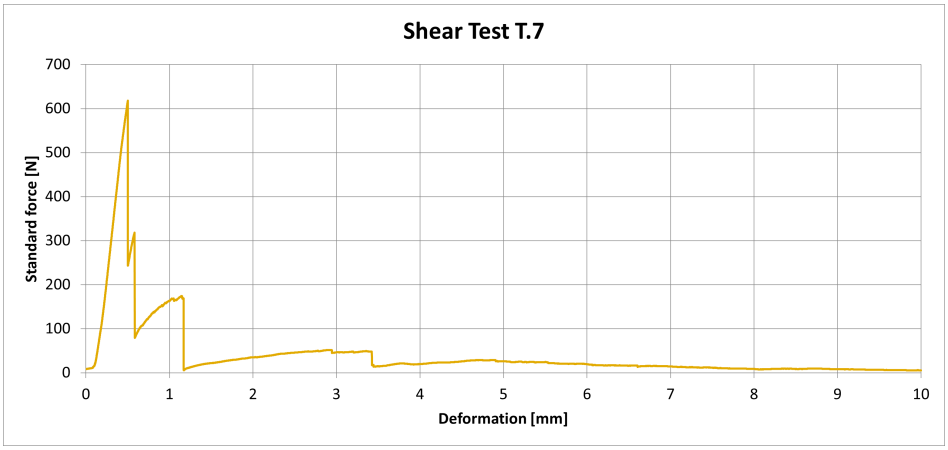

Figure 6.8: Load-displacement curve of a typical sample during an in-plane shear test

Table 6.2: Overview of the peak loads observed for the shear test samples

Test ID	Joint Type	Peak 1 [N]	Peak 2 [N]
T.1	10 mm foil	196	45
T.2	10 mm foil	204	38
T.6	15 mm foil	248	271
T.7	15 mm foil	618	174
T.11	Epoxy	1126	364
T.12	Epoxy	1344	326
T.16	15 mm foil	382	239
T.17	15 mm foil	244	240

Although these loads provided some insight into the failure characteristics of the welded joints, more information could be obtained by looking at the fracture surface. Here, a striking observation was made: The PMMA foil and epoxy adhesive both remained mostly intact and remained adhered to the middle member. Instead, fibres were observed to have broken out of the diagonal members, adhering to the foil/epoxy and leaving a fracture surface on the diagonal members that could be described as 'fuzzy', with fibres protruding from the composite. A close-up of the PMMA side of the fracture surface can be seen in Figure 6.9.

Figure 6.9: Close-up of the failure area in a shear test sample

Buckling Tests

For the buckling tests, significantly less variety was observed in the load peaks as compared to the shear tests, with loads ranging between 2.1 kN to 3.2 kN (excluding sample IT.18 with the steel middle member). Instead, many more different failure modes were observed for these samples, occurring in a variety of orders. The load-displacement graph of a typical buckling test sample is presented in Figure 6.10.

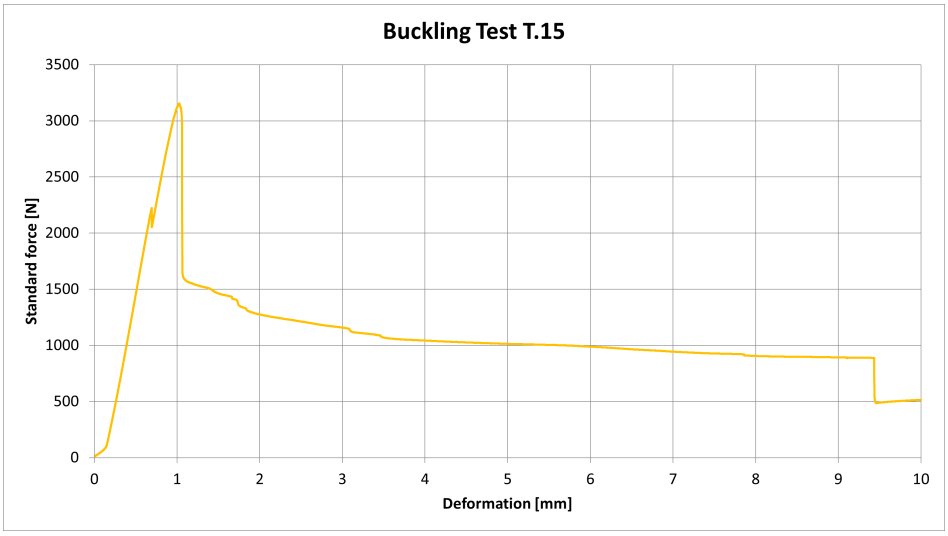

Figure 6.10: Load-displacement curve of a typical sample during a buckling test

This graph shows several notable phenomena that were observed across samples. In half of the samples, a slight decline in load would occur before the maximum load was reached.

However, this did not lead to a significant reduction in the slope of the curve. Load would continue to increase before suddenly dropping to around half its maximum value. The peaks that were observed before this drop were not as sharp as the ones observed during the shear tests, instead showing a sudden decrease and inflection in slope. The decrease in load would continue after this drop, showing another sudden drop in load for the samples that did not show the slight peak before the maximum, before stabilising at a somewhat constant load. A sample which clearly shows this behaviour is the sample with the steel rod: IT.18. While testing this sample, not one but two peaks could be observed far before the maximum load was reached. After reaching the maximum load, the load would decline more gradually, before stabilising at a constant load.

As an overview, the maximum load for each buckling test sample is presented in Table 6.3. For the other load-displacement graphs, the reader is referred to Appendix C.2.

Table 6.3: Overview of the peak load observed for the buckling test samples

Test ID	Joint Type	F_{max} [N]
T.3	15 mm foil	2460
T.4	15 mm foil	2215
T.5	15 mm foil	2333
T.8	15 mm foil	2433
T.9	15 mm foil	2268
T.10	Epoxy	2379
T.13	15 mm foil	2121
T.14	15 mm foil	2797
T.15	15 mm foil	3153
T.18	15 mm foil	3957
T.19	15 mm foil	-
T.20	Epoxy	2528

The most striking observation during these tests was the variety in failure modes, most of which occurred in the middle member. Some of the samples highlighting these modes are shown in Figure 6.11. For the middle member, failure could be classified as either kinking, like the kinking observed in previous tests, or splitting over a large portion of the length of the member either above or below the intersection. While most of the time, continued loading would lead to out-of-plane deflection of the middle member, another post-failure shape was rarely observed, as can be seen in Figure 6.11c. Here, continued loading after splitting of one end of the sample caused to other intact end to be wedged in between the two split ends, leading to a more symmetric shape of the middle member reminiscent of pure compression failure. Other than failure of the middle member, other types of failure observed were separation from one or both of the diagonal members and, very rarely, kinking of one of the diagonal members at large out-of-plane deflections of the middle member.

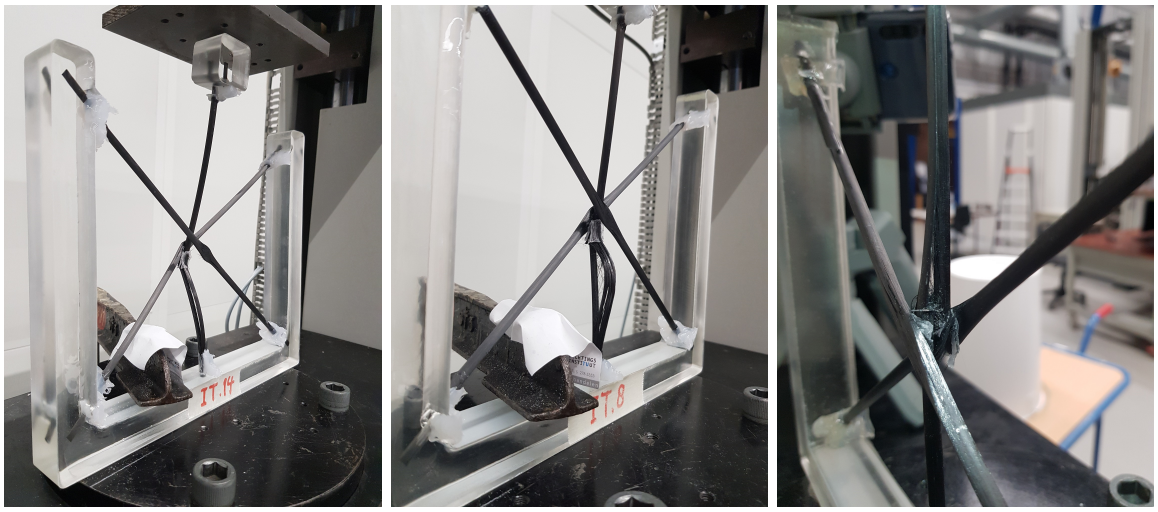

(a) Kinking and splitting **(b)** Extensive splitting **(c)** Symmetric compression

Figure 6.11: Representations of the observed failure modes

6.4 Discussion and Recommendations

After extensive experimentation with different concepts for the welding of intersections in an iso-truss structure, substantial progress was made in assessing the feasibility of this production aspect. This section aims to provide an overview of the lessons learned during this experimental phase, both in terms of production of the samples and in terms of physical test results.

6.4.1 Production

For the welding of intersections of circular cross-section iso-truss members, a production process had to be developed from the beginning, as a high degree of material deformation had to be taken into account.

Although the application of ultrasonic welding was initially considered as the most feasible method to create these intersections, it was quickly learned that it had limitations. Especially the lack of the ability to heat the transition from the weld area to the member's original shape proved to be the main limitation. While ultrasonic welding would be the fastest process to produce welded intersections, current sonotrodes are not designed for this kind of desired heat distribution. Attempting to weld the material lead to splitting of the members, partly because of the rigidity in the transition zone, but also because of the small initial contact area on which the sonotrode introduced the vibrations.

Heated mould welding on the other hand provided the possibility to increase the weld area to include the transition zone, while also allowing for differences in heat distribution due to adaptable contact between the members and the heated mould surface. The current mould surface design provided an advancing heat distribution: Upon contact between the members and the mould surface in the middle of the weld, the outer members would deform, allowing the contact front to advance through the transition zone. Although relatively slow when

compared to other welding processes, this provided the most controllable process tested so far. It should be noted that this method was designed to heat mostly the outer members of the intersection, as their shape was less critical compared to the middle member. It was believed that significant flattening of the middle member would reduce its resistance to buckling. Although the temperature of the moulds was measured and controlled throughout the welding process, the temperature distribution within the members remains unknown. As a recommendation to this test setup, the temperature of the middle member should be recorded during the welding process to make sure the member reaches an acceptable temperature for welding. If this temperature proves insufficient, the welding time or heat introduction into the members should be adapted to improve this.

Although the members were shown to deform well enough to create a sufficient area of intimate contact, estimated to be around $75\,\mathrm{mm}^2$, initial tests failed to create samples with an appropriate bond strength. This is because the material proved too dry to allow for reasonable diffusion of resin between the members. To combat this issue, the use of PMMA foil in between the sample proved quite effective. Although still a brittle connection sensitive to peel, as proven by some samples having to be rewelded, the connection proved strong enough to test. The use of adhesive, after shaping the members separately, was also considered as a workaround to the high V_f, and significantly improved both the shear and peel strength of the joint. However, only an Araldite 2012 epoxy adhesive could be tested, so it would be recommended to continue assessing the effectiveness of different adhesives, including an acrylic based adhesive that would be employed later.

From the welding experiments, it was observed that the material, especially the outer diagonal members of the intersection, deformed well under little load. Although fibre bundles generally shifted quite easily in this process, the low resin volume content lead to a small degree of splitting between the fibre bundles, with the resin unable to fill the created gaps. In order to allow the resin to flow for longer, the welding time could be easily controlled by varying the weight used to deform the members. This weight/load could be separated from the consolidation load used to hold the members in place after deforming to allow for diffusion of the resin. However, within the scope of this thesis, the moulds were designed to contact each other during consolidation. Because of this, the weight on top was distributed over both the members and the mould surface, leaving the final consolidation pressure to be determined in future research.

The casting mould proved to be an effective method of producing compression loading frames for the samples. Still, several aspects about its design could be improved. First of all, the casting process turned out to be the bottleneck in the production process for intersection test samples. The long curing time of the epoxy meant that only up to three samples could be prepared per week. Although this curing time could likely be shortened, while still leaving enough time for the resin to expel air introduced through the casting process, the most effective way to reduce this bottleneck would be to produce several instances of the casting mould. This way, several samples can be cast in parallel. During the casting process itself, other points of improvement were found. The mould did not perfectly seal between the aluminium base plate and the POM block above, allowing for a thin film of cured epoxy in between each cycle. While this film was removed as best as possible after each casting cycle, some pieces could not be removed entirely, preventing proper contact between the two mould halves on the subsequent cycle. This process gradually worsened the state of the casting mould, leaving a slightly thicker layer of resin after each cycle causing demoulding to become

more difficult as well. At some point, the force required to release the sample would lead to damage on either the mould or the sample. To prevent this in the future, a better sealing should be incorporated in the edges of the mould, for example by means of a rubber o-ring inside a groove along the contour of the POM block. Additionally, the draft angles in the POM block should be increased slightly to make demoulding easier in the future.

6.4.2 Physical Test Results

From the physical tests, more quantitative results of the intersection weld strength could be obtained. While the current welding strength is nowhere near optimal, the obtained load graphs showed promising results, while the observed failure modes showed a clear direction for future improvement.

From the tests, especially the shear tests, it was observed that existing damage in the samples proved detrimental to the bond strength. Because the shear test samples lacked support on both ends of the longitudinal member during demoulding, they were prone to peel during this process. On top of this, a large leak in the mould would also complicate the demoulding process, sometimes causing damage to the sample. Peeling along with separation of the joint occurred for sample IT.4 and later for samples IT.16, IT.17 and IT.19 due to a declining ability of the casting mould to release samples. Although the samples were rewelded, the resulting strength proved to have severely reduced: In the shear tests, samples IT.16 and IT.17 failed at loads lower than some of their counterparts. This was evident by the first failure peak, resulting from separation from one side of the intersection, sometimes being lower than the second, implying that the other side of the intersection could resist more than double the shear stress.

In-Plane Shear Tests

The most interesting characteristic to observe during the shear tests was that the intersection proved to be somewhat damage tolerant: Separation of a member would only occur between two members at a time, leaving the remaining member connection to resist around half of the peak load at larger vertical deflections before separating as well. Even after full separation, the local flattening of the vertical member allowed some small degree of mechanical interlocking, which could still resist a small percentage of the original failure load until this section of the member had been fully pushed through.

After inspecting the failure area of the intersection samples, it was concluded that failure during shear was almost exclusively within the adherend. This was evident by the fibre bundles visible on the PMMA foil surface after failure, which indicated that they were pulled out of the original composite. The surface of the composite in the joint area could be described as 'fuzzy', with dry fibres protruding from the material. This is in line with previous indications that the material is too dry for welding, as there is apparently not enough resin to prevent the fibres from breaking out of the composite. Alternatively, it could be another indication of a poor fibre-matrix interface.

The shear tests showed that it was possible to significantly improve the joint strength by changing certain process parameters. While welding temperature was not observed to significantly influence the test results, the size of the PMMA foil was shown to greatly improve

the bond strength. Of course, this could only be done up to a point. Tests T.1 and T.2 clearly showed that the 10 mm × 10 mm foil was smaller than the area of the members in contact, so 15 mm × 15 mm foil was used from that point on. While this lead to a significant improvement, perhaps the most impacting choice was to bond the samples using the epoxy adhesive. As can been seen from the results, the epoxy vastly improved the load carrying capabilities of the joint by up to a factor two. While this improvement can be related to the somewhat increased cross-sectional area of the joint from the hardened adhesive that seeped out from the sides, it is also believed that the epoxy compensated for the high fibre volume content by penetrating into the composite and stabilising the fibre bundles to an extent.

As already lightly touched upon before, the cross-sectional area of the joint was estimated in order to provide a better comparison between samples, and to provide an estimate for the shear strength as a stress instead of a load. To do this, the failure area of one of the samples was photographed. In the digital image, a screen ruler (which could count pixels) was used, first to measure the thickness of the vertical member, and second to measure the height and width of the failure area. As the thickness of the member was known, a scaling factor could be found in order to express the height and width of the failure area in mm. Assuming that the failure area was a perfect ellipse, its size was estimated by using the height and width as major and minor axis of the ellipse respectively. With this, the total cross-sectional area was estimated to be around 75 mm^2 (taking into account both sides) for most samples. For samples IT.1 and IT.2 a value of 50 mm^2 was estimated, while the adhesively bonded joints were estimated to have had a cross-sectional area of around 100 mm^2 due to the adhesive seeping out on the side of the joint. Although this provided a rough estimation of the maximum shear stress in the joint, a more precise area determination method should be used to obtain the stress in the future. The resulting estimated shear stresses can be found in Table 6.4. Here, the cross-sectional area is given as the sum of both supporting members. Because failure of the second diagonal member occurred after the middle member had separated from the first diagonal member, the second failure stress is estimated using half this cross-sectional area. Cases where the second failure stress was higher than the first are indicated in bold.

Table 6.4: Estimated maximum shear stresses of the shear test samples (* = rewelded)

Test ID	Joint Type	Area [mm^2]	F_{max_1} [N]	F_{max_2} [N]	τ_{est_1} [MPa]	τ_{est_2} [MPa]
T.1	10 mm foil	50	196	45	4	2
T.2	10 mm foil	50	204	38	4	2
T.6	15 mm foil	75	248	271	4	**7**
T.7	15 mm foil	75	618	174	8	5
T.11	Epoxy	100	1126	364	11	7
T.12	Epoxy	100	1344	326	13	7
T.16*	15 mm foil	75	382	239	5	**6**
T.17*	15 mm foil	75	244	240	3	**6**

Buckling Tests

While the shear tests provided somewhat consistent results between different samples, the buckling tests showed a variety of different failure modes, sometimes occurring in different

orders when compared between samples. No relation between the process conditions and the order of these failure modes could be found. The most striking observation was that, with the exception of sample IT.18 with the steel vertical member, the maximum loads were somewhat similar, regardless of the order of failure modes. Although sample IT.10 failed at a different vertical deflection with respect to the other buckling samples, this was most likely due to insufficient curing of the epoxy frame: During the test, which was conducted on the day after the sample had been demoulded, the frame could clearly be seen to deflect far more than in other samples. As the sample had not been cured in an oven, it was believed that the time between mixing the epoxy and testing was simply too short, leaving the epoxy frame only partially cured.

Contrary to the desired outcome, it was observed that buckling of the longitudinal member occurred in the first mode in every physical test. While intersections in an actual iso-truss are meant to increase the buckling mode of longitudinal members based on the number of intersections, the test results do not necessarily contradict this. In this buckling test, the upper and lower side of the longitudinal member were clamped inside the epoxy frame, in other words imposing a constraint on the member's rotation within this support. This imposed a higher boundary condition compared to the intersection itself, where the constraint could be seen as a hinge at best: Due to the limited shape stiffness of the diagonal members, out-of-plane deflection was still permitted within the middle of the test section, although it was likely somewhat more constrained. In an iso-truss of sufficient length, clamped boundary conditions of the longitudinal member are considered more as end-effects, while the diagonal members would likely exhibit a higher shape stiffness due to their helical shape.

Throughout the tests, a variety of failure modes were observed. These included 'buckling' of the vertical member (observed as kinking near the intersection), separation from one of the diagonal members (sometimes observed in multiple stages), splitting of the vertical member over a large portion of its length, and kinking of the remaining diagonal member as the buckled vertical member forced it into a three-point bend. Additionally, there were tests where the vertical member did not deflect out-of-plane significantly. In these tests, the vertical member would split along its length either above or below the intersection, causing it to be forced onto the remaining portion of the vertical member (visualised in Figure 6.11c).

The failure modes in the buckling experiments appeared to be somewhat independent of each other within the same test. Interestingly, buckling did not quite occur as general column buckling, but as kinking of one side of the vertical member, similar to the kinking observed in oven tests. This process appeared to be material dominated, which is likely why the maximum loads were similar regardless of joining conditions. In every test, this kinking was observed to be in the thinnest portion of the vertical member, that is within or just outside the intersection itself. Interestingly, separation from one of the diagonal members sometimes occurred before kinking of the vertical member, without affecting the load at which kinking occurred. This is likely because the diagonal member did not significantly contribute to the buckling strength. However, for the samples where separation could be observed before kinking, the kink would always occur on the separated side. It is believed that if the tensile strength of the intersection joint can be improved, the diagonal members could aid in preventing the vertical member from kinking, as they provide support on the outside of the member.

In post-buckling/kinking of the sample, the longitudinal member would usually split along its length due to the differences in stress on both sides of the cross-section. This was another

indication of the material's limited shear strength. It is believed that without the diagonal members, the vertical member would have lost any significant load carrying capabilities beyond this point. Instead, the remaining diagonal member, supporting the vertical member more through interfering contact than actually through the bond, would help stabilise it during continued loading. This would cause the diagonal member to be loaded in both tension and three-point bending, which rarely resulted in kinking of the member in its thinnest cross-section, as was observed in test T.5. An interesting experiment would be to construct a test sample consisting of only a vertical member, to provide a comparison for the intersection test against a baseline.

As a comparison to a certain baseline, the sample IT.18 with steel vertical member was thought to eliminate the splitting and kinking failure modes that were observed in vertical members, allowing for a more consistent post-buckling shape. In this test, both diagonal members were observed to separate before any significant out-of-plane deflection, likely due to limited adhesion to the steel member. However, with a maximum load of around 3.96 kN, the buckling load was still significantly higher than for other samples. This could be explained by the slightly higher stiffness of the material. For the composite, using the rule of mixtures for tensile modulus and assuming a fibre volume fraction of 0.7, the E modulus can be estimated to be $0.7 \cdot 230\,000\,\text{MPa} + 0.3 \cdot 3170\,\text{MPa} \approx 162\,\text{GPa}$ (based off of the given E modulus for both fibre and matrix materials). With an E modulus of 200 GPa, steel would be about 20% stiffer. Using these two stiffness values, the theoretical buckling load can actually be calculated for both samples, assuming they are constant in cross-section and that no diagonal members are used to support them. For the steel rod and the composite respectively, the buckling load can be estimated to be the following, assuming clamped conditions:

$$F_{buckling_s} = \frac{4\pi^2 E_s I}{L^2} = \frac{4\pi^2 \cdot 200\,000\,\text{MPa} \cdot \frac{\pi}{4}\left(\frac{5\,\text{mm}}{2}\right)^4}{(290\,\text{mm})^2} \approx 3900\,\text{N} \tag{6.2a}$$

$$F_{buckling_c} = \frac{4\pi^2 E_c I}{L^2} = \frac{4\pi^2 \cdot 162\,000\,\text{MPa} \cdot \frac{\pi}{4}\left(\frac{5\,\text{mm}}{2}\right)^4}{(290\,\text{mm})^2} \approx 3100\,\text{N} \tag{6.2b}$$

Strikingly, this closely matches the observed buckling load during test T.18 for the steel rod (3.96 kN), and the maximum observed buckling load for the composite, observed during test T.15 (3.15 kN). This indicates that the diagonal members did not prevent buckling by forcing it into a higher buckling mode, instead only providing some support in post-buckling.

In several of the tests, namely T.3 and T.13, failure was observed without significant out-of-plane deflection. These test samples were therefore classified as pure compression failures. Although the samples appeared to deflect out-of-plane initially after kinking followed by immediate splitting, kinking of the vertical member on the second split side would align it once more in the loading direction. In test T.3, the portion of the vertical member above the intersection was observed to split first, forcing the lower portion to wedge itself in between the two split ends. During test T.13, the opposite was observed. Progressive deformation led to continued splintering of either end of the vertical member, until the maximum deflection of the test was reached. Unfortunately, no relation could be found between the production conditions and the occurrence of this failure mode. Instead, it is assumed that it is related to differences in the pultrusion material.

Chapter 7

Helical Winding Demonstration

This chapter describes the detailed design process and testing phase for the Helical Winder Demonstrator described in Section 4.3.3. As the design presented in Chapter 4 was only conceptual, Section 7.1 elaborates on all the detailed aspects required for the production of this demonstrator. Section 7.2 presents the tests that were performed after the demonstrator was built. In Section 7.3, the results of these tests are discussed.

7.1 Winding Test Design

After discussing the conceptual design for the Helical Winder Demonstrator with involved parties, a detailed representation of the design could be made. This version would then later be prepared for production and assembly. This section highlights the decisions made during this process and how the current mechanical setup came to be.

7.1.1 Mechanical Setup

As a general design rule for the mechanical setup of the demonstrator, it was decided to limit the need for custom-made parts as much as possible. This way, the design of the demonstrator could be realised in as short a time as possible by simultaneously ordering off-the-shelf parts and machining the parts that could not be ordered. The off-the-shelf parts could be divided into several categories, which would later translate to the different suppliers for these items. The main categories were frame, drivetrain and miscellaneous (bearings, fittings etc.). For the frame of the device, it was decided to collaborate with Item Systems B.V. (ITEM), as they provided a vast array of high-tolerance, stiff, easily assemble-able and ready-to-order frame components in the form of aluminium profiles. Additionally, the headquarters of the Dutch distribution facility was located in close proximity to the faculty of Aerospace Engineering, making short-notice support and feedback possible. With this decision, the production-ready design of the demonstrator was based around standard ITEM profiles and fittings.

Compared to the conceptual design, several changes were made. First of all, to make the design simpler and easier to set up, the machine would be manually operated, in contrast to the initially envisioned motor control. With two dependent degrees of freedom in the system, being the rotational motion of one fixture end for the composite samples and the translational motion of the other fixture end, it was decided to make the former one the controlled degree of freedom. This way, with the samples in place, a controlled input could be given to the rotation angle, while the top fixture would be 'pulled down' to accommodate the height change of the samples wrapping around a central cylinder. Manual control of the rotational angle would be realised through use of a geared crank arm located on the side of the structure, connected to the central cylinder by use of belts. A gearing of 10:1 ensured a small input force would be enough to rotate the samples. Another design choice was made with regards to the support structure and guidance of the top platform. To provide a stiffer support for the torsional loads that would be generated between the top and bottom fixture, an external frame was preferred over the initially envisioned guiding shafts. With these decisions made, the design was split up into several sub-assemblies: The external frame, the bottom fixture, the top fixture, the central cylinder, the crank support structure and the drivetrain components for rotational control. As a comparison, both design iterations are visualised in Figure 7.1.

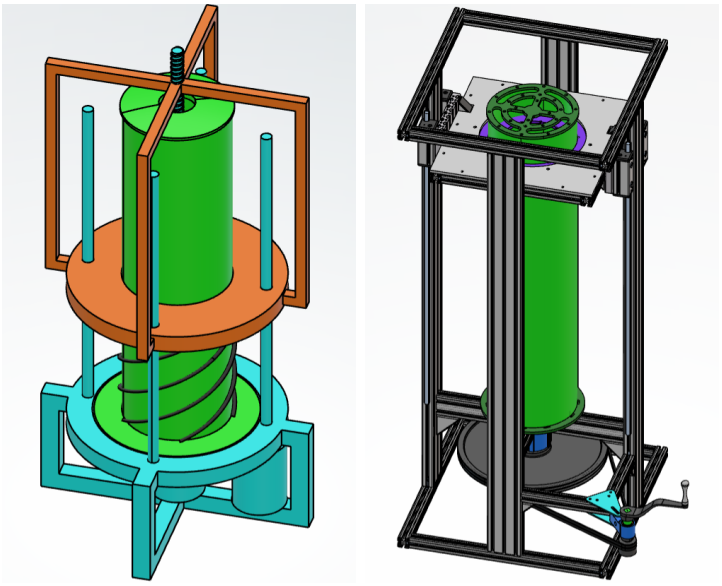

(a) Conceptual design in CATIA **(b)** Final detailed design in CATIA

Figure 7.1: Comparison between the two design phases of the Helical Winder Demonstrator

With all the design considerations and final designs of the components discussed in Appendix D, the final assembled design of the Helical Winder Demonstrator could be presented. In Figure 7.2, this design is visualised, showing the winding of five composite samples for a 300 mm helix with a 150 mm pitch between the different members.

Construction was carried out over a period of about two months and in close collaboration with DEMO. During this process, several changes and additions were made to the design, including adaptable counter weights for the top fixture, an upper bearing housing for the central cylinder and limit stops for the top fixture's travel. An overview of the completed mechanical setup, excluding the incorporation of heating, can be seen in Figure 7.3.

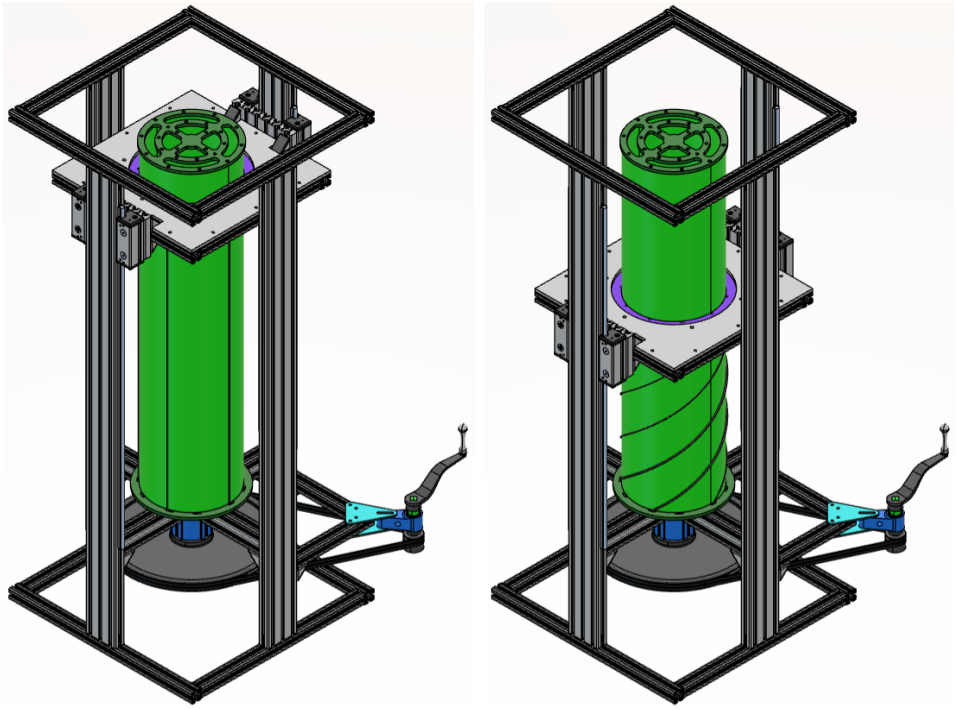

(a) Unwound configuration **(b)** Wound configuration

Figure 7.2: Final design overview of the Helical Winder Demonstrator

Figure 7.3: Completed setup of the Helical Winder Demonstrator, excluding heating method

7.1.2 Heating Methods

After the mechanical design for the Helical Winder Demonstrator was completed, methods for heating of the composite samples could be tested. Some options were eliminated from the beginning, like heating the complete setup in an oven, for the reason that the ITEM components and transmission systems were not designed to operate under these temperatures. Instead, heat had to be focused on the central cylinder, which should be isolated from as much of the structure as possible. This would provide a stable temperature in close proximity to the samples, so that they would not suffer from large temperature fluctuations during the winding process.

Concept 1: Heat Cage

To mimic the use of an oven for the setup, an initial idea was to construct a heat cage around the central cylinder. To prevent viewing obstruction, this cage was designed with glass plates in mind, as available transparent plastics like Acrylic and Polycarbonate would not withstand the required temperatures for the forming process. The use of glass plates limited the shape of the cage to a square box, to limit costs. One major challenge to the design of this cage however was the need for a telescoping mechanism, as the cage could only be connected to the top fixture to prevent interference with the bearing units during operation. The simplest option would be to construct a lower stationary half of the cage that would be connected to the lower fixture in the frame, and a larger perimeter upper half of the cage that would be suspended from the top fixture. However, a logistic problem visualised in Figure 7.4 meant that this could only be done if the maximum total distance between the bottom and top fixture was less than two times the maximum desired travel of the top fixture. Since this was not the case, maximum extension of the top fixture would lead to a gap between the two cage halves. While this could be solved by more telescoping mechanisms, it was deemed that this design became too complicated for effective use within the device, and that it would drastically limit accessibility to the inner components of the setup.

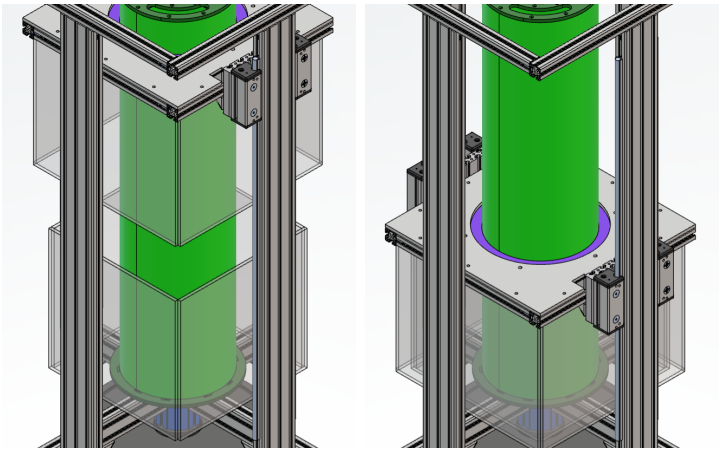

Figure 7.4: Logistic challenge to the heat cage design, taking into account the maximum (left) and minimum (right) height positions of the upper fixture

Concept 2: Cylinder Contact Heating

Another method considered for heating the composite samples was through contact with the central cylinder. As the cylinder was made of aluminium, had a large heat capacity and was hollow on the inside, a heating mechanism like silicon heating blankets against the inner surface could be used to reach the required temperatures. This way, a sample pressed against this heated surface would heat up through contact heating. However, heating in this case would be rather one-sided, and would rely on a small contact patch between the cylinder and the circular sample. In the worst case, this contact patch would increase from local softening of the samples, leading to undesired deformation, and perhaps cracking in the portion of the sample furthest away from the heating source. Still, the method of heating up the cylinder was in itself an idea to consider, if only to provide a stable temperature region in proximity to the samples.

To test the effectiveness of heating the cylinder using a silicon heating blanket, two tests were conducted. First, an aluminium plate of 10 mm thick was cut to the size of an available heating blanket. Several thermocouples were connected to this plate in order to monitor the temperature distribution. The plate was then vacuum bagged together with the blanket to ensure proper contact, as seen in Figure 7.5. During this test, temperatures in excess of $(160 \pm 3)\,°C$ were achieved on the opposite side of the plate. Even with the incorporation of breather as insulation, heat still radiated from the product. After turning off the blanket, a cooling rate of around $3\,°C\,min^{-1}$ was observed in the upper temperature region.

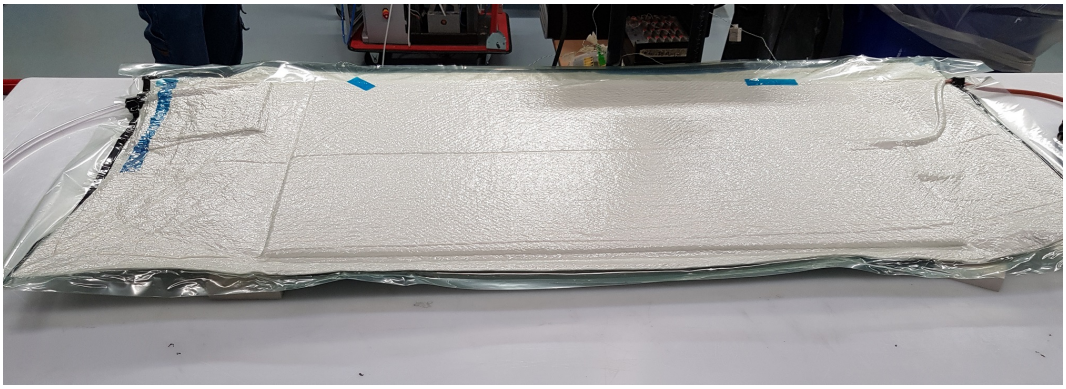

Figure 7.5: Vacuum bag containing aluminium plate with silicon heating blanket

As a second test, the same heating blanket was incorporated inside the 200 mm central cylinder, which was around the same size as the blanket in terms of height and (inner) circumference. Several options were considered to press the blanket against the cylinder, but as a first test, the simplest option was chosen: Wrap a smaller diameter aluminium tube in breather, creating a diameter larger than the inner diameter of the central cylinder, and slide it into the cylinder to press the blanket against the inner surface, while creating a barrier of still air to limit convection cooling. During the test, the cylinder was encased in a layer of breather, creating another barrier of still air around the outside of the cylinder. This test setup can be seen in Figure 7.6.

In this test, thermocouples could be used to measure interesting zones: The middle and end of the outer surface of the cylinder, the inside surface of the cylinder at the gap in the heat-

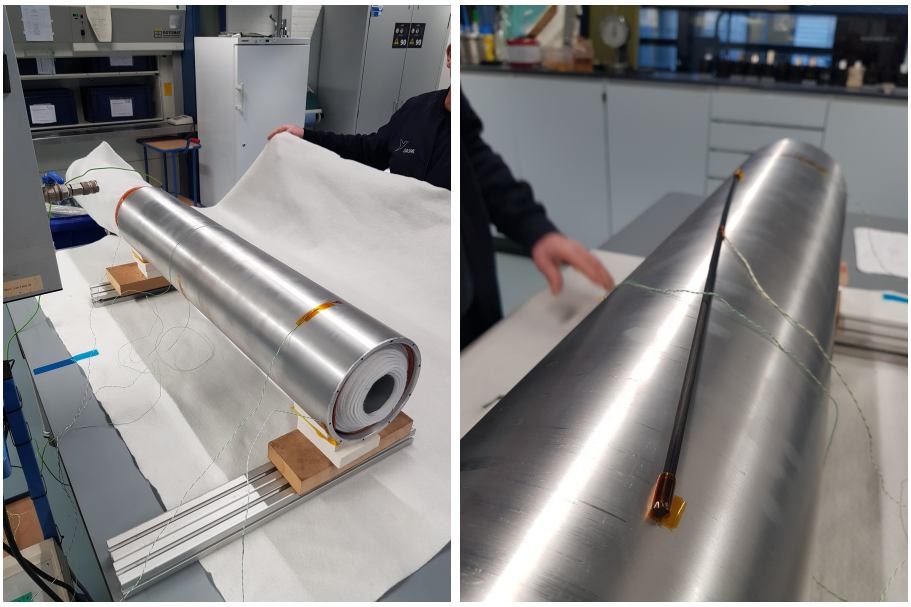

(a) Overview of the setup **(b)** Sample pressed against the cylinder

Figure 7.6: Silicon heater mat incorporation into 200 mm central cylinder

ing blanket and the surface of the heating blanket not in contact with the cylinder. From the readings of these thermocouples, heating rates of around $10\,^{\circ}\mathrm{C\,min^{-1}}$ were observed during the initial heating stage. As the heating blanket reached the set temperature far earlier than the cylinder, especially in the area not contacting the cylinder, heating rates slowed to about $0.5\,^{\circ}\mathrm{C\,min^{-1}}$ to $2.5\,^{\circ}\mathrm{C\,min^{-1}}$ while the blanket was in its temperature regulating phase, switching on and off at consistent time intervals. To prevent overheating of the blanket, readings from the thermocouple directly in contact with the blanket were kept under 180 °C. Even under these conditions, temperatures of $(135 \pm 5)\,^{\circ}\mathrm{C}$ could still be easily achieved. During this process, a composite sample was pressed against the cylinder at a shallow angle with respect to the cylinder axis to observe its forming behaviour under these conditions. From this sample, it was observed that deformation was fairly easy, with somewhat consistent radius of curvature throughout the length of the sample, though some small kinks still occurred.

Concept 3: Sample Ohmic Heating

As a more direct approach to heating the composite samples, a method similar to the heat generation in resistance welding was considered: Since the composite was based on unidirectional carbon fibre filaments, it was envisioned that these would conduct well enough for a steady current to be able to pass through, similar to the metal mesh for a resistance welding interface. The resistance against this current would generate heat within the material evenly over the length of the sample regardless of its total length. However, it was uncertain whether the conductivity of the sample would be enough to be able to pass the current over a reasonable distance.

To test this concept, a sample was connected to a current supply with crocodile clips, with several (insulated) thermocouples connected to different regions of the sample, as can be seen

in Figure 7.7. Additionally, a thermal camera was used to provide an indication of the heat distribution over the full length of the sample.

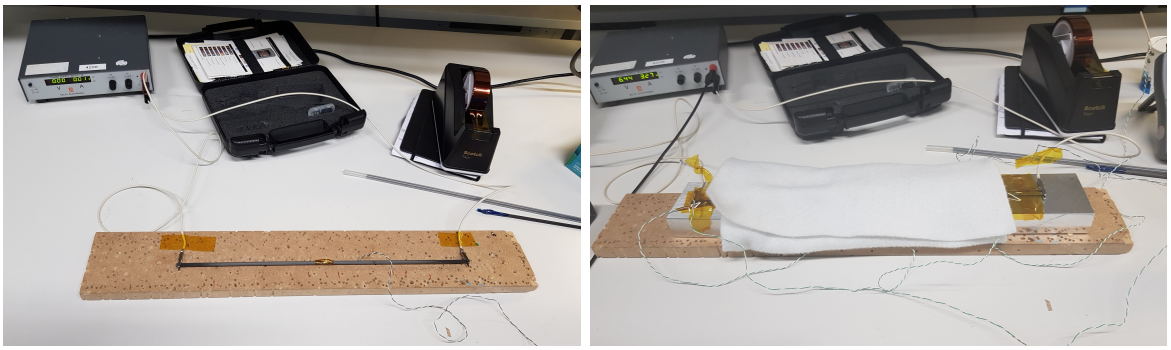

(a) Composite sample connection to a power supply **(b)** Heat management solution

Figure 7.7: Setup for the testing of Ohmic sample heating

As the current was increased, readings from the thermocouples were monitored to prevent overheating of the sample. As could be expected, heat generated within the sample peaked at the interface between the clips and the composite, though heat was also generated along the length of the sample. Temperatures were seen to stabilise for certain current readings, so the current was slowly increased until the center section of the sample was able to reach a temperature of around 120 °C, above the glass-transition temperature of the resin. At this temperature, readings of the thermocouples near the clips indicated temperatures around 190 °C, close to the degradation temperature of the resin, even after attempts to provide heat sinks for these areas. For this temperature, a relatively low power of around 22 W (a current of 3.4 A causing a voltage difference of 6.5 V) was needed for the 400 mm sample, indicating that this concept could be proven to be feasible.

However, incorporation of this method into the current design would likely prove difficult, as significant changes to the layout of the Helical Winder Demonstrator would have to be made. Firstly, the central cylinder would have to be electrically insulated to prevent current from leaking away through it. Technically, this could likely be achieved through use of a Kapton adhesive sheet, though economically this would be quite expensive to implement. Furthermore, the end supports for the composite samples would have to be completely redesigned, firstly to provide insulation and secondly to allow the samples to protrude on the other side of the support. This would allow the sample ends to be pre-processed for a more efficient current introduction while they would remain unstressed during the winding process. Finally, the sole use of this heating method would still prove ineffective, as heat could quickly dissipate from the samples due to their low thermal mass when compared to the central cylinder. Though combination of this heating method together with pre-heating of the central cylinder through use of a silicon heating blanket would still likely be possible, resistance heating was disregarded within the scope of this thesis for the reason that it would require too many design changes.

Final Heating Method

As a final solution to heating of the samples for use within this project, a combination of some of the methods discussed before was chosen: Heating up the central cylinder by use of a silicon heating blanket, while containing the heat generated by use of a simple heat cage around the samples. This way, the setup could be used without extensive modification. This heat cage was based on flexible aluminium ducting, for its telescoping abilities and direct availability in an appropriate diameter, even though it would limit visibility of the samples during the process. Suspended from the top fixture, the ducting created a small enclosed air chamber around the central cylinder, in which the samples would be heated up through convection. To further insulate this chamber and contain the heat, breather was placed around the aluminium ducting and around the portion of the central cylinder above the top fixture. To further insulate the cylinder, the top bearing housing was removed, and the cylinder was placed on top of struts (several nuts in between the bottom disc and the cylinder) to create a small offset. The final setup, excluding the breather, can be seen in Figure 7.8. It should be noted that due to the availability of silicon heating blanket sizes, only the 200 mm central cylinder could be used in this setup.

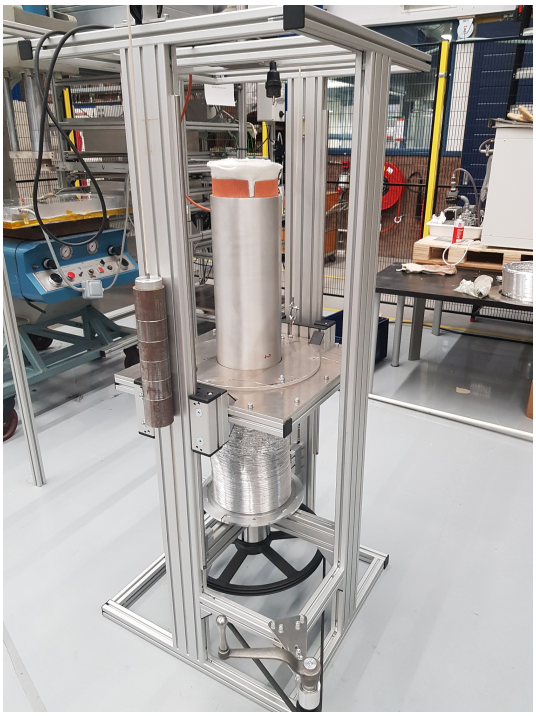

Figure 7.8: Setup of the Helical Winder Demonstrator incorporating the silicon blanket heating method

7.2 Winding Sample Production

With the setup for the Helical Winder Demonstrator completed, the testing phase could commence. Testing would be focused on the creation of helical samples, wound from straight

carbon-Elium composite samples using the demonstrator. First, it was investigated how the composite samples behaved in this setup, both at room temperature and above the glass-transition temperature. After the kinking phenomenon was observed in this setup as well, modifications were defined and implemented to circumvent these production difficulties.

7.2.1 Initial Tests

Deformation at Room Temperature

Before heating was incorporated, a decent indication of the behaviour of the samples could be obtained from deforming samples at room temperature. Though it was suspected that this deformation would be mostly elastic, it was believed that this test would provide a benchmark for the deformation process. For this test, five samples of roughly 500 mm were cut and then bundled together so they could be sanded to the same length. The samples were then positioned in the machine in the slots for clockwise helices. To ensure the upper fixture would move down together with the samples, two counterweights were removed to establish a constant compressive load on the samples. The winder was then operated to deform the samples, as can be seen in Figure 7.9. Safety barriers were incorporated around the device in case samples would fracture during the process, as this would likely release a significant amount of energy.

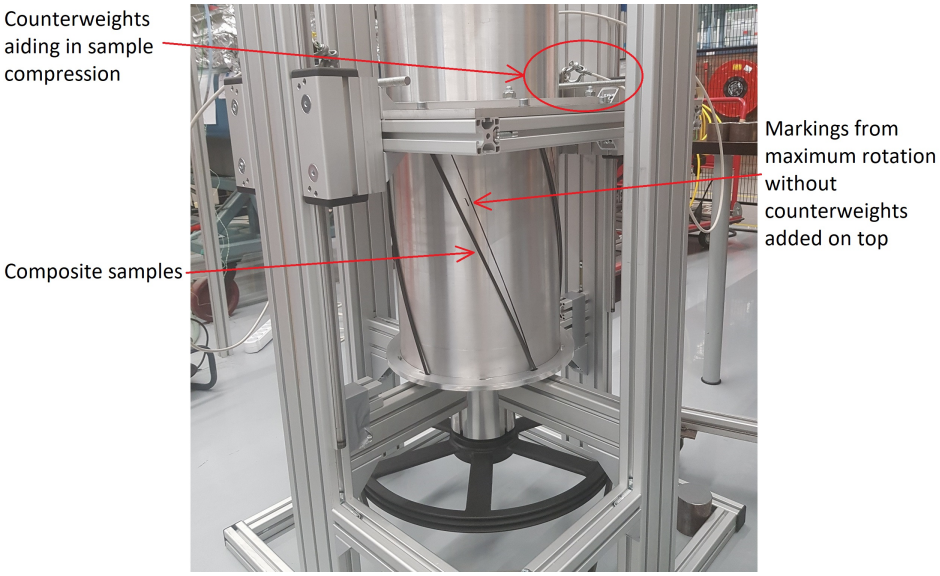

Figure 7.9: Room temperature (elastic) deformation of the composite samples

From the process, several aspects could be seen. First of all, the force required to deform the samples increased with increasing deformation as the samples were wound around the cylinder. At some point, this resistance became high enough to cause the V-belt to slip with respect to the crank. This was deemed as a welcome safety feature for the device: further deformation would be limited, preventing the samples from fracturing. The maximum rotational deformation in this counterweight setup was around 60° to 70°. Deformation was consistent over the entire length of the sample, and the samples contacted the cylinder over a

large portion of their length (being prevented from contacting the cylinder near their supports by the necessary offset in the slots). To be able to achieve further deformation, counterweights were removed one by one, until the weights were removed entirely and were positioned on top of the fixture to aid in the compressive force on the samples. It was seen that for the same rotation angle, an increase in compressive force caused the samples to bulge slightly from the cylinder. However, for every increase in compressive force, the samples could be rotated further by a small increment, causing them to contact the cylinder once more. After all weights were positioned, a final rotational deformation of around 100° was observed, translating to a helical pitch of around 300 mm. Interesting to note was that, after the samples were slowly wound back, they remained as straight as they were before the process, indicating a fully elastic deformation process.

Deformation at Elevated Temperatures

With a heating mechanism incorporated into the Helical Winder Demonstrator setup, the machine could be used to produce the first helical samples. For initial testing, composite samples of 500 mm in length were used, similar to the ones described in the previous subsection. To prepare the machine for this test, thermocouples were connected to different areas of interest within the device, as visualised in Figure 7.10. These areas of interest included the middle of three out of five composite samples (1-3), the outer surface of the central cylinder within the sample space (4), just outside the sample space (5) and close to the top (6), the portion of the silicon heating blanket protruding from the cylinder (7), the surface of the top (8) and bottom (9) supports for the samples and finally the ends of one of the composite samples (10-11).

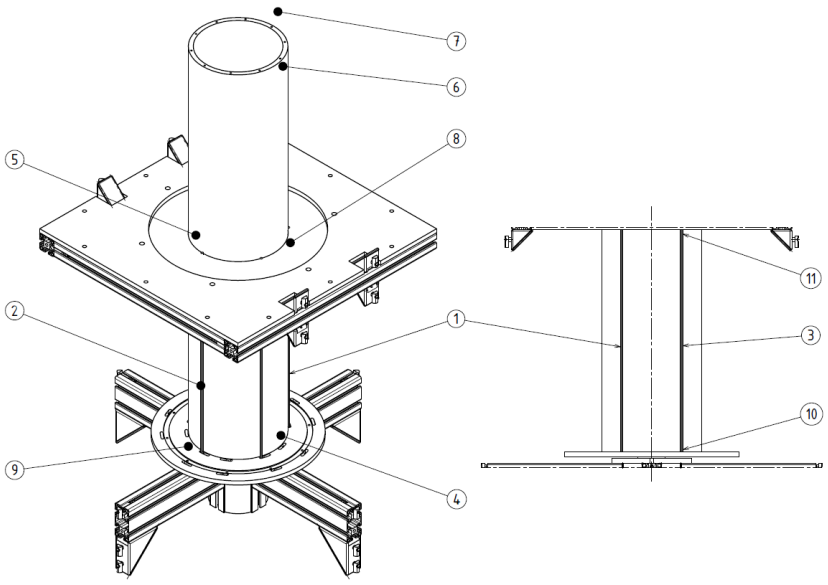

Figure 7.10: Layout of the thermocouples used for testing with the Helical Winder Demonstrator

Based on the oven experiments described in Section 5.5, it was decided to aim for a testing temperature in the range of 100 °C to 120 °C, as it was observed that a large decrease in stiffness of the matrix occurred in this temperature region. Before the samples reached the

desired testing temperature, they were rotated to a small extent so that they would contact the central cylinder, speeding their heating rate. When the desired temperature was reached, the samples were slowly rotated in increments of around 45° until a final rotation angle of around 180°, all while monitoring the temperatures recorded by the thermocouples.

Two tests were conducted in total, the results of which can be seen in Figure 7.11. Instead of neatly wrapping around the cylinder as expected, the samples kinked in several places along their length in order to curve around the cylinder. These results are consistent with the oven tests performed before, where the resin became too soft to support any kind of compressive loading without kinking. At this point it was deemed that the current setup of the Helical Winder Demonstrator would not prove feasible for the production of helical samples, as the samples could only be loaded in compression. To improve the results, two options were considered: pre-twisting the samples and modifying the setup. The first option is elaborated on further in the next subsection. The latter option was considered under the assumption that a tensile pre-load on the samples would be beneficial to their forming characteristics. To achieve this, the supports for the samples would have to be modified to allow the top platform to pull on the samples with an adjustable tensile load.

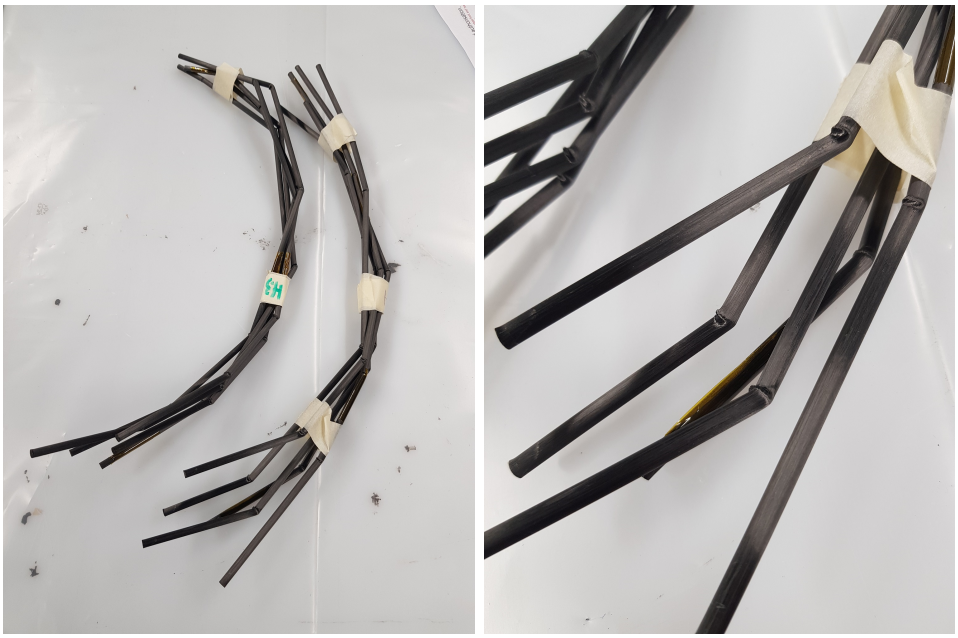

(a) Overview showing both tests **(b)** Close-up of the kinks

Figure 7.11: Result of initial helical testing

7.2.2 Concept of Pre-Twisting

Pre-twisting of the composite samples was considered under the assumption that a twisted rod would be less sensitive to buckling, similar to steel cables: By twisting the rods, fibre bundles would alternate between different circumferential positions along the length of the rod. When bending the rod, it was expected that a fibre bundle could then compensate length changes in both inner and outer radius of the bend. Tensile loads in the upper bending radius

and compressive loads in the lower bending radius could then cancel out, provided the fibre bundle would be able to shift along its length (depending on the degree of twist and the softness of the resin). This way, buckling at the inner radius of the bend could likely be prevented.

To test this concept, a setup was designed with several requirements in mind. First, the setup was to be made as much as possible from directly available parts, as its production time was limited due to the time frame of this thesis. Secondly, to heat up the rods effectively, the setup was to be used in a temperature controlled environment like an oven, meaning all components had to be able to withstand temperatures in excess of 150 °C. In terms of functional requirements, the setup was to allow for rotation of one sample end in one direction only to prevent the sample from springing back during the forming process. Furthermore, the sample should be able to be pre-loaded in tension in case this would prove beneficial to the forming process.

The final design of the setup can be seen in Figure 7.12. The design features an external frame made out of ITEM profiles, an upper support responsible for suspending a composite sample of roughly 30 cm in length, a 'floating' lower support featuring a one-way bearing to restrict the rotational degree of freedom of the sample, and a lower clamp to rotate the sample with and allow for the inclusion of weights underneath in order to preload the sample.

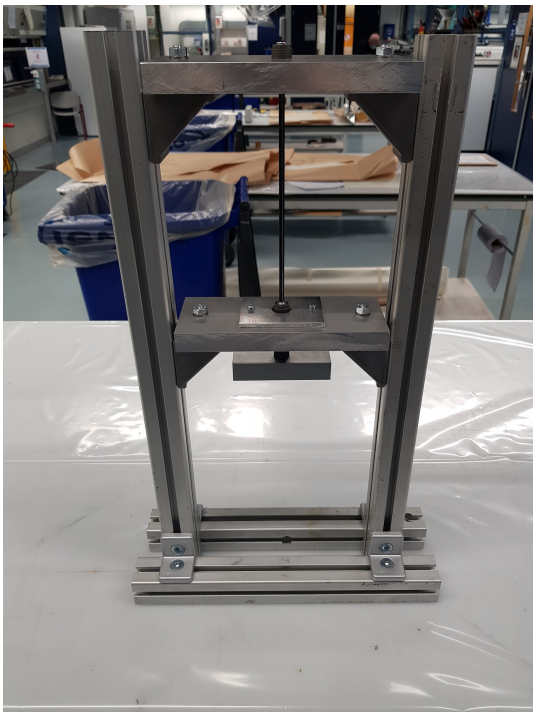

Figure 7.12: Overview of the twister setup, containing a 300 mm composite sample

Samples were prepared by using a white paint marker to mark the usable section of the rods (around 20 cm to leave enough space for the clamps and the lower block) and to paint a white line along the length as a reference for the degree of twist of the sample. Desired rotations were expressed in number of turns, with one full turn used as a reference for most samples. A temperature range was chosen between 120 °C (above glass transition) and 150 °C

(the maximum use temperature of the bearing). To limit the amount of samples, tests were performed at both extremes. For pre-loading the samples a similar philosophy was used: samples were tested either with no added weight, or with a weight of 5 kg. A final testing parameter was the amount of time the sample would be left in its loaded state, assuming creep had an effect on the final permanent deformation. To provide an estimation of the residual stress left in the sample after deforming it, a sample would be laid in an oven to raise its temperature to above glass transition, leaving the rod able to spring back. Samples would be labelled with the prefix "O." as a continuation to the oven tests discussed in Section 5.5.

The first sample, O.22, was formed at a temperature of 120 °C with no extra weight added to pre-load the sample. The rod was slowly rotated in the oven in one increment of 1.5 turns, then immediately taken out and left to cool down to room temperature before being released from the fixture. From this test, the sample showed consistent twist over the test length of the rod, with the exception of 3 or 4 small 'knots' similar to the ones observed in previous oven tests. These knots were several tenths of millimeters wider in diameter compared to the rest of the sample, and were spaced at somewhat consistent intervals. When put back in the oven at 120 °C, the sample rotated back to its original shape, with no significant deformation remaining in the rod. The knots could also not be identified visually anymore, seeming to have disappeared completely.

Further tests (samples O.23 to O.27) showed similar results. The knots still appeared even with the addition of weight and with rotating the sample in smaller increments. Still, significant improvement was obtained with regards to the residual stress left in the sample: Higher testing temperatures and longer loading times (with one sample left in the oven in its rotated state overnight), improved the final degree of twist left in the sample after being allowed to spring back. However, samples twisted by one turn would still only retain up to around 120°, roughly a third of their initial rotation.

Sample O.28 was rotated to 4 turns in increments of 45° to evaluate when and to what extent the knots would form. They were initially observed at a rotation angle of around 270°, and were seemingly not affected by the turning rate. Further deformation lead to an increase in diameter of these knots and decrease in spacing between them, with more knots forming along the length of the sample (around 11 total at the final rotation angle). Unlike the other samples, O.28 was not put back in an oven to release the stress in order to show the extremity of this phenomenon, as can be seen in Figure 7.13. An overview of other samples (after their second heat cycle) can be found in Appendix A.3. Sample O.29 remained untested.

Figure 7.13: Overview of the twisted sample O.28

With the knots considered as an undesirable side effect to pre-twisting the samples, it did not appear that they could be eliminated entirely. Furthermore, the ever-present springback of the samples also provided a limitation to the usefulness of this technique to try to limit kinking of the samples during the winding process. As this springback could not be eliminated, it was

hypothesised that there was a maximum permanent deformation that could be achieved with the composite material. To prove this, it was decided to compare these tests to a baseline using a similar thermoplastic material. As the Elium resin is acrylic in nature, some pure acrylic rods were subjected to similar tests. In these tests, it was observed that the bending behaviour of this material was far more consistent, with no kinking due to the absence of any significant buildup of stress. Furthermore, these rods showed little to no springback after their temperature was raised again to above the glass-transition temperature. For this reason, pure acrylic rods of the same diameter as the composite samples were ordered in order to conduct more tests using the setups designed for the initial samples.

7.2.3 Redesign of the Winding Tests

As a proof of principle, it was decided to test the feasibility of winding fully thermoplastic rods in the Helical Winder Demonstrator, as this would take any fibre and fibre-matrix interface effects out of the equation. The rods in question were chosen to be similar in diameter and chemical formulation to the carbon-Elium samples to ensure compatibility with the winding machine. Based on availability, a small testing batch of ten 2 m long Perspex (PMMA) rods with a diameter of 5 mm were ordered at DS-Groep Almere. These rods were also used as a reference for the welding tests discussed in Chapter 6.

Test Setup Redesign

Similar to the carbon-Elium samples, initial oven tests with the acrylic rods showed a significant loss of stiffness above the glass-transition temperature. While this would benefit formability of samples, it was expected that the current setup of the Helical Winder Demonstrator, which relied on a compressive load to retain the ends of the samples, could not work: the samples would simply not be able to carry any form of compressive loading without buckling. To solve this issue, changes to the design of the support plates were made so that they could retain the samples while also introducing a tensile load. This retention design, similar to the already present grooves in the support plate, would rely on interference to prevent the rods from slipping out of their support, while allowing for rotational freedom. This rotational freedom was necessary in order to accommodate the change in angle between the sample and the axis of the central cylinder during the winding process. A new groove profile was designed to satisfy these requirements and was then machined into the three existing support plates. The new retention system relied on a spherical bead that would be bonded to the ends of the rods, creating an interference between the new groove and the bead, which would be free to rotate. This interference connection was tested with 10 mm poly-propylene spheres bonded to the ends of the samples using an acrylic based adhesive especially designed for bonding to acrylic and poly-propylene. Other than this change, a vacuum bag was also incorporated inside the central cylinder of the winding demonstrator in order to provide better heat conduction from the silicon heater mat to the cylinder.

Initially, five 500 mm long rods were prepared for simultaneous winding, similar to the first helical winding tests conducted with the carbon-Elium samples. However, due to some degree of eccentricity in the acrylic rods, together with other measuring inaccuracies, it proved difficult to bond all beads with exactly the same distance between them without using a

specifically designed jig for this purpose. This meant that any pre-load introduced into the system would not be evenly distributed among all five rods. Therefore, in order to quantify the pre-load per sample, and to save material, it was decided to test using one rod at a time.

Samples H.4 and H.5

For the first two rods, labelled as H.4 and H.5, the goal was to produce a helix with one end rotated by 180° (enveloping half the cylinder), once clockwise and once counter-clockwise. Temperatures were monitored like before using the thermocouple layout shown in Figure 7.10, although thermocouples 1 and 2 were omitted as only one sample was present in the winder. Additionally, thermocouple 6 was dedicated to monitor the outlet tube of the vacuum bag to be able to prevent it from overheating.

The first sample H.4 was wound at a temperature of around 90 °C in increments of around 45° at a relatively slow rate (roughly $45\,^\circ\,\mathrm{min}^{-1}$). An additional 5 kg counterweight was used to establish pre-load on the sample, though it should be noted that this weight also compensated for the added weight of the suspended aluminium ducting. The sample was left overnight before taking it out of the winder. A similar procedure was followed for sample H.6, though the winding temperature was increased to 100 °C and the twisting rate per interval was slower (around $15\,^\circ\,\mathrm{min}^{-1}$ for every 45° interval). The sample was cooled down faster by cooling the upper part of the central cylinder (outside the testing area) using pneumatic pressure. The sample was taken out after the cylinder had cooled down to below 60 °C.

What was interesting to observe was a striking length difference between the two samples: Even though the rods started out at the same length, sample H.5 was significantly longer than H.4. Upon closer inspection, there was a notable change in diameter along sample H.5: the upper end showed a diameter decrease of around a millimetre, confirming that the sample had significantly stretched. On the other hand, while sample H.4 did not show this effect, it did have a noticeably smaller radius of curvature near the upper end of the sample.

Samples H.6 and H.7

For the next two helical samples (H.6 and H.7), the goal was to aim for a specific helical angle (once clockwise and once counter-clockwise), so that the helical samples could be more easily welded to the carbon-Elium rods using the existing mould block design. As visualised in Figure 7.14, using basic trigonometry and assuming a constant helix, a given helical angle α could be related to the rotation angle θ of one of the fixture ends through Equation 7.1. Using Pythagoras' theorem, the height change of the upper end of a helix can also be related to the rotation angle, as shown in Equation 7.2.

$$\sin\alpha = \frac{\frac{\theta}{360}\pi D}{l} = \frac{\theta\pi D}{360l} \tag{7.1}$$

$$\Delta h = l - h = l - \sqrt{l^2 - \left(\frac{\theta}{360}\pi D\right)^2} \tag{7.2}$$

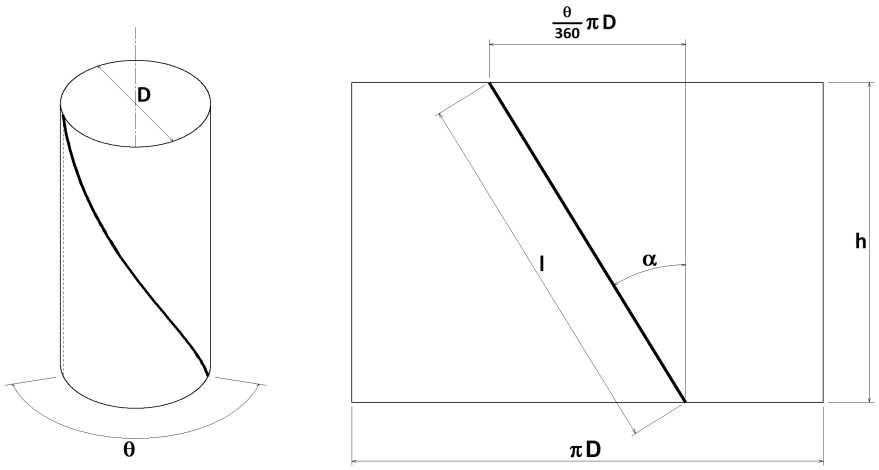

Figure 7.14: Visualisation of helix parameters in 3 dimensions (left) and unwrapped (right)

In this equation, D is the diameter of the helix, while l is the length of the sample and α and θ are given in degrees. Given by Equation 6.1b, the mould blocks used a helical angle α of 51.5°. Assuming a helix diameter of about 203 mm (taking into account the actual diameter of the central cylinder and the thickness of the rod) and a sample length of roughly 490 mm (distance between the two bead centres), this implied a total rotation angle of 216°, 36° more than the previous samples. While not a large increase in rotation angle, due to this extra rotation the theoretical height change of the upper platform would be 185 mm, a significant increase compared to only 118 mm for a 180° rotation. This is because the maximum rotation (in other words, when $\alpha = 90°$ and $\delta h = h$) for a sample with a length of 490 mm would be 276°.

Both samples were wound separately at a temperature of roughly 90 °C to avoid stretching of the samples as observed with sample H.5. To further limit distortion effects, samples H.6 and H.7 were wound in one interval at a rate of around $40\,° \,\mathrm{min}^{-1}$. When the desired winding angle was achieved, both samples were cooled down to a temperature below 60 °C before they were taken out of the setup. Under these conditions, the two samples showed little difference in height between one-another: only around 2 cm. However, this height difference was observed to be the result of an increase in curvature of sample H.7 towards the top end of the sample, similar to sample H.4. Furthermore, the total travel of the upper platform (Δh) was consistent with the theoretical calculated value and there was no significant diameter decrease observed along the length of either sample.

Samples H.8 and H.9

With the pure acrylic samples demonstrating the feasibility of producing helices using the Helical Winder Demonstrator, it was deemed worth investigation whether the new test setup would influence the kinking phenomenon observed for the carbon-Elium samples. The reasoning behind this was that the new setup could pre-load the samples in tension, thereby limiting the chance for a sample to buckle.

For this purpose, two carbon-Elium samples were prepared, labelled as H.8 and H.9. They were prepared in a similar way as the PMMA rods: they were cut to a length of 500 mm,

and poly-propylene beads were bonded to either end of the sample using the acrylic based adhesive. The goal was to rotate both samples to an angle of 180°, similar to samples H.4 and H.5. Different from the previous samples, sample H.8 was pre-loaded using a 10 kg weight and the target temperature for winding was 100 °C to 110 °C due to the slightly higher glass-transition temperature of the Elium resin. For this sample, the adhesive between the sample and the bead failed during the heating phase at a temperature of around 90 °C, prematurely terminating the test.

For sample H.9, the weight responsible for pre-loading was reduced back to 5 kg, the same as for the pure acrylic samples. This allowed the sample to be successfully heated to a temperature of 105 °C, although the adhesive failed during the winding process instead. While the sample itself was kept within the groove of the upper fixture, limiting its lateral movement, the pre-load on the sample was lost, leading to a kinked rod similar to H.2 and H.3. However, while winding the sample, the first kink could already be felt through the transmission even before the bead separated, indicating that the end result would have been similar regardless of loss of pre-load.

Sample H.10

As a final test with the Helical Winder Demonstrator within the scope of this project, the last acrylic sample was wound as far as physically possible to assess the upper deformation limit of the material and the test setup. Looking at Equation 7.1, this would be for an angle of α close to 90°, implying a fixture rotation angle θ of a little over 276°. To be able to accomplish this, the aluminium ducting used for insulation had to be removed, leaving only bleeder around the test area to prevent convection cooling. The pre-loading weight was kept at 5 kg and the target test temperature was slightly increased to 95 °C to allow for easier deformation of the sample.

Although initial deformation of the rod seemed similar to previous samples, further rotation became increasingly harder after rotating the rod close to the angle for sample H.6 and H.7. The absence of the aluminium ducting allowed to view the top of the sample during rotation, which was seen to be unable to slide over the central cylinder at this point. Instead, further rotation of the sample would lead to stretching and further curving of the upper end of the sample, until the point where the plastic bead separated from the rod due to the high involved loads.

Iso-truss Welding Demonstration

As a proof of concept, the pure acrylic helical samples were welded to a carbon-Elium sample using the welding setup discussed in Chapter 6 to form the very first representation of an iso-truss using this manufacturing method. From the tests discussed in Section 6.1.3, the welding temperature was limited to 160 °C to limit gas formation within the pure acrylic rods. For samples H.4 and H.5, the composite rod could only be oriented in a circumferential direction with respect to the helicals due to a mismatch between their helical angle and the grooves present in the welding moulds. The created structure can be seen in Figure 7.15a. Due to the lower welding temperature, the carbon-Elium sample hardly deformed, leaving a very weak connection.

Since samples H.6 and H.7 were wound with the required helical angle in mind, they could be welded to several carbon-Elium rods, creating the first crude sectional representation of an iso-truss, seen in Figure 7.15b. It should be noted however that since the mould blocks were designed for straight diagonal members, they locally straightened the helices within their welding area, creating a section of an iso-truss with a diameter greater than 200 mm. Without the presence of an appropriate welding jig, the welded joints could not be accurately positioned, meaning the longitudinal samples were not perfectly parallel to each other. Additionally, due to the limited strength of the intersection, the samples were instead bonded using the acrylic based adhesive.

(a) Helical samples 4 and 5, welded to a single composite sample

(b) Helical samples 6 and 7, welded to several composite samples

Figure 7.15: Results of fully thermoplastic helical testing

7.3 Discussion and Recommendations

After conducting a variety of experiments and testing different aspects of the Helical Winder Demonstrator, the results had to be interpreted in order to form recommendations for further research. In this section, these results are discussed so that some initial conclusions can be drawn with regards to the winding related aspect of this thesis. This discussion can be split into two topics: the design process for the Helical Winder Demonstrator, treated in Section 7.3.1, and the testing phase with this setup, treated in Section 7.3.2.

7.3.1 Design

The Helical Winder Demonstrator design was meant to be a prototype for the demonstration of winding helical members for iso-truss structures. This also meant that it served as a testing ground for future versions of the device, as many forming related aspects could only be identified through testing. The modular design allowed for the replacement of components by later improved iterations. One of these iterations was already elaborated on in Section 7.2.3: The end support plates for the samples were redesigned to allow for sample tensioning. While this design change was necessary in order to create the first successful helical samples, there are many more improvements that could be made.

Changes to Improve Current Design

The main improvement to the test setup is a more refined iteration of the heating mechanism. Currently, the silicon heater blanket in combination with the 200 mm central cylinder is able to create a somewhat stable temperature environment, although there is around a $\pm 10\,^{\circ}\mathrm{C}$ temperature variation along the length of the cylinder. This variation is likely caused by insulation differences between the top and the bottom. The current setup uses insulation that is far from ideal, being comprised of layers of breather around the cylinder to limit convection. Additionally, although the bottom of the cylinder has been offset from the much colder bottom support plate, it is still in contact through the steel nuts and bolts used to accomplish this. While this likely accounts for some heat loss, there is also the aspect of heat loss through the testing chamber. This chamber, created from the space between the central cylinder and the aluminium ducting around it, is not perfectly sealed, allowing for some degree of convection within it. During testing, it was seen that the top of the sample was warmer than the bottom of the sample, likely contributing to inconsistent curvature of the sample during forming. It is hypothesised that this is because the top of the test chamber is still relatively open, allowing the warmed up air inside the chamber to escape through it. Because the bottom of the test chamber is also not perfectly sealed, this likely creates an air current where hot air rises and escapes, being replaced by colder air coming in through the bottom. For a test environment, this is far from ideal, as it leads to temperature variations along the length of samples and general temperature inconsistencies. To improve this, it is recommended to redesign this test chamber to offer better sealing. Additionally, the area above the test chamber around the central cylinder should be improved as well to offer better insulation, making higher heat-up rates and maximum temperatures possible.

Another aspect to be improved is the counterweight system used for establishing a pre-load on the samples. While weights can be removed selectively, the current counterweight setup is designed to counteract the weight of just the top platform with the lighter sample support plate (the one for 300 mm diameter helical samples). This means that additional weights have to be attached to the existing counterweight setup when using a combination of the 200 mm support plate, the aluminium ducting suspended from the top fixture platform and the pre-load on the samples. This attachment procedure is less than ideal if a specific pre-load is to be applied. To offer a more controlled tension load on the samples, the counterweights should be redesigned or replaced with another system.

Due to production choices, the diameter of the central cylinder is not exactly as intended. This is because the cylinders were produced as aluminium extrusions with the intended diameter,

but due to the low tolerances of this production process they were post-processed on a lathe to a slightly smaller diameter (about 2 mm to 3 mm smaller than intended) to ensure roundness. On top of this, the grooves in the support plates that hold the samples had to be offset from the cylinder in order for them to fit, creating an inconsistent helix diameter on the outer ends of the sample. Still, this could be seen as a benefit, as the ends of the sample were not in contact with the central cylinder, creating some cooling effect which was needed in order to successfully clamp the samples. In the production of helices, these ends could actually be trimmed off at a later stage. Although the length of these ends could not be exactly measured during production, it is estimated to be around 5 cm. As for the helix diameter, it is proposed to investigate the possibility of adding padding with variable thickness around the central cylinder. This would make it possible to make small incremental changes to the produced helix diameter, which would be beneficial to account for springback and compaction considerations for the Assembly Demonstrator discussed in Chapter 8.

Finally, there are small aspects to improve the current design of the Helical Winder Demonstrator that were discovered during production of the device and subsequent testing. One of these is the incorporation of a lock ring for the bottom fixture plate, as it is subject to unscrewing itself if the torsional load caused by winding exceeds a certain threshold. Another is the incorporation of another structure above the central cylinder capable of aligning its rotation axis, one that also fits the current heating setup. Although an upper support fixture was realised, the silicon heater blanket currently protrudes from the 200 mm cylinder, and cabling would be in the way of the lid of this setup.

Conceptual Design Changes

On a conceptual level, many recommendations can be made that would significantly improve the use of the Helical Winder Demonstrator. They were not considered for this thesis topic because they would require far more testing time, without actually adding value to demonstration of the process itself. However, they would provide a testing ground for automation of the process, making them important for future consideration.

The first of these recommendations is the incorporation of motor control on the rotational motion of the bottom end fixture. Although the manually actuated motion provided valuable feedback to the user during winding, an electric motor would make the process more accurate, reproducible and easier to automate. With regards to the layout of the Helical Winder Demonstrator, little changes would have to be made, as the motor could easily replace the currently employed crank. Similarly, accurate temperature and sample pre-load control could be incorporated to improve the reproducibility of the design.

As another recommendation for future improvements to the design, it is proposed to redesign the central cylinder and the end fixture plates to support helix diameters different from 200 mm and 300 mm. While it should initially be acceptable to produce more cylinders with different diameters, as this requires no major redesign of this sub-assembly, it is recommended to investigate other concepts. One of these concepts would be a variable diameter cylinder with integrated heating, like a cylindrical inflatable balloon. The balloon would be able to expand or contract based on the amount of fluid inside of it, creating the possibility to vary its diameter through a controlled input. If oil is used instead of air inside this balloon, the system can ensure a stable temperature environment for the creation of helical samples. Of course,

this system would require extensive design considerations, taking into account the expansion of oil while heating up, the required pressure for a somewhat solid outer surface, the need for an outer surface with a low friction coefficient, and an adapted end fixture structure which allows for diameter changes, to name a few. While the system would likely fit in the current setup for the Helical Winder Demonstrator for diameters up to 350 mm, the aluminium profile components that make up the frame would have to be changed for larger diameters. While this would not change the design of the Helical Winder Demonstrator, it would require a complete dis- and re-assembly of the device.

Although the design of the Helical Winder Demonstrator was envisioned as the most simple way to investigate the shaping of straight pultrusions into helices, it was never considered to be the final solution for the production of iso-trusses. In a setup that would integrate all the iso-truss production steps (that is, pultrusion, helical forming and joining of the members), the setup would not be able to fit without severely affecting the pultrusion and welding steps. Instead, it was envisioned to integrate the forming of helical members with the pultrusion step by creating curved instead of straight pultrusion members. Although this manufacturing method does exist, as shown by Thomas-Technik Radiuspultrusion [39], it would have created many uncertainties for the research of this topic. On top of this, while it would be theoretically possible to create pultrusions with a varying curvature over their length (allowing for a tapered diameter iso-truss structure for example), such a production process has likely not been demonstrated as of writing this report.

7.3.2 Testing

From the experiments conducted with the carbon-Elium composite and pure PMMA materials, many conclusions could be drawn with regards to the feasibility of forming helical members from thermoplastic pultrusions.

First and foremost, it appeared that the composite's material characteristics proved limiting for formability. No setup was found that could eliminate kinking of the carbon-Elium samples. The only way in which it could be avoided was to deform the samples at room temperature so they would maintain their stiffness. Here, it was observed that a combination of compressive and torsional loading could be used to force the members around the central cylinder in a consistent curvature along their length, although the required force to shape the samples would scale up with the amount of deformation. The limiting factor for this method was therefore the stiffness of the samples. It was shown that this process was fully elastic, as no permanent deformation remained on the samples after they were taken out of the setup. It is hypothesised that forming at slightly elevated temperatures (around 60 °C as observed from the oven tests) would be possible through the use of creep, although the process would take a considerable amount of time to complete, scaling up with the length of the samples as fibres would have to slide over their entire length. Because of this, it is not seen as a feasible alternative for the production of iso-truss structures.

While pre-twisting was thought to reduce the tendency for the material to kink, no samples usable for helical testing could be produced due to the high degree of stress-release at elevated temperatures and the decompaction of the samples in the form of knots. If this decompaction could be prevented through the use of support around the sample, perhaps this method could be investigated further. The degree of stress-release, observed as a reduction in the degree

of twist of an unloaded sample at elevated temperatures, did appear to be dependent on the amount of time the sample was left at elevated temperatures during twisting. However, it still appears that the process of twisting of rods would depend on the length of the sample, limiting feasibility of this process in the production of iso-truss structures.

Through the use of pure PMMA samples, it could for the first time be seen that it was in fact possible to produce helical samples using the Helical Winder Demonstrator. This was because the material did not show any fibre related phenomena like the decompaction and kinking observed with the carbon-Elium samples. Although the setup had to be redesigned slightly to allow for pre-tensioning of the samples, the production of helices proved highly effective. Helical samples could be produced with relative ease with mostly constant parameters like helical angle and radius of curvature. The only additional phenomenon that was observed was stretching and increased curvature of the samples near their upper end. From helical test H.10, it could be seen that these phenomena occurred as a result of friction between the sample and the central cylinder. While friction itself was constant over the length of the cylinder, the current layout of the cylinder (rotating together with the bottom fixture) meant that a sample would travel the largest distance over the surface of the cylinder near the upper fixture. It was observed that at some point, this travel was no longer possible, instead leading to stretching and increased curvature of this upper end upon further rotation of the sample. It is hypothesised that this phenomenon is also somewhat related to the temperature in the device, as the PMMA material would become tackier the warmer it was.

As a general recommendation, it is advised to perform more experiments in order to investigate the phenomena explained above in more detail. While the forming of composite pultrusion samples could be limited in terms of feasibility, this should still be proven by varying the material's characteristics: Possibly, a better fibre-matrix interface and higher resin volume content could greatly improve the results. The PMMA samples on the other hand showed no clear limitations. Better samples could likely easily be produced by changing certain aspects about the production process, like the surface friction of the central cylinder.

Finally, a recommendation is made with regards to the investigated method of heating up samples using resistance heating. Although this would only be possible for carbon and other conducting fibre materials used in the pultrusion composite, it proved to be a highly effective way of heating up samples over their entire length. The only consideration for future pursuit of this method would be to ensure an even heat distribution over the length of the sample, including its ends. This could be done by providing a conducting path to the head of the rod so that current can be evenly distributed over all fibre bundles in the cross-section, and by designing a heat sink to account for any increase in temperature at these ends.

Chapter 8

Assembly Demonstration

This chapter describes the detailed design process of the Assembly Demonstrator described in Section 4.3.4. As the design presented in Chapter 4 was only conceptual, Section 8.1 elaborates on all the detailed aspects required for the production of this demonstrator. As construction of the device did not take place as part of this thesis, Section 8.2 focuses on recommendations for further steps.

8.1 Assembly Test Design

After discussing the conceptual design for the Assembly Demonstrator with DEMO, a detailed representation of the design could be made. This version would then later be prepared for production and assembly. This section highlights the decisions made during this process, and how the current detailed design came to be. Design rules for the Assembly Demonstrator were similar to the ones described for the Helical Winder Demonstrator: The setup should be constructed from off-the-shelf parts as much as possible, limiting the amount of parts that would have to be produced by DEMO. In this regard, the setup was again designed around standard ITEM profile components and other miscellaneous parts like bearings and fittings.

8.1.1 Top Level Design Changes

Based on the tests described in Chapter 6, several changes could be made to the welding related aspect of the design. With the final choice for welding being the use of heated moulds, there was no longer a need for the setup to interface with an external welding device, like an ultrasonic welding machine. Instead, heating and consolidation could be integrated into the design by use of an arm that could be repositioned over the setup. To generate the forces necessary for consolidation of the welding points, a pneumatic piston was selected for its ease of setup. This piston could be connected to the centralised pressurised air system anywhere in DASML, leaving a large amount of flexibility in the placement of this setup. The consolidation force could then be easily controlled by incorporating a pressure regulator within

the air pressure supply line. For the heating aspect of the welding design, a setup similar to the one shown in Figure 6.4 was envisioned: Two aluminium mould halves would be connected to separate soldering irons in order to reach the temperature required for welding. One of these mould halves would be connected to the end of the pneumatic piston arm, while the other mould half would be part of the internal support structure of the Assembly Demonstrator.

Other changes made to the conceptual design included cost savings in the bearing aspect of the design. The initial design was based on a need for one-sided access to the welding site, requiring that the entire structure to be assembled could be rotated. While this requirement was not changed, this degree of freedom could be achieved simply through the central rotation core interfacing directly with a roller bearing housing, instead of through the outer fixture for the composite samples. This way, the required bearing would be far smaller, limiting cost and increasing the likelihood of direct availability. With these changes in mind, the design of the Assembly Demonstrator could be divided in the following sub-assemblies: A base frame, the rotating core, the end fixture for the samples, modular support for the welding sites and a repositionable consolidation arm. As an overview, the differences between the conceptual design and the final production ready design can be seen in Figure 8.1.

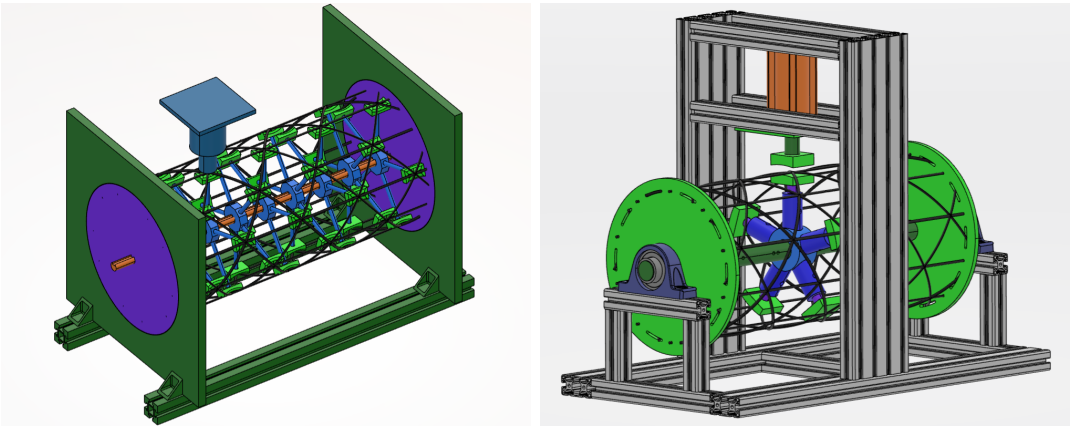

(a) Conceptual design in CATIA **(b)** Detailed design in CATIA

Figure 8.1: Comparison between designs of the Assembly Demonstrator

8.1.2 Frame

Requirements for the base frame of the Assembly Demonstrator were similar to the ones for the Helical Winder Demonstrator: It would be responsible for reacting any loads present in the system, including the consolidation of members and the weight of the structure. In this case, the frame for the Assembly Demonstrator was envisioned as the floor area for the setup, with vertical sections extending on either end which would contain the bearing units required for rotating the main mandrel. Besides this interface, the frame should also interface with the repositionable consolidation arm.

Similar to the Helical Winder Demonstrator, a design satisfying these requirements could again be realised through the sole use of off-the-shelf parts. In this case, the base frame would be constructed from standard ITEM profiles, while two integrated bearing houses were

selected from RS-Components to interface with the rotation core of the rotating mandrel. The detailed design is visualised in Figure 8.2.

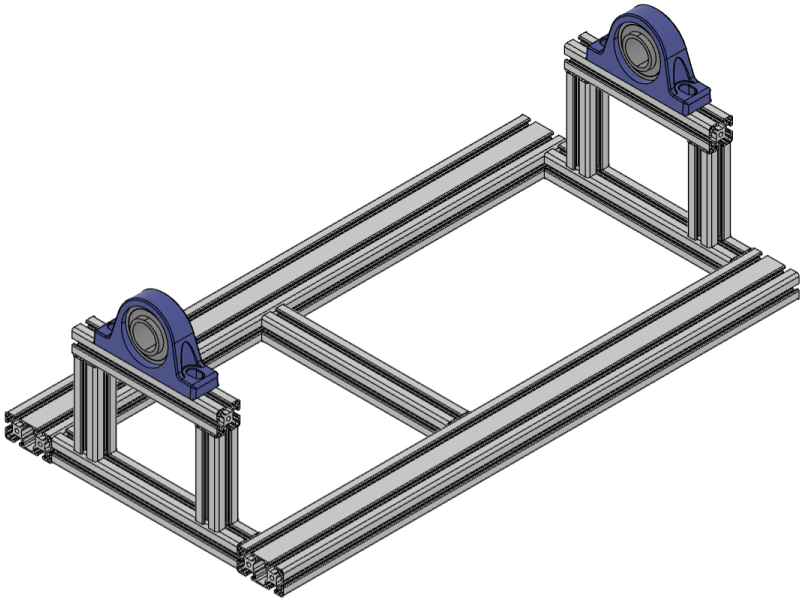

Figure 8.2: Detailed design of the base frame

8.1.3 Core

The main requirement for the core of the rotating mandrel was relatively straightforward: It should provide support for the internal modular supports for the composite samples, while interfacing with the bearing houses. Preferably, within the scope of this project, the core should contain alignment points for the modules, making it easier to set up the demonstrator for the two considered helical pitches of 50 mm and 75 mm. Two other components of the setup that were considered part of the rotating core were the two fixture ends on either side of the composite samples. This decision was made in order to create a dependency between the reference points for the modules and the positions of the composite samples. While one end of the mandrel had to be removable in order to release the finished iso-truss sample, one end could remain in place for the duration of experiments. Both these end fixtures should contain slots for the fixation of composite samples, which they should keep in place during the entire operation. As a last requirement, the core should be stiff enough to resist consolidation forces without significant deflection, even at the point furthest away from the outer support.

To fulfil these requirements, the core was designed as a single solid shaft made of steel, 40 mm in diameter. This shaft would contain threaded holes at predetermined positions to interface with the modular supports, which would be slid over the shaft. Additionally, holes would be present for positioning the end fixtures. Both these end fixture were designed as a single plate of aluminium with slots for a 200 mm and 300 mm diameter iso-truss. For alignment with respect to the compressor arm of the setup, holes were drilled in the fixed end-fixture which would interface with a single locking pin in the external frame. This could be used to lock the rotating mandrel in position for welding. With these considerations, the detailed design for the rotating core is presented in Figure 8.3.

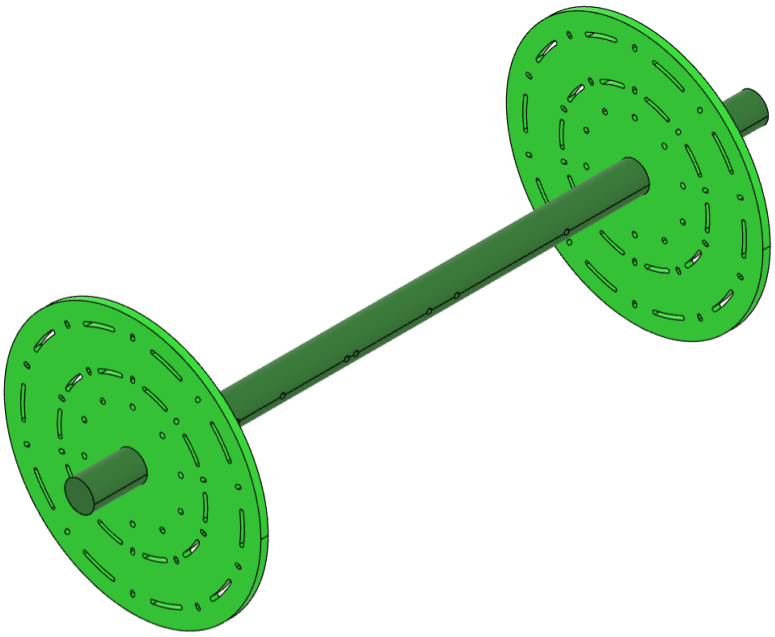

Figure 8.3: Detailed design of the rotation core, including both end fixtures

8.1.4 Module

The module sub-assembly was the first component that would be responsible for the shape of the iso-truss to be produced, creating an interface between the composite samples and the core. First and foremost, it should contain the surfaces against which to consolidate the iso-truss members, providing internal mould surfaces similar to the lower mould half of the experiments discussed in Chapter 6. Consequently, it should be rigid enough to resist the forces of consolidation, while also being flexible enough to allow for different iso-truss diameters and to be able to release the finished product. For the scope of this thesis, access to the modules during the welding of the iso-truss would be limited, requiring that all modules to be place before welding. As a last requirement to the module, it should provide access for a soldering iron in order to heat up at least one mould block at the time.

With the above requirements in mind, the design could not simply be made from off-the-shelf components. To make construction as simple as possible, a design which would fulfil these requirements was discussed with DEMO. This design consisted of a five-arm collar, which would be one welded-together piece. The collar itself would interface with the core, and would contain one hole for alignment to the threaded holes in the core. The tubes welded around the perimeter of this collar would likely be large in diameter and thickness, on the order of 40 mm × 10 mm, to be able to resist the forces of consolidation. Each of these tubes would also feature a through-hole for a locking pin. This locking pin would be responsible for locking the module ends in place so they could resist the consolidation forces, while also allowing them to be retracted to fit different diameter iso-truss samples. The module ends that would fit inside the five tubes, featured three parts. One of these parts would be a solid shaft containing holes for the locking pin to fit through. On top of this shaft, an insulating material would be mounted, on the end of which one mould half would be attached. This mould half would be removable and could only be attached in one orientation to allow for

simple alignment. Within the scope of this thesis, two different instances were considered for this mould half: One for a 200 mm diameter iso-truss, and one for a 300 mm diameter iso-truss. Other than this, the mould halves would be similar to the ones used for the experiments discussed in Chapter 6. It should be noted that with this in mind, these mould halves had to be somewhat mass-produced. A total of 45 mould halves would be needed per iso-truss sample. As such, they were designed to be produced on a 3-axis CNC machine from several blocks of aluminium, depending on the maximum reach of the CNC machine. While the detailed design would be up to interpretation by DEMO, a representation of the design can be seen in Figure 8.4.

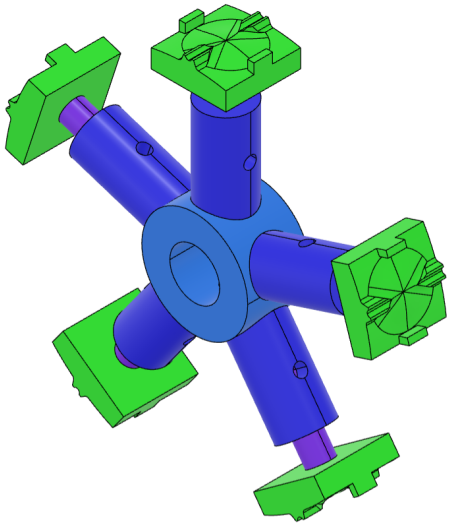

Figure 8.4: Detailed design of one of the modules for internal support, with changeable mould blocks

8.1.5 Compressor

As the centre piece in the welding operation of the Assembly Demonstrator, the compressor structure required many design considerations. As main requirement, it should provide a stable platform for the incorporation of the pneumatic cylinder, while at the same time being repositionable for welding different modular sections of the iso-truss.

A structure satisfying these requirements was designed mostly from standard ITEM profile options. Two wide vertical profiles were selected to be able to accommodate the space required for a pneumatic cylinder, to which a single upper welding mould half would be connected. Four cross-members would interface between these vertical members and the cylinder, as can be seen in Figure 8.5. The cylinder would interface with these cross-members by means of a bolted connection or a transitioning bracket if required. The pneumatic cylinder would be connected to the existing pneumatic network in DASML, which is believed to operate at a pressure of around 6 bar. The connection would be established by means of a pneumatic quick connect coupling of a CEJN (Euro) standard. In between the network and the pneumatic cylinder, a pressure regulator and a ball valve would be incorporated. The pressure regulator would allow for a control of the applied force of the cylinder, while the ball valve would be

used for extension and retraction of the cylinder's piston. All these components would be connected by an appropriate type of pneumatic hosing.

Selection of the cylinder was based on the available space, force required for both forming and consolidation, total possible extension of the piston and maximum operating temperature. The force applied by the cylinder is related to the operating pneumatic pressure through the diameter of the cylinder's piston, which can be selected as part of Festo's product configurator, similar to the total travel of the piston. Estimated values for these parameters are tabulated in Table 8.1.

Table 8.1: Overview of estimated pneumatic cylinder parameters

Parameter	Estimated Value
Width	80 mm
p_{op}	0.5 bar to 6 bar
Travel	150 mm
T_{max}	15 mm foil

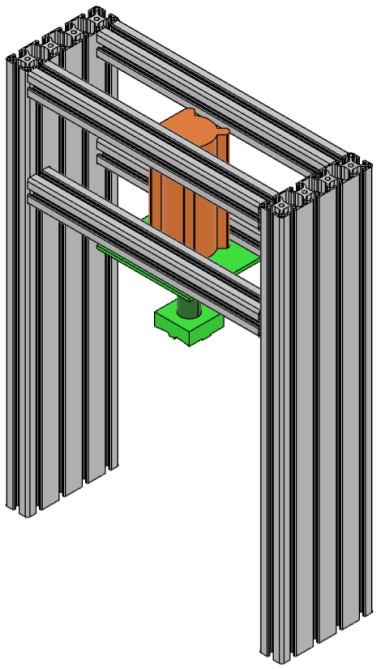

Figure 8.5: Detailed design of the compressor arm with integrated pneumatic cylinder

8.1.6 Complete Design

With all the design considerations of the components discussed before, the current state of the design of the Assembly Demonstrator can be presented. In Figure 8.6, this design is visualised, showing the use of the demonstrator in the construction of a 200 mm diameter iso-truss with 50 mm pitch and a 300 mm diameter iso-truss with 75 mm pitch.

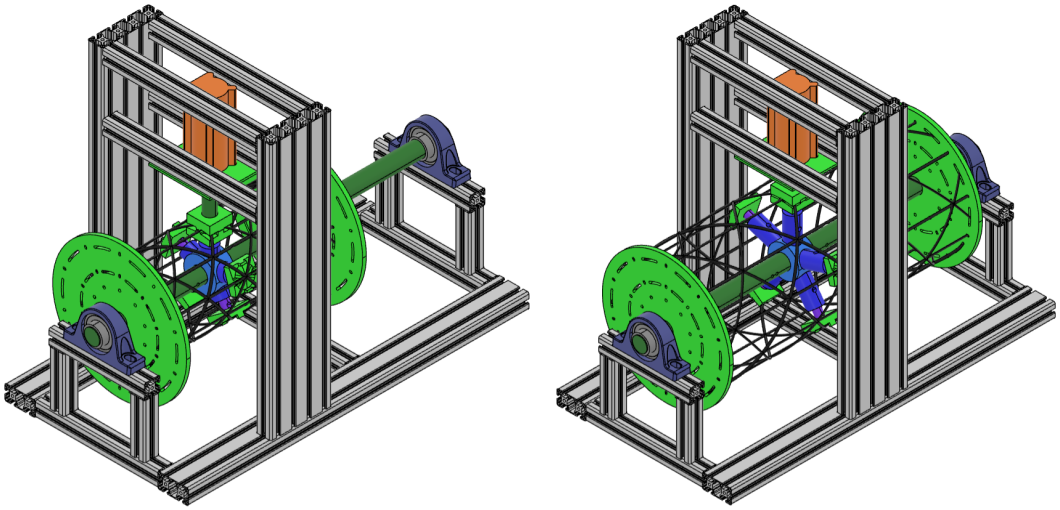

(a) $D = 200\,\text{mm}$, $l_p = 50\,\text{mm}$ **(b)** $D = 300\,\text{mm}$, $l_p = 75\,\text{mm}$

Figure 8.6: Detailed design overview of the Assembly Demonstrator

8.2 Discussion and Recommendations

At the start of this project, the design and production of the Assembly Demonstrator was seen as feasible within the time frame of this thesis. However, as the production of iso-truss structures with this demonstrator depended on the success of helical winding, the design was pushed back until the problems observed with winding could be solved. Because of the extensive delay caused by current limitations of the carbon-Elium composite material, the design had to be left in its current state in order to prevent further delay of this project. Finalisation of the design is therefore seen as a direct continuation of this project, using PMMA based rods as a stepping stone to achieve demonstration of iso-truss production. The discussion section of this chapter therefore focuses on finalisation of the design, as well as a preliminary testing procedure. Additionally, even though a final design was never presented, recommendations can still be made to further adapt the design for fully automated iso-truss production in the future.

8.2.1 Design Finalisation

The main focus in the finalisation of the design of the Assembly Demonstrator is on the assemblies that directly interact with the iso-truss members, being the mould blocks and the end fixtures. Secondly, the different mechanisms within the demonstrator have to be finalised, namely the pneumatic cylinder, compressor positioning system, rotational fixation of the mandrel and the accommodation of heating.

Mould Blocks

Although a recommended shape accommodating a 300 mm diameter iso-truss has been designed for the mould blocks, several aspects have yet to be incorporated.

The first of these is the design of a mounting system to either the module or the pneumatic cylinder of the compression arm, taking into account the integration of thermal insulation. Although a threaded connection would be advisable for alignment and disassembling purposes, most threaded connections do not provide decent thermal insulation due to their reliance on metal threaded parts. Well-insulating materials on the other hand are usually too soft (for polymer based insulation) or too brittle (for ceramic based insulation) to support a threaded connection. The selection of a proper mounting system has therefore yet to be determined.

In addition to a mounting system, the moulds should accommodate alignment of the two halves during welding. As the pneumatic cylinder only supports vertical travel, it is recommended to design a planar floating connection between the cylinder and upper mould block. This way, conical pins on one mould half and corresponding holes on the other would allow the upper mould half to align itself to the lower one, eliminating any prior misalignment between the compressor arm and the modules.

Finally, a mating hole should be included for accommodation of the soldering iron tip to heat up the mould halves. This hole should be positioned such the the protruding soldering iron does not clash with any of the assembly's components. Additionally, for the mould blocks incorporated in the modules, the hole should make it as simple as possible to disconnect the iron and reconnect it to the next mould block.

End Fixtures

Finalisation of the design of the end fixtures requires a trade-off between two clashing requirements: Although the fixtures are responsible for aligning all members before fixation of the first joint, requiring tight alignment tolerances, they should also accommodate a certain amount of travel and possible misalignment. For the longitudinal members, this resulted in a vertically elongated hole profile, as horizontal alignment is not difficult to accomplish. The helical members on the other hand will likely contain a certain amount of misalignment from the forming process. It is therefore believed that a rotationally oriented elongated hole profile is best suited to constrain the samples in the end fixture, leaving room for rotational adjustment before welding. Concepts for this design would need to be tested before incorporation into the final design.

Additionally, a mounting system for the end fixtures should be designed which relates the rotational position of the fixtures to that of the modules. For one of the ends, an additional bracket with mounting holes for both the core and the fixture would likely be an appropriate solution. The other fixture end on the other hand should account for horizontal travel of the fixture to be able to release the iso-truss sample and to accommodate iso-trusses with different intersection pitch. For this purpose, it is believed that a groove within the core for the mounting of a sliding bracket would offer the best solution.

Compressor Arm

With the incorporation of horizontal alignment in the mould block design, the mounting system of the compressor arm can be slightly simplified. Standard horizontal travel options available for ITEM components should be able to accommodate this. A guide rail able to support the pressure from the consolidation process in combination with a clamp to fixate

the position of the compressor arm is thought to be the best solution to approximately align the assembly.

Another interface to finalise is the connection between the compressor arm and the pneumatic cylinder. It is currently believed that transition brackets are used best for this purpose, although their design depends on the final selection of the cylinder. The cylinder itself, a standard option from Festo, is to be selected for the required loads. These loads are currently estimated to be between 50 N for forming and 500 N for consolidation. With the pneumatic network present at DASML supporting pressures of up to around 6 bar and this load range in mind, a cylinder with a piston diameter of 32 mm should suffice. Festo pneumatic cylinder options from either the DSBC or DFM range are recommended, with an estimated possible travel in between 100 mm and 200 mm. For the regulation of consolidation load, especially when shifting from forming to consolidation, a pneumatic pressure regulator should be connected in between the pneumatic network and the cylinder. This regulator could be selected from either the MS4 or MS6 range from Festo, with an estimated regulation range from 0.5 bar to 6 bar.

Finally, an interface with the soldering iron would likely make the setup easier to use. It is therefore recommended to design a bracket or other mounting location for the iron itself, taking into account the travel of the device.

Modules

For the modules holding the inner mould halves, it is believed that the current option using a locking pin with three different mounting holes would offer the simplest solution. This way, the mould height can be easily adapted for a 200 mm diameter iso-truss, a 300 mm iso-truss or the release position. Still, there is concern for the diameter accuracy in helical members after winding. If the diameter of the helix does not match the height of the mould block both before and after compaction, the iso-truss might become deformed. For this reason, it is recommended to accommodate a certain amount of spacers of a given thickness in the design of the modules so that the height can be set to an appropriate value after fitting the iso-truss members.

For the interface with the core, it is believed that a single locking screw should suffice. When designing a connection between a module arm and a mould half, care should be taken to accommodate thermal insulation and the previously mentioned spacers. The connection should fully constrain the rotational freedom of a mould half, aligning it properly to the direction of a longitudinal member.

Finally, it is recommended to design a separate tool to set the height of the module arms, as access to the inside of the iso-truss is limited after the members have been positioned, especially in the case of the 200 mm diameter iso-truss. Access can be achieved only through openings in the lattice, which likely will not provide enough space for hands to unlock the module arm. A tool which is specifically designed for undoing the locking pin, or designing the locking pin such that it can be released with a normal hex key, are two recommended options.

Rotational Fixation

In order to lock the mandrel in place during the welding process for one of the iso-truss intersections, a locking pin is to be incorporated in one or both of the end fixtures. This pin would interface with a bore in the horizontal aluminium profile underneath the bearing housing, which can be incorporated as a standard option for ITEM profiles. Through the use of threaded holes in the end fixtures, the locking pin could be incorporated as being a standard M8 threaded bolt. However, it should be investigated if such bolts can cover the maximum distance between the end fixture and the bearing support on the adaptable side of the mandrel.

Heating Incorporation

Currently, solder heating is thought to be the simplest way to heat up separate mould blocks. This method allows for separation of the heating control unit and the welding mandrel, requiring only that the irons themselves interface with the setup. Although these irons are connected to the control unit by means of a flexible cable, positioning them inside a mould block may still prove to be a challenge due to the limited space around the mandrel. For this reason, the size of the soldering iron should be accommodated within the Assembly Demonstrator design. Additionally, the mounting holes inside the mould blocks should be designed for a maximum trasfer of heat.

It should be noted that although simple, solder heating is not the fastest way of heating up the mould blocks. Heating times for a single mould block are estimated to be around 20 minutes. Taking into account consolidation time and cooling time as well, a single intersection weld may take up to an hour to complete, requiring more than 45 hours to produce one iso-truss sample. Although this production time would likely suffice for a follow-up project, it should be investigated whether this welding time can be reduced by speeding up either the heating or the cooling process. For heating, a device with more power transfer would be required, while cooling is likely best realised through air convection cooling.

8.2.2 Testing Procedure

Although an iso-truss sample could not be produced as part of this thesis project, a recommended testing procedure can still be described, taking into account the lessons learned during the welding and forming experiments.

After producing a set of five clockwise helical members and five counter-clockwise helical members with the Helical Winder Demonstrator, it is recommended to make use of the beads still remaining on the member ends in order to restrain the samples in the Assembly Demonstrator. The demonstrator itself should be prepared by setting the end fixture to the appropriate distance and retracting all module arms to their minimum height. Five of the helical members, all with the same winding direction, should then be fed through one of the end fixtures until they pass through the other end fixture. After this, the longitudinal members should be fed through the appropriate fixture holes, making sure they pass over the previously positioned helical members. Then, the other five helical members can be positioned, and the module arms should be set to the appropriate height. Alignment of the

helical members needs to be ensured in order to line up properly over each mould half. The helical members should then be fixed in place by tightening them using the movable end fixture.

For the welding of intersections, it is recommended to work from the middle of the truss outwards to each end fixture, welding each circumferential row by step-wise rotation of the mandrel after each weld. For a single weld, two separate soldering irons should be used to heat up the mould half supporting the intersection in question and the mould half of the compressor arm. Before welding, the user should make sure to set the air pressure for the pneumatic cylinder to the value required for forming, which is likely lower than for consolidation. After heating both mould blocks to the test temperature in the range of 180 °C to 200 °C, the valve to the pneumatic cylinder can be opened to press the upper mould half on top of the intersection, heating it up through contact and forming the members. After reaching the required distance between the two mould halves, the pressure in the pneumatic cylinder can be increased to ensure intimate content between the members. The soldering irons can then be removed to allow the mould halves to cool down. It is recommended to cool down to below the glass-transition temperature of the material, so to roughly 90 °C, before retracting the upper mould half and moving on to the next weld.

After all intersections have been welded, the finished iso-truss sample can be released from the setup. This is done by retracting all inner mould halves and releasing the tension created from one of the fixture ends. This then allows the beads of the helical members to be cut from the member ends, making it possible to pull the sample out of the fixture ends. One end of the Assembly Demonstrator can then be disassembled to be able to take the iso-truss sample out of the setup.

8.2.3 Future Improvements

As the Assembly Demonstrator is only designed to assess the feasibility of producing an iso-truss, it is not yet optimised for automated iso-truss production. To do this, the entire design would have to be revised, taking the following into account:

1. Integrated heating and cooling in the mould blocks to speed up the welding time of a single intersection
2. The use of (hydraulic) pistons to set the height of the inner mould blocks for each module arm
3. For the continuous production of an iso-truss, the tube itself would be continuously translated through the welding setup. Rotation of the product would likely not be possible, meaning the compression arm should rotate around it to create each joint. Consequently, a single module would need to be able to translate from one welding row to the next

Chapter 9

Conclusions

Through the execution of this project, an answer to the following research question was sought:

Can composite continuous fibre reinforced iso-truss structures be produced using a scalable and cost-effective automated manufacturing method?

The focus of this thesis was on the investigation of all the aspects necessary for a production of this iso-truss structure, focusing on a (collection of) process(es) suited for later automation. The conclusions to the investigation of these aspects are discussed in the following sections.

9.1 The Iso-truss Concept

Through the use of thermoplastic composite materials, the process steps required for the production of an iso-truss could be split up from each other, allowing curing and consolidation to be moved to the very beginning of the process in the form of pultrusions. The structure would make use of straight pultrusion rods, acting as the longitudinal members in the truss, and curved pultrusion rods, which would act as helical members. The iso-truss structure would be created by joining these members together at intersections by means of thermoplastic welding, forming a continuously produced open lattice tubular structure.

With this, conceptual production of an iso-truss was based on three key steps: pultrusion, forming, and intersection welding. The pultrusion process was outsourced to an outside company, vDijk Pultrusion Products (DPP), due to its high required equipment cost. It was not the aim of this thesis to re-invent this process, as it has already reached a sufficient state of maturity. Nevertheless, the process has not yet been optimised for thermoplastic-based composites, leaving room for improvement in this area. Materials for the concept were based on availability. Elium® resin (a PMMA based thermoplastic polymer developed by Arkema) was chosen for its similarity to existing process materials and its direct availability from DPP. As reinforcement, a Toray T700SC type carbon fibre was used.

By taking pultrusion out of the research scope, forming and welding were left as processes to demonstrate. A separate welding test was isolated to provide a way to perform standardiseable tests. Simultaneously, a forming process demonstrator was designed together with a welding jig to demonstrate assembly of the iso-truss.

9.2 Test Setup

The material batch used for execution of this project was the result of a first successful attempt by DPP to make rods of this diameter. To assess the quality of this material and to estimate important composite material parameters, several tests including SEM, TGA and DSC were performed. From these tests, the fibre volume fraction could be estimated to be around 70%, while the onset of T_g was estimated to be 95 °C by definition of maximum loss modulus. Additionally, several interesting phenomena were observed at elevated temperatures in the form of fibre kinking when bent and circumferential decompaction when twisted, indicative of a weak fibre-matrix interface. More indications of this limited fibre-matrix interface were obtained from SEM images, some of which showed small voids around fibres. Dynamic mechanical analysis showed a steady decline of the material's (shear) stiffness over a large temperature range, including before the onset of glass transition. This can likely be attributed to the amorphous nature of the polymer.

After considering several joining techniques for the creation of iso-truss intersections, heated mould welding was selected as the best currently feasible option. After performing numerous experiments to fine-tune the method of heated mould welding, a standard setup was designed around this technique. This setup addressed methods for heating, alignment of members to be welded, a compaction mechanism, physical test preparation and physical testing.

A detailed design for a helical winder demonstrator was made and produced, mostly focusing on the demonstration of the mechanical aspect, leaving heating as a secondary concern. Similarly, a more detailed concept of an assembly demonstrator was discussed and designed, although a production-ready design did not prove feasible within the time frame of this project.

9.3 Intersection Testing

The main goal of the intersection welding experiments was to optimise the weld strength by optimising the processing conditions. Due to the limited resin volume content, PMMA foil and epoxy adhesive were used to locally increase resin volume, greatly improving the bond strength compared to initial samples. Using mould temperatures in between 180 °C to 200 °C, a large degree of deformation could be achieved to maximise the joint area, creating mostly consistent intersection samples.

Physical tests proved that the PMMA-based joints were very fragile, while epoxy adhesive based joints performed significantly better. Estimated shear strengths for the samples varied from 3 MPa for some of the lower performing PMMA-based intersections which were believed to have sustained prior damage, to as high as 13 MPa for the epoxy based intersections. For the buckling tests, maximum loads in between 2.1 kN to 3.2 kN were observed. In the final

buckling test setup, diagonal members did not increase the buckling load by forcing higher-mode buckling. Instead, they offered some support in post-buckling by resisting out-of-plane deformation. Failure modes in both shear and buckling tests were within the adherend, occurring as a combination of fibre break-out, member kinking and member splitting, more indications of a poor fibre-matrix interface. In summary, the experiments proved that the investigated welding method is feasible if the base material can be improved. As of writing, such improvements have already been reported by DPP through increased process stability and (likely) better fibre sizing, so more tests could already be performed with improved batches.

9.4 Helical Testing

The physical test setup of the Helical Winder Demonstrator was designed to offer continuous support of the members over their full length, realise a gradual increase in radius of curvature and allow torsional and axial forces to be introduced independently. This setup proved to be a feasible solution for the production of helical samples. Additionally, the method of heating the central cylinder and introduction of heat to soften the samples through both contact and convection proved the most feasible solution within the time frame of this project. It did not prove feasible to produce carbon-Elium composite helices due to the current material limitations, that is the fibre kinking observed in previous tests. Instead, the process was demonstrated using pure PMMA rods at forming temperatures of around 90 °C, which proved highly effective. The process showed the potential to create constant curvature helices with controllable helical angle, although more testing should be performed to achieve accurate and repeatable results.

9.5 Design Feasibility

Through the performed experiments, preliminary answers to some of the research sub-questions posed in Chapter 3 can be given. By answering these questions, an answer to the main research question can be formulated which, in turn, is an answer to the feasibility of this project.

1. **What is the definition of an iso-truss structure for this thesis project?**

   An iso-truss is defined as a tubular structure consisting of a number of longitudinal members and a number of helical members. The structure is manufactured from a continuous fibre reinforced thermoplastic polymer composite material. The structure is fully defined by a length (or number of repeating units), a major diameter of the tube, a helical pitch, a number of helical members, a number of longitudinal members and separate thicknesses for both the helical and longitudinal members.

2. **How can iso-truss bundle intersections be designed to fulfill as many of the automation requirements as possible?**

   Intersections between members are joined by means of thermoplastic welding. In each of these intersections, the longitudinal member is positioned in between two rotationally opposing helical members. To maximise contact, the helical members are flattened at

the intersection to bring as many fibre bundles in contact as possible. Heated mould blocks are specifically designed to shape and join the members through the transfer of heat and the application of pressure, a process which can be automated by means of a (repositionable) welding jig.

3. **What is the best combination of materials to use for the iso-truss structure, considering their possible degree of automation?**

   Currently, it appears that thermoplastic continuous fibre reinforced composite materials offer the highest possible degree of automation because of their reshape-ability. This allows for the separation of conflicting manufacturing aspects, which makes the entire process simpler and more cost-effective. The final selection of materials will be based on both process-ability and structural requirements, though the former set weighs heavier. Elium resin is seen as a stepping stone to the incorporation of higher grade thermoplastic materials like PPS and PEEK, which need to be optimised for use in a pultrusion process. In search of the best combination of materials, focus should be placed on optimising both fibre volume and fibre-matrix interface strength.

4. **How can a production method be designed to offer the highest degree of automation?**

   In order to reach an automatable process, it is deemed most beneficial to split the production process up into two different manufacturing steps. These steps can be formulated as: producing fibre reinforced thermoplastic members of a certain length and diameter through means of pultrusion and assembling all members together by means of thermoplastically welding each member intersection to produce the final iso-truss structure. In this process, the shaping of helical members would be integrated in the pultrusion step by means of fixed or flexible curvature pultrusion dies, forming a production line capable of continuously outputting an iso-truss structure.

5. **How can the shape of the iso-truss structure be accurately controlled during the manufacturing process?**

   In the envisioned automated production line, the cross-sectional shape and size of members together with fibre volume content would be controlled within the pultrusion process. The process would also control the helical angle and diameter of helical members. A welding jig with heated moulds would ensure accurate positioning of intersections and control their shape, fully defining the iso-truss parameters.

6. **How can the quality of the members of the iso-truss structure be maximised, similar to the quality benefits of conventional vacuum bagging and autoclave procedures for composite plates?**

   By separating the production of the members from other production steps, the quality of individual members can be maximised in the pultrusion process. By minimising deconsolidation during welding through the optimisation of the welding pressure, the final quality of the product should be on par with current aerospace certified composite structures.

7. **How can the manufacturing process of the iso-truss structure be made independent of the desired length of the structure?**

The current iso-truss manufacturing process designed as part of this thesis assumes an iso-truss tube with a fixed length. However, by integrating the helical winding step in the pultrusion phase, it would theoretically be possible to design a production line capable of continuously outputting an iso-truss structure. This is because neither the pultrusion process nor the welding of intersections depend on the length of the product.

With these preliminary answers, it is concluded that it is theoretically possible to produce continuous fibre reinforced iso-truss structures using a scalable and cost-effective automated manufacturing method. The process would rely on existing production capabilities which can easily be scaled up or down, without greatly affecting the cost of equipment. The pultrusion, helical shaping and intersection welding processes can all be easily automated using existing techniques to be able to produce an iso-truss tube of indefinite length. The only limitation of this manufacturing method would be the variation of process parameters within the same iso-truss sample. While it is theoretically possible to vary the radius of curvature of pultrusion dies during the pultrusion process, enabling the possibility of varying the outer diameter and the intersection node-to-node distance along the length of a tube, the current state-of-the-art does not accommodate such a design. While it would also be possible to vary the cross-sectional area of each member along their length, it is considered undesirable as it would negatively affect the fibre volume content for a pultrusion-based process. Instead, it is recommended to construct an iso-truss structure in stages, being connected by a structure that is to be envisioned and produced in future research.

Chapter 10

Recommendations

Due to the time frame of a thesis, many aspects of a research topic simply can not be treated. These aspects form the recommendations for further research, guiding the reader to a continuation of the project in the most interesting directions. For the design of an iso-truss manufacturing method, decisions were made at the top level design to be able to devise a test setup that could be completed within the given time frame of this thesis. However, if given more time, these decisions would likely be altered as well to be able to reach a better end result. These decision changes are discussed in Section 10.1. Furthermore, during the execution of the experiments, aspects to the test setup were discovered that could be improved upon, as can be read in Section 10.2. Perhaps the most important set of recommendations however are with regards to the continuation of this project. With the end result taking longer to attain than was initially believed, a new timeline can be made, taking into account the lessons learned during the execution of the experiments. These recommendations, given as a timeline, are treated in Section 10.3.

10.1 Top Level Design Changes

From a top level design view, several other aspects could be considered to increase feasibility of automated iso-truss manufacturing. First and foremost, a production-ready design for the continuous automated production of iso-truss structures should be designed as an integrated process from the very beginning. In other words, a process should be designed where pultrusion, helical forming and welding are stations inside a single production line. Helical forming would be integrated in this case within the pultrusion process using curved instead of straight dies. The line would then be able to continuously produce these members, which would be fed through a station that welds one circumferential row of intersections at a time. Logistical challenges for this design would include a fibre tensioning system at the end of the line, avoiding the clashing of helical and longitudinal pultrusion dies, which need to output members at similar locations, and a factory large enough to accommodate the full iso-truss length, as it can not be folded once it has been produced.

Other variables to consider from a top level point of view, include the selection of a different set of materials. For example, other thermoplastics can be considered with higher specific properties and better fibre interaction. Additionally, concepts of dual matrix systems could be explored, for example by altering the matrix system in the longitudinal members as compared to the helical members, since they both have different sets of requirements. For the longitudinal members especially, reshaping is not a strict requirement, so perhaps a thermoset matrix system (compatible with the thermoplastic matrix of the helical members) could be considered.

In terms of shape, different concepts can be explored as well. For example, there is currently no requirement that specifies that the helical members must be circular in cross-section. Perhaps rectangular cross sections would make it easier for the members to be formed and reshaped for welding. All of these parameters should be considered from the very beginning of the design process in order to determine the best solution.

10.2 Adaptations to Experimental Setup

After conducting numerous experiments, it was learned that many test setup related aspects could be improved in the future. This section highlights these recommendations, which can be divided into improvements for material characterisation tests, setup for the welding experiments, improvements to the Helical Winder Demonstrator and recommendations for the design and production of the Assembly Demonstrator.

10.2.1 Recommendations on Material Characterisation

As the material characterisation related aspect of the experiments was not the main focus of this project, many details about its test setup could be improved. In general, a standardised test should be designed for characterising the base material of an iso-truss, including SEM, TGA, DSC, DMA and other characterisation experiments. If implemented successfully, these tests could be used to assess different batches of base materials supplied by external companies like DPP and Arkema, providing them with valuable feedback. This collaboration would provide a ground of common interest, where both supplier and user would benefit from an improvement of the product during this process.

The main point of improvement for the characterisation experiments is repetition and varying of the test conditions. This way, aspects like fibre distribution, thermal degradation and outgassing of the material could be better understood. Especially the TGA and DSC experiments should be performed again under different conditions, as these parameters were shown to have somewhat of an effect on the results. Besides this, proper sample preparation and handling should be observed, as this was not done as part of the work performed during this project.

10.2.2 Recommendations on Welding Test Setup

The intersection welding test setup proved to be a simple way of representing a single flattened iso-truss intersection. Using this setup, many different processing conditions could be

investigated in the future to find the best way of joining members of an iso-truss for a given material. To do this, a more standardised and reproducible physical test should be created to assess the joint strength of iso-truss intersection, focusing especially on the boundary conditions: As a simple representation, all member ends were clamped in the current test setup, while in reality the intersections in an iso-truss would not limit rotational freedom.

In order to create this standardised test setup, more production parameters for welded intersections should be changed. It should be designed for more high volume production, providing better alignment for the two mould halves, integrated and faster heating and cooling of the mould blocks and accurate compaction force control, to name a few of the most important parameters. Using this, different mould shapes, compaction forces, temperatures and bonding methods (like adhesive types if thermoplastic welding does not prove feasible) can be assessed. The production setup could also be designed so that different joining techniques can be (re-)assessed, like ultrasonic welding or induction welding, to be able to choose the most suitable method for commercial production.

Additionally, the casting mould for clamping these intersections should be redesigned to reflect the intended boundary conditions, for example using cylindrical or spherical end supports to provide rotational degree of freedom. To make the mould suitable for high-volume production, limitations that were discovered during testing should be addressed. The most important ones include better sealing, higher draft angles to aid in release and more instances of the same mould for parallel production, as this proved to be the bottleneck in producing test samples. Additionally, jig elements should be designed that properly interface with both the machine and this cast support, eliminating the need for external tools during testing, like glue clamps.

For the physical test itself, focus should be placed on the improvement of data collection and on failure analysis. In buckling tests especially, the out-of-plane deformation of the middle member could be recorded over its entire length using a line scanner. Furthermore, strain gauges should be included at key points within the intersection, at least one for every member. As a comparison, a detailed model of a single iso-truss intersection could be created, taking into account the boundaries of an actual iso-truss and perhaps even the failure mechanisms observed in testing, with the exception of fibre-matrix interface failure provided this can be improved in the future.

10.2.3 Recommendations on the Helical Winder Demonstrator

Due to its extensive design, production and fine-tuning process, experimentation with the Helical Winder Demonstrator was limited. Although demonstration of helical winding could be achieved at the end, the process can still be improved in a variety of ways. Most importantly, this should be done by continuing current experiments to assess different processing temperatures and winding speeds. The most important improvements to the design itself include a better sample retention mechanism (for example using inserts or threaded connections instead of bonded beads) and more consistent heating and insulation to improve the temperature distribution in the test chamber. Additionally, the counterweight system should be improved to provide a more controlled and measurable pre-load on the samples, and friction between the central cylinder and samples should be reduced to prevent the phenomena observed during testing.

After optimising the process for fully thermoplastic samples, the setup could be adapted for use with composite materials. While improvement of this method would likely focus mostly on material-related aspects like fibre-matrix interface and resin volume content, other concepts can still be re-assessed. These concepts would include re-assessment of the possibility to pre-twist samples or establishing higher pre-tension to limit kinking, as well as the possibility of using resistance heating in the winding test setup for more consistent heating of carbon based composite samples.

As recommendations for future improvement of the design to assess the feasibility of automated production, the current crank system could be replaced by a motor controlled assembly, to provide a controlled and repeatable input to both the winding angle and the winding rate. On top of this, the central cylinder could be redesigned to offer adaptability in the diameter of the helices.

10.2.4 Recommendations on (the design of) the Assembly Demonstrator

Because it was not possible to reach a production-ready design stage for the Assembly Demonstrator, it is important to establish recommendations for improvement and finalisation of the design.

Firstly, recommendations from the welding tests should be incorporated into the detailed design of the mould blocks for the Assembly Demonstrator, including the shape of the moulds, effective heating (and perhaps cooling), determination of the pressure on the samples and alignment of the mould halves. Secondly, the modules for the assembly demonstrator should be designed for easy alignment of the mould blocks at the correct reproducible height (which is to be determined), as well as insulation from the heated moulds. Another important aspect to consider is the design of the end fixtures for the iso-truss members, as they provide initial alignment of unwelded samples. They should provide a rigid and precise connection for the samples on one hand, while allowing for flexibility to accommodate inaccuracies in helical shape and compaction travel of the members on the other hand.

Finally, for future improvement of the design, the mould blocks should be designed with integrated heating and cooling in mind, similar to the welding tests. Mechanically, the setup should be adapted to accommodate an iso-truss structure which is only able to translate as part of a continuous and automated production line. This can be done by using a retractable translating module for inner support and a single circumferentially positionable mould block on the outside of the iso-truss.

10.3 Project Timeline

Taking all the discovered recommendations into account, a road map can be made for continuation of research into the automation of iso-truss production. This road map can be seen as a multi-year plan, which is believed to best be executed as part of a PhD project. It is believed that the most crucial steps can be taken within such a time frame, providing a definitive answer to the original research question within four years. For this question to be answered, the following steps are thought to be of crucial importance:

1. Continuation of helical winding tests and production of helices using PMMA rods
2. Development of the Assembly Demonstrator and demonstration of iso-truss production using PMMA rods as helicals
3. Establishment of a collaboration project with material suppliers to improve material characteristics
4. Development of a standardised test method for composite pultrusion samples
5. Extensive testing of different material batches from suppliers and selecting the best batch for use in iso-truss production
6. Demonstration of iso-truss production using currently established shape parameters
7. Demonstration of iso-truss production using different shape parameters
8. Design, production and physical testing of the first iso-truss optimised for a given load case

These steps are to be distributed over a four year planning. It is believed that step 1,2 and 3 can be executed within the first year, as elaborated on below. During the second year, research should be focused on step 4 and 5, after which the third year focuses on the execution of step 6. This leaves the execution of the final two steps for the fourth year, although these steps could be seen as supplementary if the project would inevitably be delayed. Additionally, a road map can be set out for continuation of this project beyond this scope.

10.3.1 Year 1

The first step, the production of helical samples using PMMA rods, focuses on the continuation of current tests, although with a few adjustments. Firstly, a test setup or jig should be designed for the simultaneous bonding of beads for five PMMA rod samples so that they can be wound together in one process. If bead bonding proves ineffective, other high-temperature rod retention mechanisms like aluminium bonded or threaded inserts should be investigated. Furthermore, the current heating mechanism should be adapted to work with the 300 mm diameter cylinder by ordering a silicon heating blanket of the appropriate size. Heat insulation should be improved as well to provide a stable and even temperature environment inside the test chamber. This is done by improving retention of the currently employed aluminium duct. After these improvements have been realised, testing of 500 mm long PMMA rods can resume until samples with constant curvature and repeatable height change can be produced. As part of these tests, stress relaxation of the produced samples at elevated temperatures should be assessed as well, and should then be accounted for in the winding process. As a milestone to this process, the first helical samples for intended use in an iso-truss are to be be produced.

In parallel with this process, focus should be directed to step 2: Continued development of the Assembly Demonstrator. Finalisation of the design of this demonstrator has already been discussed in this chapter, focusing on the production of both 200 mm and 300 mm diameter iso-trusses. Before this can be done however, the welding mould blocks for use with these

helical samples should be developed, produced and tested. After welding has been successfully demonstrated, the final design can be produced in collaboration with DEMO, paving the way for the second milestone: Production of the first iso-truss structure using PMMA based helices and carbon-Elium based longitudinal members.

In order to ensure continued experimentation, this year should be used for the establishment of a collaboration project together with the carbon-Elium material suppliers (DPP and Arkema). While the project itself would be executed during the second year, several conditions could already be met. These would include the planning of feedback meetings with both DPP and Arkema, as well as the establishment of parameters for different test batches. Through collaboration with DPP, the fibre-matrix interface of the carbon-Elium composite could be improved by experimenting with different fibre sizings, while discussing the possibility of varying the fibre-volume fraction as part of the batch parameters. Through this collaboration, small testing batches with different samples can be developed instead of having to work with one large batch of material.

10.3.2 Year 2

The main focus in the second year of this project is on extensive testing of the different material batches made by DPP. To do this, the current test setup for the assessment of the the joint strength will be adapted for high experimental repeatability, while all important test conditions will be recorded for every sample. In addition to these experiments, material characterisation tests, including oven and winding experiments, SEM, TGA, DSC and DMA, will be included in a standardised test setup to be able to compare different material batches. For physical testing, the current compression test casting mould design will be adapted to accommodate improvements, and several instances of this mould will be produced for parallel compression sample production. This way, a welding testing batch of at least 50 samples can be produced, creating a solid test base. After conducting these physical tests, feedback shall be created for the material suppliers for a final material iteration for use in an iso-truss.

10.3.3 Year 3

After the development of a final material iteration with improved fibre-matrix interface and optimal fibre-volume fraction, focus can finally be shifted to the production and physical testing of several full carbon-Elium composite iso-truss samples. As initially envisioned, around four of these will be produced, each with a different combination of helical pitch (50 mm and 75 mm) and outer diameter (200 mm and 300 mm). At least one of these iso-trusses will be physically tested by encasing the ends of the tube in a supporting material and loading the truss in compression until failure. If possible, this test will be compared to an IsoTruss tube of similar shape and size, normalising the results with respect to the weight of either sample.

10.3.4 Year 4

With the production process fully demonstrated, emphasis during the fourth year will be on adapting the already existing production facilities to be able to produce composite iso-trusses

with parameters outside the initially envisioned design parameters. In parallel, using the physical test data obtained from previous iso-truss tubes, an iso-truss will be designed and optimised for a given load case. Without prior knowledge of the resulting design during the adaptation of the production process, it should then be possible to produce this iso-truss design using the improved facilities. Final validation can then be obtained by physically loading the iso-truss until failure, and comparing these results to the predictions. This would be an important milestone, envisioned as a completion of the PhD requirements by providing a definite answer to the original research question:

Can composite continuous fibre reinforced iso-truss structures be produced using a scalable and cost-effective automated manufacturing method?

10.3.5 5+ Years

Even after conclusion of this project, improvements to the design can still be made. During this stage, focus is shifted to commercialising the existing production process and allowing pultrusion based iso-truss structures to compete in markets for both the IsoTruss (civil applications) and open lattice structures (Aerospace applications). This is seen as a project that exceeds any single academic endeavour in terms of length, while also providing little added benefit to the body of science. It is therefore recommended that a pursuit of this project is better suited to a company interested in investing in its potential.

The road map for this project can be divided into the following steps:

1. Adapt the current production process for a more high-performance thermoplastic material
2. Develop a continuous production process for an iso-truss with one set of shape parameter
3. Adapt the production process for the creation of different iso-truss shapes by adaptable inputs
4. Conceptualise and produce an iso-truss end cap design for the introduction of different loads
5. Create a load case optimisation tool specifically for iso-truss structures
6. Adapt the iso-truss production process for commercial applications

References

[1] D. W. Jensen, "Using External Robots Instead of Internal Mandrels to Produce Composite Lattice Structures," in *International Conference on Textile Composites (TEXCOMP10)*, 2010, p. 2019.

[2] V. V. Vasiliev, V. A. Barynin, and A. F. Razin, "Anisogrid composite lattice structures - Development and aerospace applications," *Composite Structures*, vol. 94, no. 3, pp. 1117–1127, 2012.

[3] L. Pavlov, I. te Kloeze, B. J. R. Smeets, and S. M. S. Simonian, "Development of mass and cost efficient grid-stiffened and lattice structures for space applications," ATG Europe, Tech. Rep. September, 2016.

[4] V. V. Vasiliev, V. A. Barynin, and A. F. Rasin, "Anisogrid lattice structures - Survey of development and application," *Composite Structures*, vol. 54, no. 2-3, pp. 361–370, 2001.

[5] M. J. Jensen, D. W. Jensen, and A. D. Howcroft, "Continuous manufacturing of cylindrical composite lattice structures," in *Recent Advances in Textile Composites*, 2010, pp. 80–87. [Online]. Available: https://www.scopus.com/inward/record.uri?eid=2-s2.0-79952382503&partnerID=40&md5=c6989334f48bf640d76e19d5b62c1af0

[6] B. Asay and D. W. Jensen, "Manufacturing of carbon/epoxy isobeam lattice structures," Brigham Young University, Tech. Rep., 2015. [Online]. Available: https://www.scopus.com/inward/record.uri?eid=2-s2.0-84966589278&partnerID=40&md5=9219cabceb61969eac2df52d3bae9e5c

[7] V. Barynin, V. Bunakov, A. Rasin, and V. Vasiliev, "Aerospace composite lattice structures," *International Conference on Composite Materials*, 1999.

[8] D. Wang, M. M. Abdalla, Z. P. Wang, and Z. Su, "Streamline stiffener path optimization (SSPO) for embedded stiffener layout design of non-uniform curved grid-stiffened composite (NCGC) structures," *Computer Methods in Applied Mechanics and Engineering*, vol. 344, no. September, pp. 1021–1050, 2019.

[9] C. Bellini and L. Sorrentino, "Mould design for manufacturing of isogrid structures in composite material," *Procedia Structural Integrity*, vol. 9, pp. 172–178, 2018. [Online]. Available: https://linkinghub.elsevier.com/retrieve/pii/S2452321618300271

[10] H. Wu, C. Lai, F. Sun, M. Li, B. Ji, W. Wei, D. Liu, X. Zhang, and H. Fan, "Carbon fiber reinforced hierarchical orthogrid stiffened cylinder: Fabrication and testing," *Acta Astronautica*, vol. 145, no. January, pp. 268–274, 2018. [Online]. Available: https://doi.org/10.1016/j.actaastro.2018.01.064

[11] G. Totaro and F. De Nicola, "Recent advance on design and manufacturing of composite anisogrid structures for space launchers," *Acta Astronautica*, vol. 81, no. 2, pp. 570–577, 2012. [Online]. Available: http://dx.doi.org/10.1016/j.actaastro.2012.07.012

[12] M. Buragohain and R. Velmurugan, "Optimal design of filament wound grid-stiffened composite cylindrical structures," *Defence Science Journal*, vol. 61, no. 1, pp. 88–94, 2011. [Online]. Available: http://dx.doi.org/10.1016/j.compstruct.2010.06.003

[13] D. Jensen, "IsoTruss Industries, LLC," 2019. [Online]. Available: http://www.isotruss.com/

[14] T. J. Weaver and D. W. Jensen, "Mechanical characterization of a graphite/epoxy IsoTruss," *Journal of Aerospace Engineering*, vol. 13, no. 1, pp. 23–35, 2000.

[15] C. M. H.-. (CMH-17), *Composite Materials Handbook, Volume 3 - Polymer Matrix Composites - Materials Usage, Design, and Analysis (CMH-17)*. SAE International on behalf of CMH-17, a division of Wichita State University, 2012. [Online]. Available: https://app.knovel.com/hotlink/toc/id:kpCMHVPM1E/composite-materials-handbook/composite-materials-handbook

[16] M. Biron, *Thermoplastics and Thermoplastic Composites*, 3rd ed. Matthew Deans, 2018.

[17] Arkema, "Elium Resins for Composites," 2019. [Online]. Available: https://www.arkema.com/en/products/product-finder/range-viewer/Elium-resins-for-composites/

[18] "Dunstone Hi-Shrink Tapes," 2019. [Online]. Available: https://www.shrinktape.com/products/hi-shrink-tapes/

[19] C. Decker, "Photoinitiated Crosslinking Polymerisation," *Progress in Polymer Science*, vol. 21, pp. 593–650, 1996.

[20] D. Bird, E. Caravaca, J. Laquidara, K. Luhmann, and N. M. Ravindra, *Formulation of Curable Resins Utilized in Stereolithography*. Springer International Publishing, 2019. [Online]. Available: http://dx.doi.org/10.1007/978-3-030-05861-6_148

[21] Y. J. Park, D. H. Lim, H. J. Kim, D. S. Park, and I. K. Sung, "UV- and thermal-curing behaviors of dual-curable adhesives based on epoxy acrylate oligomers," *International Journal of Adhesion and Adhesives*, vol. 29, no. 7, pp. 710–717, 2009. [Online]. Available: http://dx.doi.org/10.1016/j.ijadhadh.2009.02.001

[22] Y. Okamoto, P. Klemarczyk, S. Levandoski, V. Hanlon, and J. Bremmer, "Novel UV cure filament winding," in *Conference on Composites Manufacturing and Tooling '94*, 1994, pp. 94–111. [Online]. Available: https://www.scopus.com/inward/record.uri?eid=2-s2.0-0028061009&partnerID=40&md5=ee9f22a58a347762cc7f49cfaffce51c

[23] P. Apostolidis, X. Liu, C. Kasbergen, M. F. C. V. D. Ven, and A. Scarpas, "Advances in Materials and Pavement Performance Prediction," Delft University of Technology, Tech. Rep., 2018.

[24] C. Severijns, S. T. D. Freitas, and J. A. Poulis, "On the Assessment of Susceptor-Assisted Induction Curing of Adhesively Bonded Joints," *International Journal of Adhesion and Adhesives*, vol. 75, pp. 155–164, 2017.

[25] Intertronics, "Thermally conductuve gasket," 2018. [Online]. Available: https://www.intertronics.co.uk/wp-content/uploads/2016/11/TB2007-12-Thermally-Conductive-Silicones.pdf

[26] B. Jongbloed, J. Teuwen, G. Palardy, and I. F. Villegas, "Improving weld uniformity in continuous ultrasonic welding of thermoplastic composites," in *ECCM18: 18th European Conference on Composite Materials*, 2018, pp. 24–28. [Online]. Available: https://repository.tudelft.nl/islandora/object/uuid%3A22b7283a-71c1-4fdf-80db-1008ac98c076

[27] Y. Kyosev, *Braiding machine components*. Woodhead Publishing, 2015.

[28] "NLR Automated Composite Manufacturing Pilot Plant," 2019. [Online]. Available: https://www.nlr.org/article/automated-composite-manufacturing-pilot-plant/

[29] N. Minsch, F. H. Herrmann, T. Gereke, A. Nocke, and C. Cherif, "Analysis of Filament Winding Processes and Potential Equipment Technologies," *Procedia CIRP*, vol. 66, pp. 125–130, 2017. [Online]. Available: http://dx.doi.org/10.1016/j.procir.2017.03.284

[30] N. Minsch, M. Müller, T. Gereke, A. Nocke, and C. Cherif, "Novel fully automated 3D coreless filament winding technology," *Journal of Composite Materials*, vol. 52, no. 22, pp. 3001–3013, 2018.

[31] F. C. Shen, "A filament-wound structure technology overview," *Materials Chemistry & Physics*, vol. 42, no. 2, pp. 96–100, 1995.

[32] J. Driezen, "Integration and optimisation of a novel industrial Fused Composite Manufacturing process for prepreg filament," Ph.D. dissertation, Delft University of Technology, 2019.

[33] F. Di Caprio, V. Acanfora, S. Franchitti, A. Sellitto, and A. Riccio, "Hybrid Metal/Composite Lattice Structures: Design for Additive Manufacturing," *Aerospace*, vol. 6, no. 6, p. 71, 2019.

[34] "vDijk Pultrusion Products," 2020. [Online]. Available: https://www.dpp-pultrusion.com/

[35] "Torayca Product Lineup," 2019. [Online]. Available: http://www.torayca.com/en/lineup/product/pro_001_01.html

[36] C. M. H.-. (CMH-17), *Composite Materials Handbook, Volume 3 - Polymer Matrix Composites - Materials Usage, Design, and Analysis (CMH-17)*. SAE International, 2012, vol. 3, no. 1.

[37] T. Hirata, T. Kashiwagi, and J. Brown, "Thermal and Oxidative Degradation of Poly(methyl methacrylate): Weight Loss," *Macromolecules*, vol. 18, pp. 1410–1418, 1985.

[38] L. C. Thomas, "Interpreting Unexpected Events and Transitions in DSC Results," *Government Information Quarterly*, vol. 27, no. 4, pp. 423–430, 2010.

[39] Thomas-Technik, "Radius Pultrusion," 2021. [Online]. Available: https://www.thomas-technik.de/en/pultrusion/process/radius-pultrusion

Appendix A

Test Sample Details

A.1 Experimental Intersections (X)

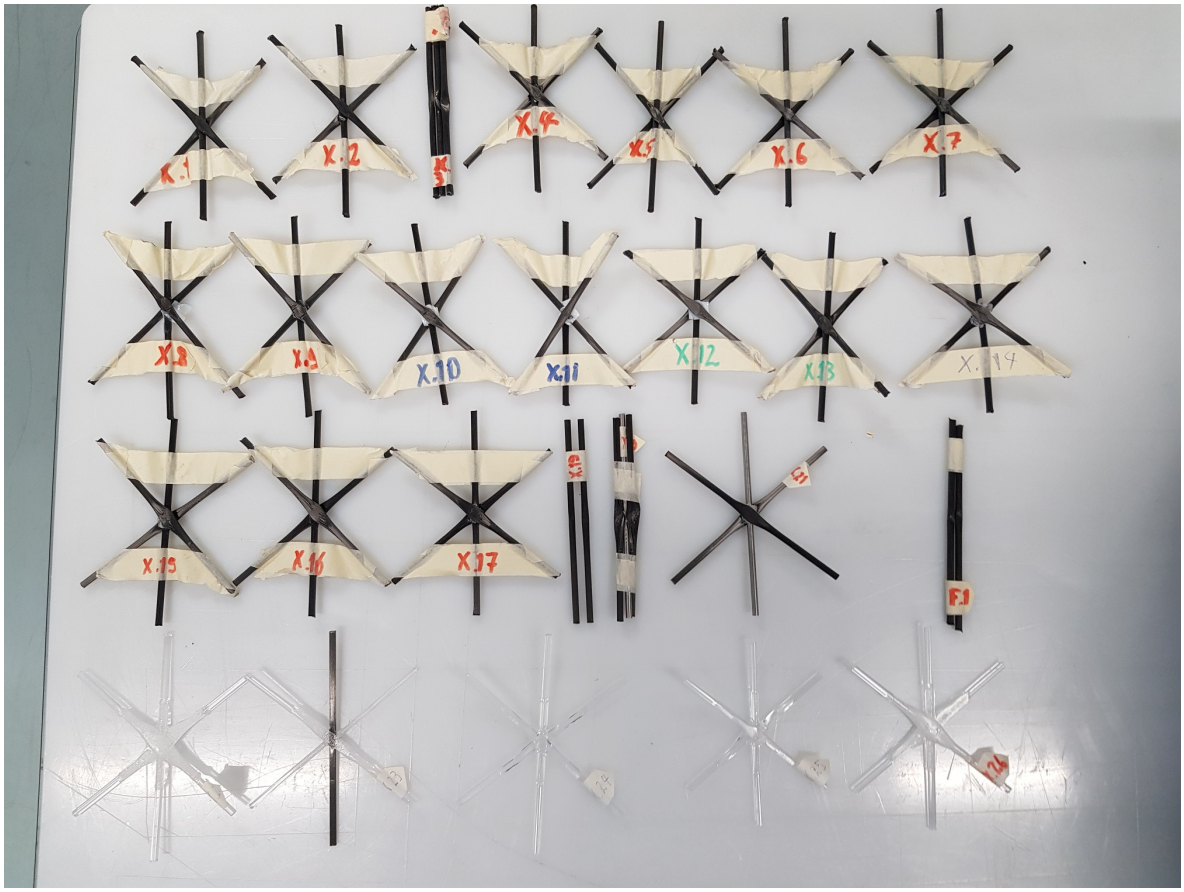

Figure A.1: Overview of experimental intersection samples

Table A.1: Experimental Intersection Sample Details (X)

ID	T [°C]	Heating	Weight	Foil	Notes
X.1	< 170	Oven	Clamp	None	RT for members, quick cool
X.2	< 180	Oven	Clamp	None	RT for members, slow cool
X.3	< 170	Oven	Clamp	None	170 °C for members, quick cool
X.4	< 170	Oven	Clamp	None	RT for members, quick cool
X.5	< 180	Oven	Clamp	None	USW alignment jig, steel core
X.6	< 180	Oven	Clamp	None	No jig, steel core
X.7	< 170	Oven	Clamp	None	170 °C for members, steel core
X.8	< 170	Oven	Clamp	PETG	Shifted foil
X.9	< 170	Oven	Clamp	PETG	-
X.10	< 170	Oven	20 kg	PETG	New alignment jig (from here on)
X.11	< 180	Oven	20 kg	PETG	Shifted foil
X.12	< 190	Oven	40 kg	PETG	Slow cool
X.13	< 170	Oven	20 kg	None	-
X.14	< 170	Oven	20 kg	PP	-
X.15	180	Oven	40 kg	PMMA	Heated again during consolidation
X.16	< 190	Oven	20 kg	PMMA	-
X.17	195	Solder	20 kg	PMMA	New setup test
X.18	180	Solder	20 kg	PMMA	Intersection Test (IT) sample
X.19	190	Solder	20 kg	Kapton	Pre-forming test
X.20	190	Solder	40 kg	PMMA	Steel core
X.21	200	Solder	20 kg	PMMA	Processed steel core
X.22	200	Solder	20 kg	None	Full PMMA
X.23	180	Solder	20 kg	None	PMMA-carbon mix
X.24	160	Solder	20 kg	None	Full PMMA
X.25	160	Solder	20 kg	PMMA	Full PMMA
X.26	160	Solder	20 kg	None	Full PMMA, long consolidation

A.2 Tested Intersections (IT)

During the production of intersection test samples, the Solder Heating Parameters Form would be filled in for each and every sample in order to record key aspects that could influence test results. The most important test parameters are already presented in Table 6.1. The standard form can be found on the next page.

Solder Heating Parameters Form

Date	

Test Conditions

Sample name	IT.
Intersection test type	
Welding temperature [°C]	
Consolidation weight [kg]	
Approximate sample compression time [s]	~
Options:	
Moulds heated together	Moulds heated separately
Members positioned before heating up	Members positioned after heating up
Comments:	

Sample Parameters

Members	Longitudinal Member	Lower Helical Member	Upper Helical Member
Length [mm]			
Diameter [mm]			
Weight [g]			

PMMA Foil	Lower Foil	Upper Foil
Size [mm x mm]		
Thickness [mm]		
Weight [g]		

Recorded Temperatures

	Before positioning samples	After positioning samples	After applying weight	Before weight removal
Upper mould [°C]				
Lower mould [°C]				

Welded weight [g]	

A.3 Oven Samples (O)

Table A.2: Oven Sample Details (O)

ID	Test	L [mm]	T [°C]	Notes
O.1	Form	160	170	Deformation test for welding
O.2	Form	490	160	Bending
O.3	Form	490	160	Twisting + bending
O.4	Form	490	160	Twisting + bending
O.5	Form	490	160	Twisting, stress release
O.6	Cylinder	490	130	Silicon heater mat test
O.7	Form	300	140	Thermocouple reference
O.8	Form	300	90	Bending
O.9	Form	300	95	Bending
O.10	Form	300	100	Bending
O.11	Form	300	110	Bending
O.12	Form	300	140	Bending
O.13	Creep	300	90	30 mm deflection
O.14	Creep	300	90	15 mm deflection
O.15	Creep	300	90	20 mm deflection
O.16	Creep	300	80	11 mm deflection, 1 h
O.17	Creep	300	60	11 mm deflection, 15 h (2x)
O.18	Creep	300	60	16 mm deflection
O.19	Creep	300	70	11 mm deflection
O.20	Creep	300	70	15 mm deflection
O.21	Creep	300	60	12 mm deflection, 15 h
O.22	Twist	300	120	540°, no weight
O.23	Twist	300	120	540°, 5 kg weight, 15 min
O.24	Twist	300	120	360°, no weight, 1 h
O.25	Twist	300	150	360°, no weight, 30 min
O.26	Twist	300	120	360°, no weight, 15 h
O.27	Twist	300	150	360°, 5 kg weight, 6 h
O.28	Twist	300	150	1440°, no weight, 5 h
O.29	Twist	300	-	Not tested

Figure A.2: Overview of the twisted samples O.22 to O.29

A.4 Helical Winding Samples (H)

Table A.3: Helical Winding Sample Details (H)

ID	Pieces	L [mm]	T [°C]	θ [°]	Material	Load
H.1	5	490	20	100	Carbon-Elium	−5 kg
H.2	5	490	115	180	Carbon-Elium	−5 kg
H.3	5	495	140	180	Carbon-Elium	−5 kg
H.4	1	500	90	180	PMMA	5 kg
H.5	1	500	100	180	PMMA	5 kg
H.6	1	500	90	215	PMMA	5 kg
H.7	1	500	95	215	PMMA	5 kg
H.8	1	490	90	0	Carbon-Elium	10 kg
H.9	1	490	105	180	Carbon-Elium	5 kg
H.10	1	500	95	270	PMMA	5 kg

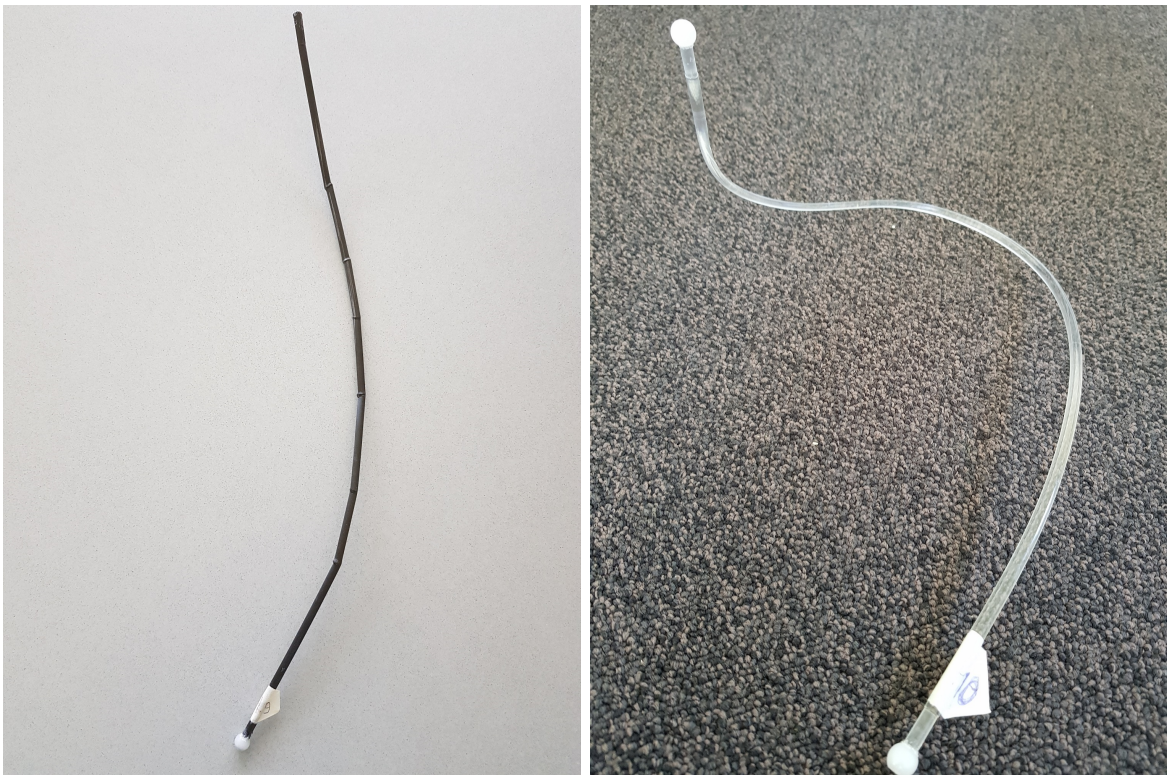

(a) Carbon-Elium sample H.9 showing kinking at several locations

(b) PMMA sample H.10 showing stretching and local curving

Figure A.3: Samples highlighting the defects observed during winding experiments

A.5 Other Samples (E/U)

Figure A.4: Resistance heating sample after bending

Table A.4: Ultrasonic Welding Sample Details (U)

ID	Pieces	US-time [ms]	Weld distance [mm]	F_{form} [N]	F_{cons} [N]
U.1	3	197	1.70	300	500
U.2	2	1697	2.12	50	100
U.3	1	1333	2.05	30	30
U.4	1	608	1.94	30	30
U.5	1	384	1.94	30	30

Appendix B

Material Characterisation Supplementary Data

B.1 SEM

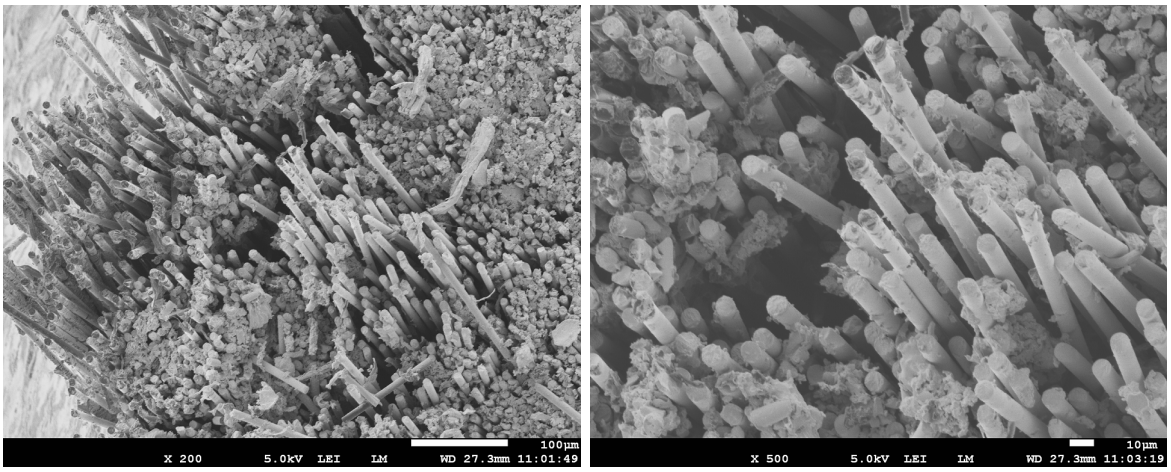

Figure B.1

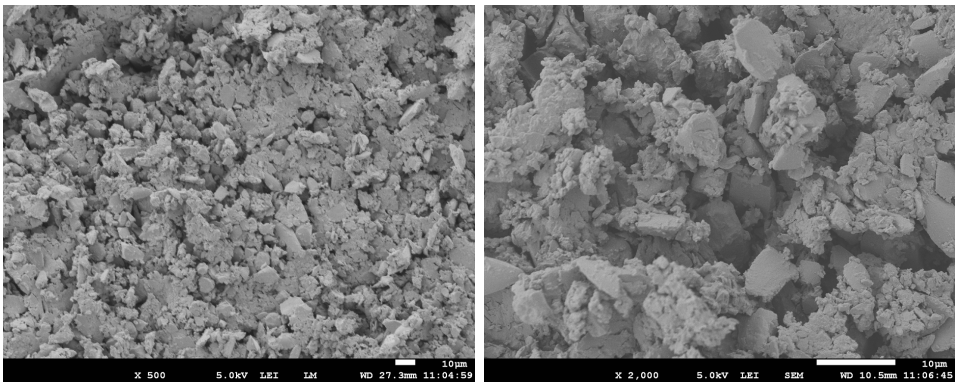

Figure B.2

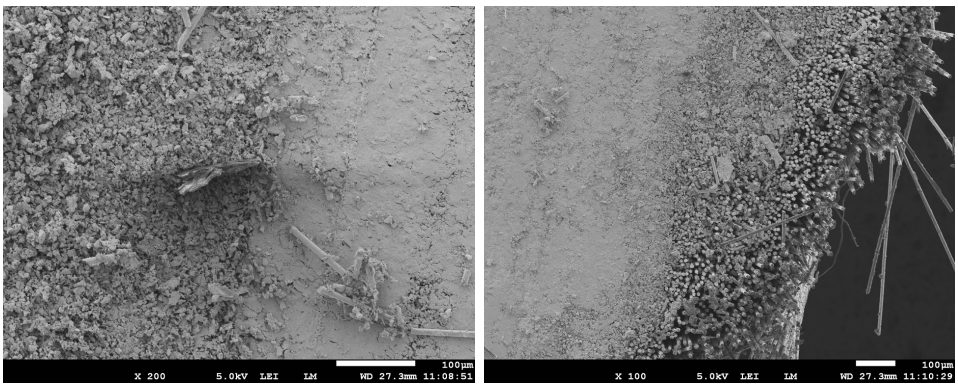

Figure B.3

B.2 DSC

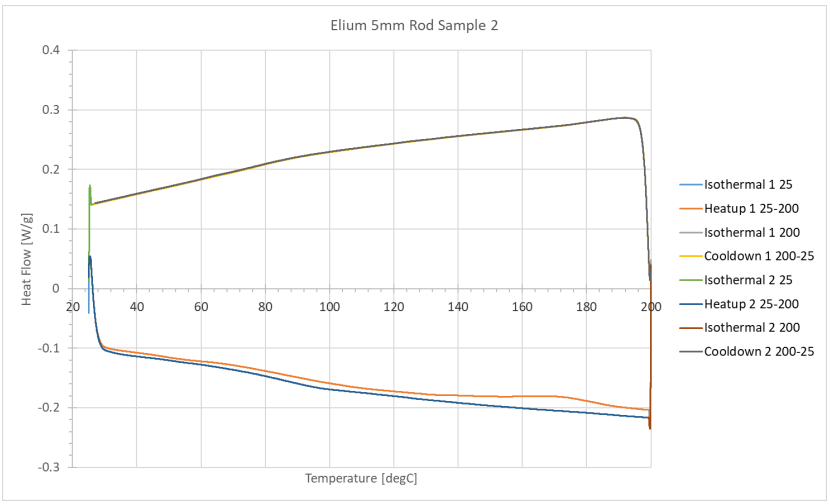

Figure B.4: Different Scanning Calorimetry of one of the Elium-carbon composite samples

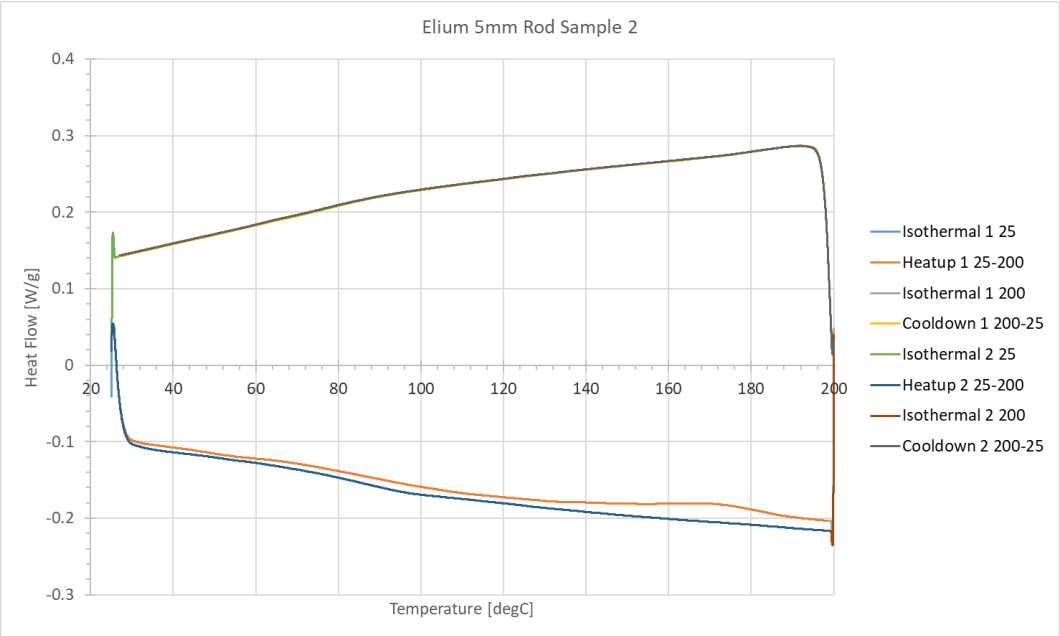

Figure B.5: Different Scanning Calorimetry of one of the Elium-carbon composite samples

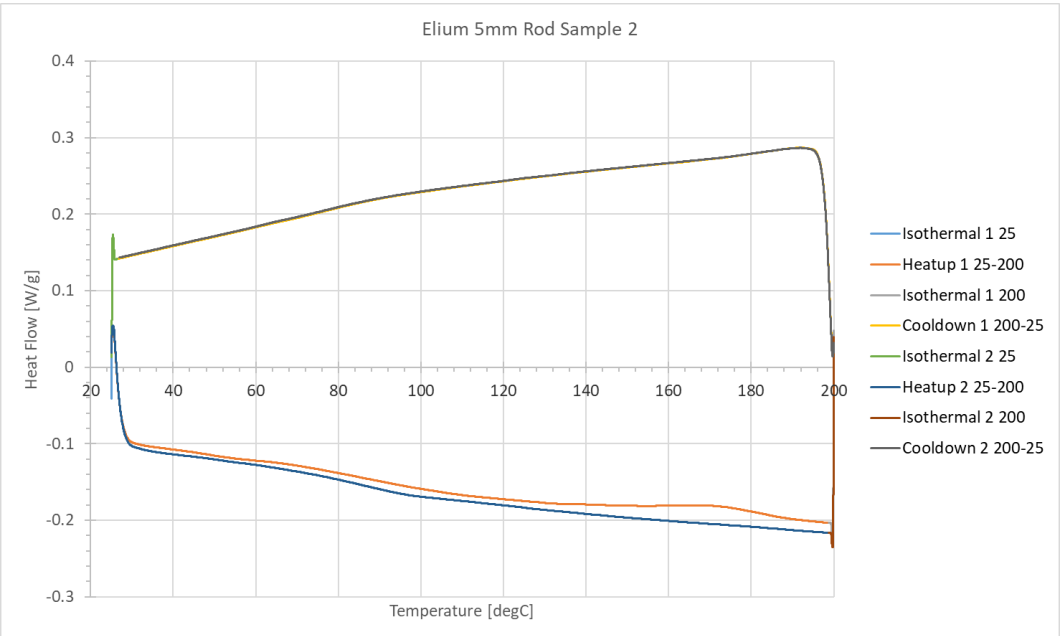

Figure B.6: Different Scanning Calorimetry of one of the Elium-carbon composite samples

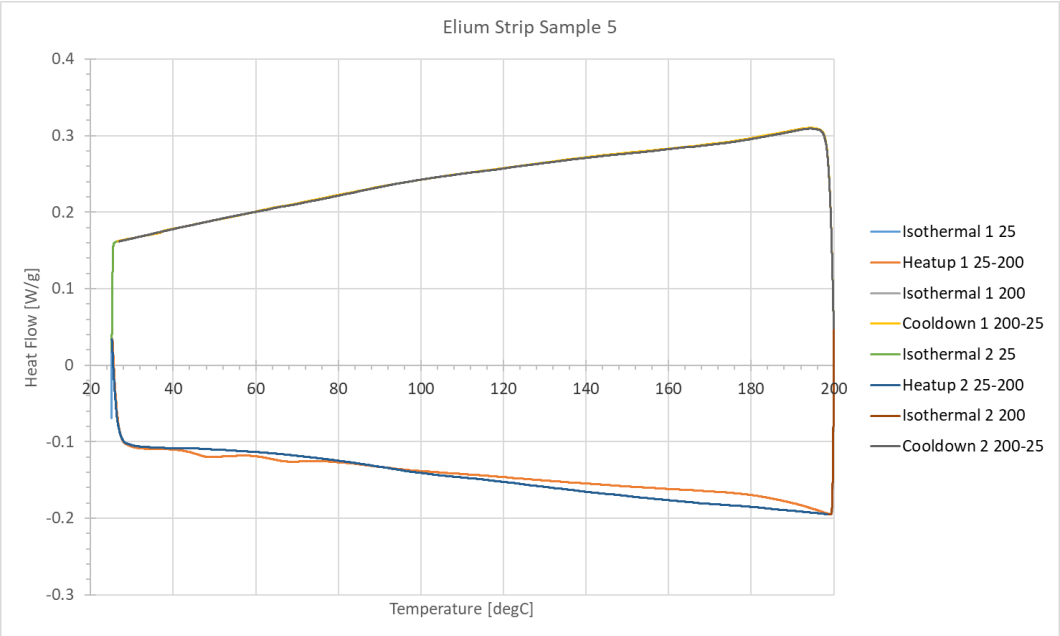

Figure B.7: Different Scanning Calorimetry of one of the Elium-carbon composite samples

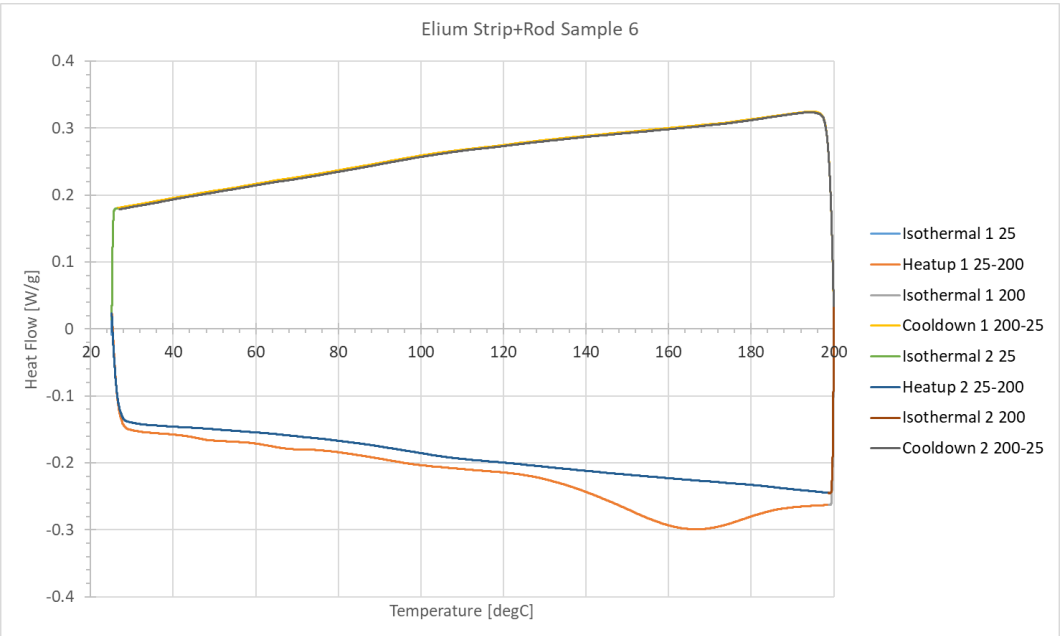

Figure B.8: Different Scanning Calorimetry of one of the Elium-carbon composite samples

B.3 DMA

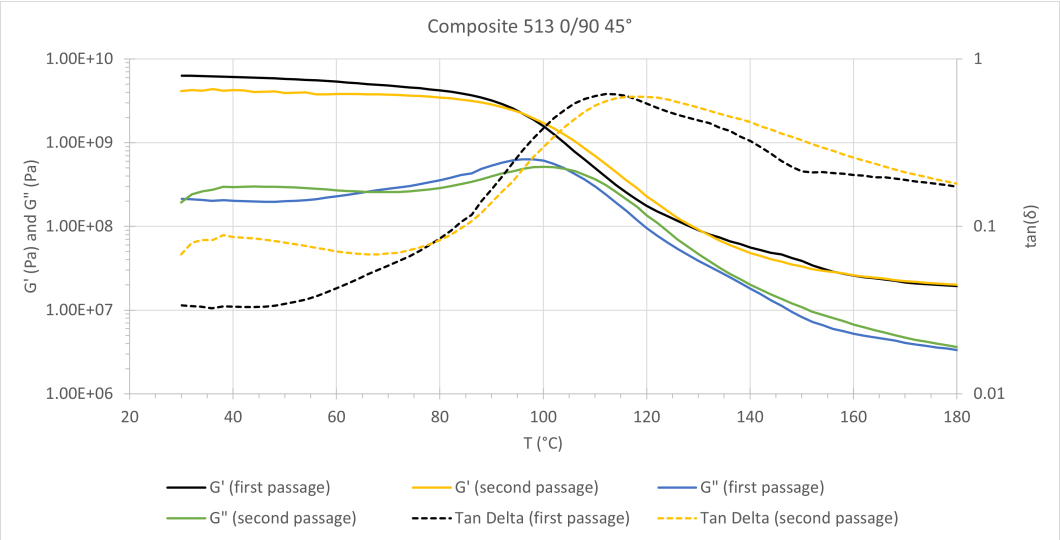

Figure B.9: Dynamic Mechanical Analysis of a carbon-Elium composite sample. Data provided by Arkema

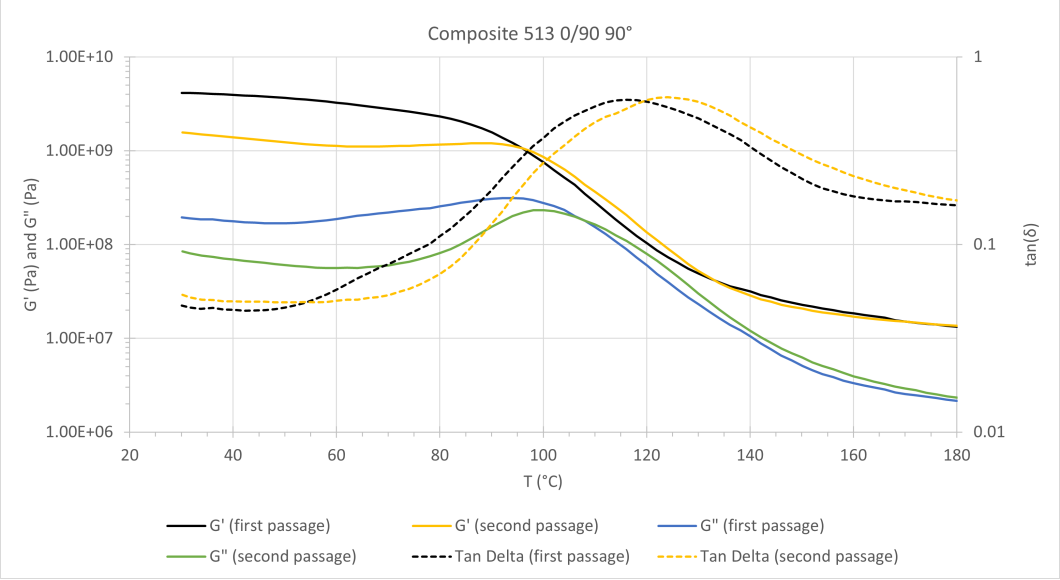

Figure B.10: Dynamic Mechanical Analysis of a carbon-Elium composite sample. Data provided by Arkema

B.4 Externally Supplied DSC

As presented on the next two pages, showing a single heat cycle each.

Sample: INS0007744-33 1263
Size: 16.3700 mg
Method: 25-220°C - 2 passages iso 5 min

DSC

File: C:...\INS0007744-33 1263 - 1er passage
Operator: AC
Run Date: 19-Jun-2020 13:06
Instrument: DSC Q20 V24.11 Build 124

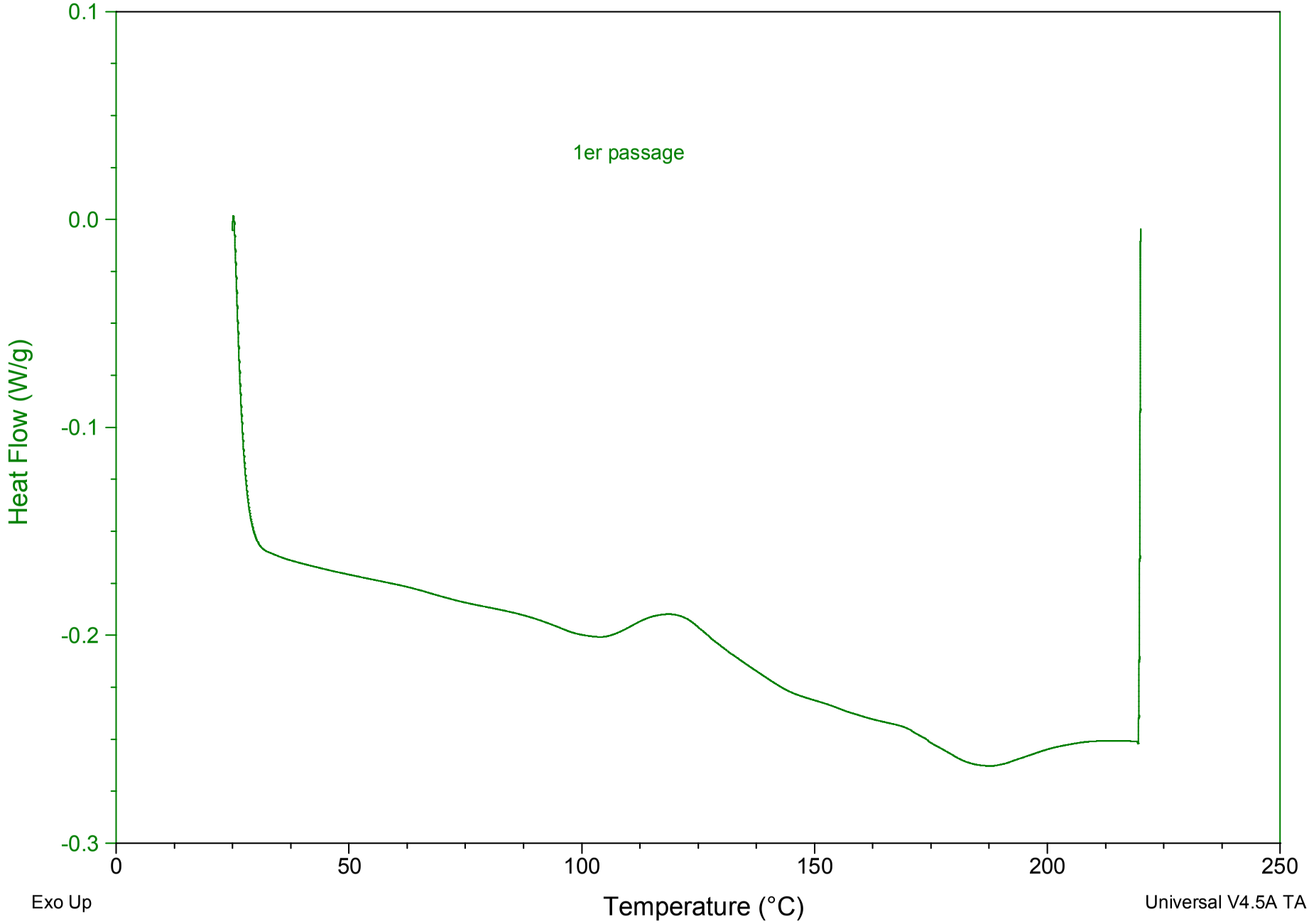

Sample: INS0007744-33 1263
Size: 16.3700 mg
Method: 25-220°C - 2 passages iso 5 min

DSC

File: C:...\ISI0126378\INS0007744-33 1263.001
Operator: AC
Run Date: 19-Jun-2020 13:06
Instrument: DSC Q20 V24.11 Build 124

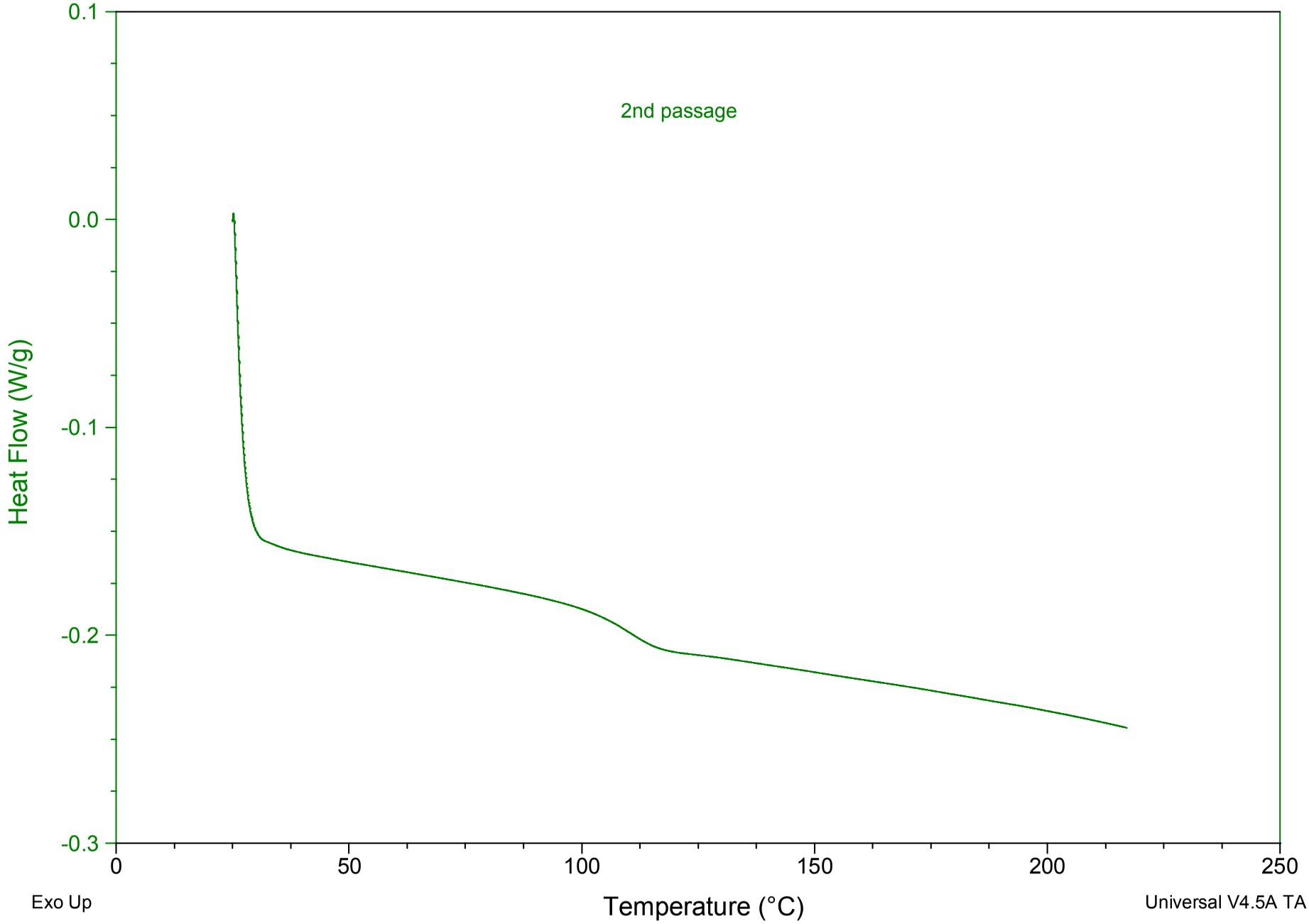

Appendix C

Physical Test Graphs

C.1 Shear Tests

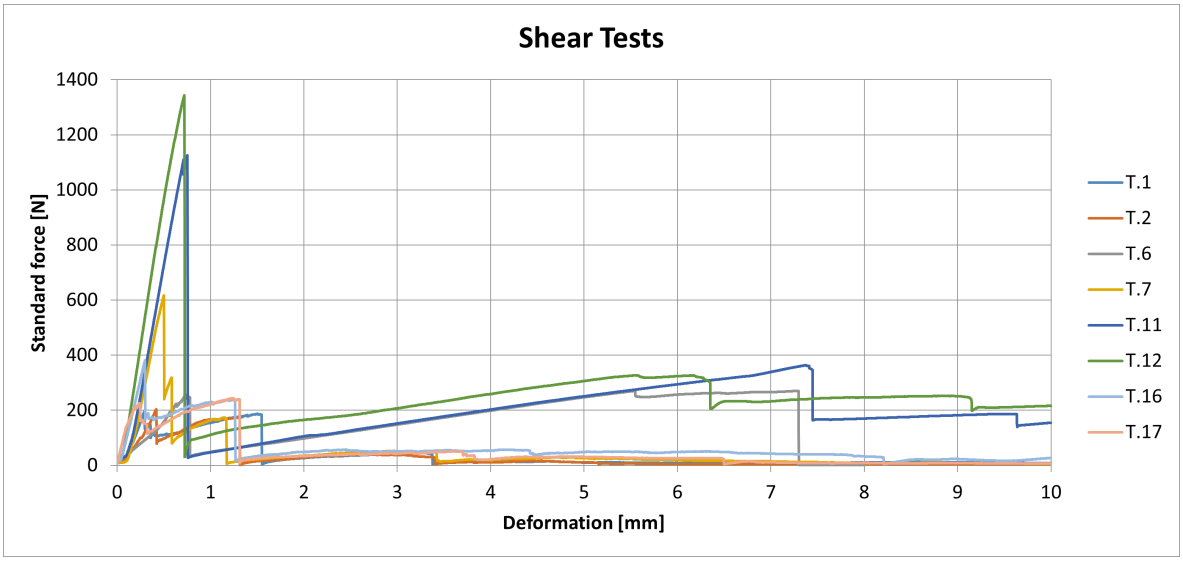

Figure C.1: Overview of all different shear tests

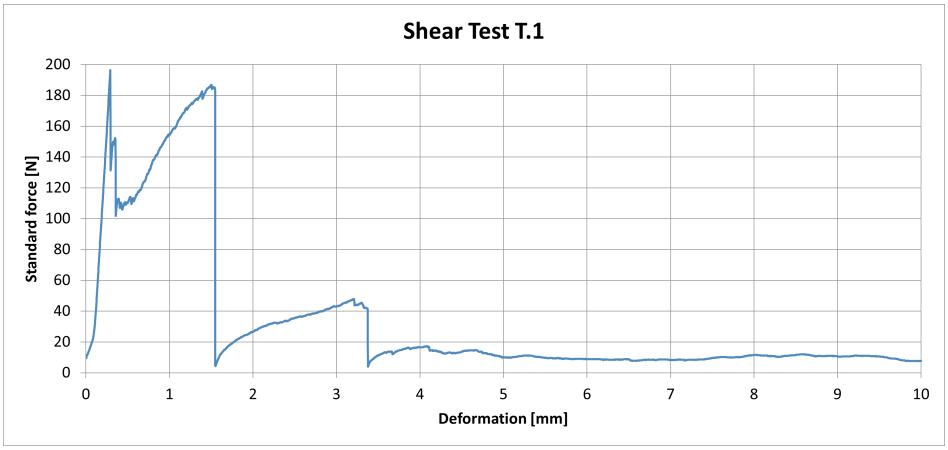

Figure C.2: Load-displacement graph for shear test sample 1

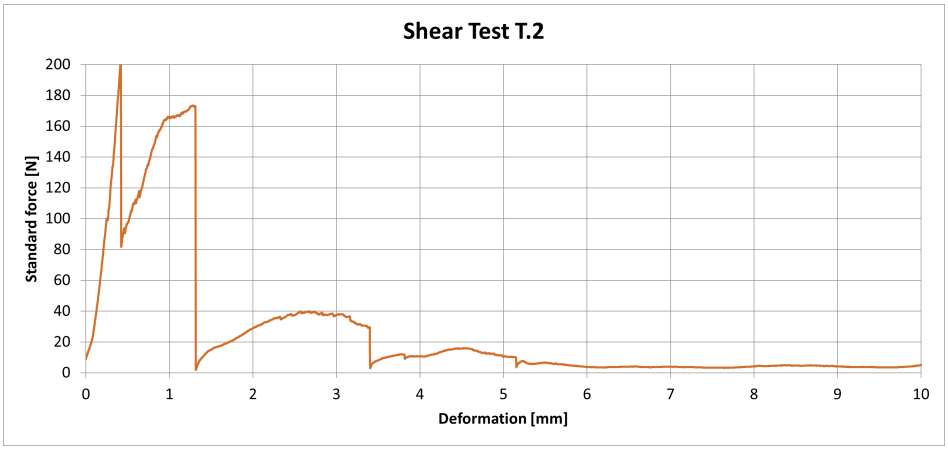

Figure C.3: Load-displacement graph for shear test sample 2

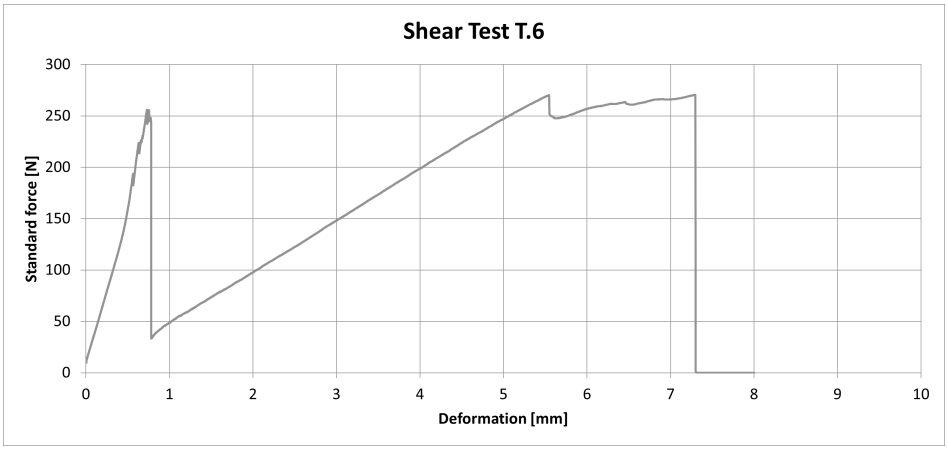

Figure C.4: Load-displacement graph for shear test sample 6

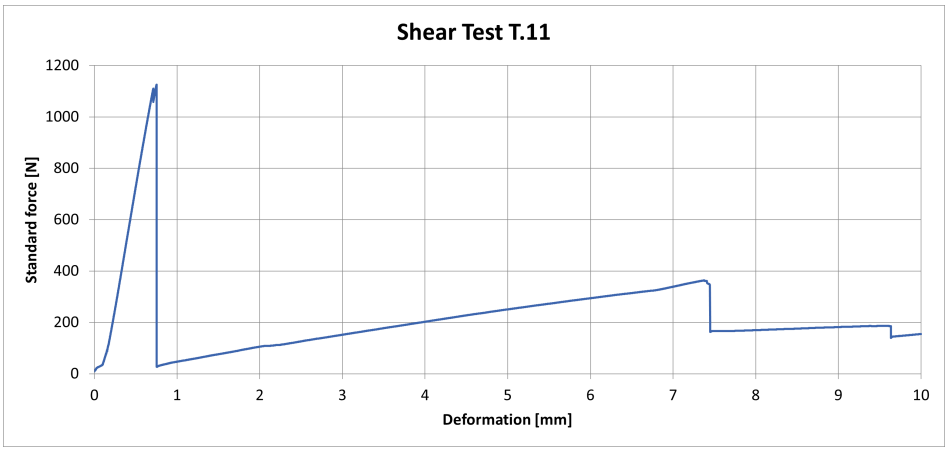

Figure C.5: Load-displacement graph for shear test sample 11

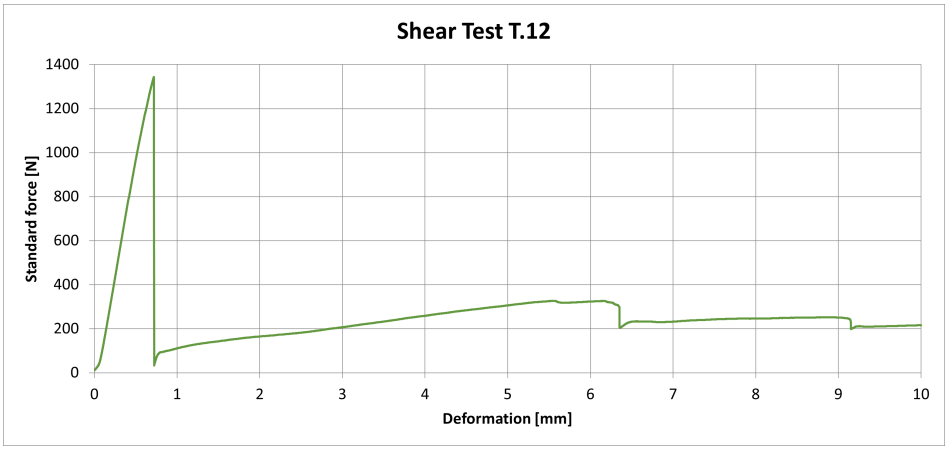

Figure C.6: Load-displacement graph for shear test sample 12

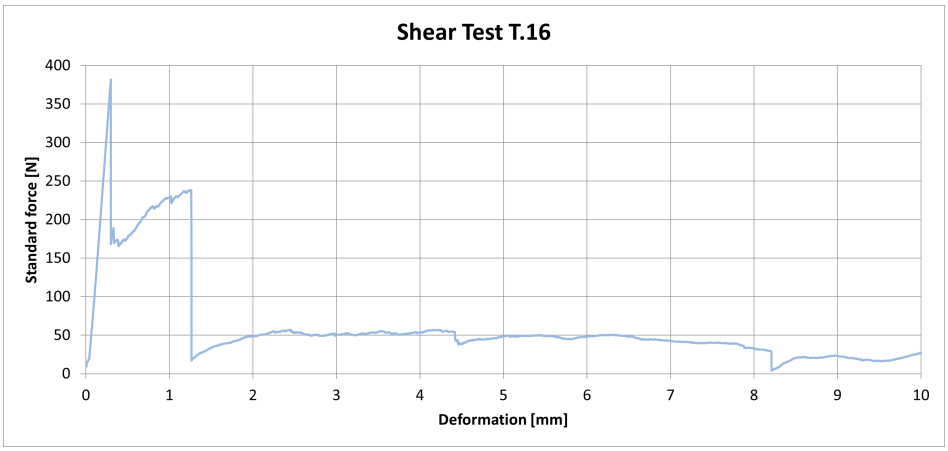

Figure C.7: Load-displacement graph for shear test sample 16

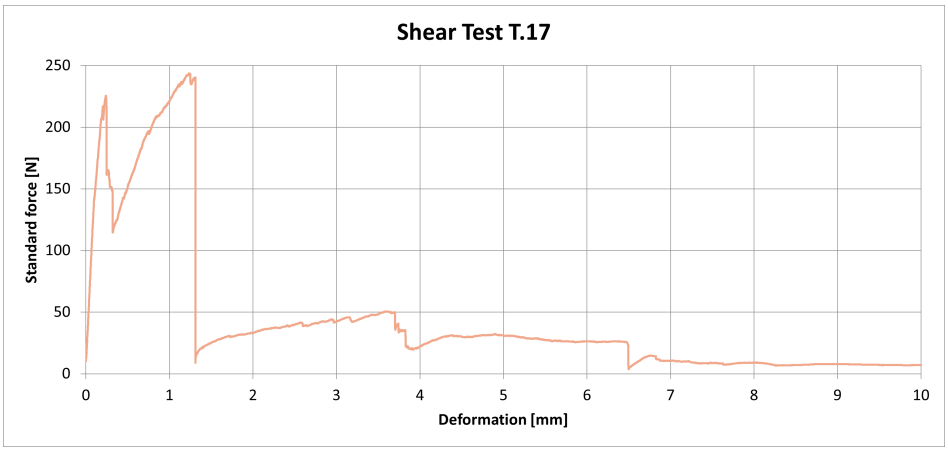

Figure C.8: Load-displacement graph for shear test sample 17

C.2 Buckling Tests

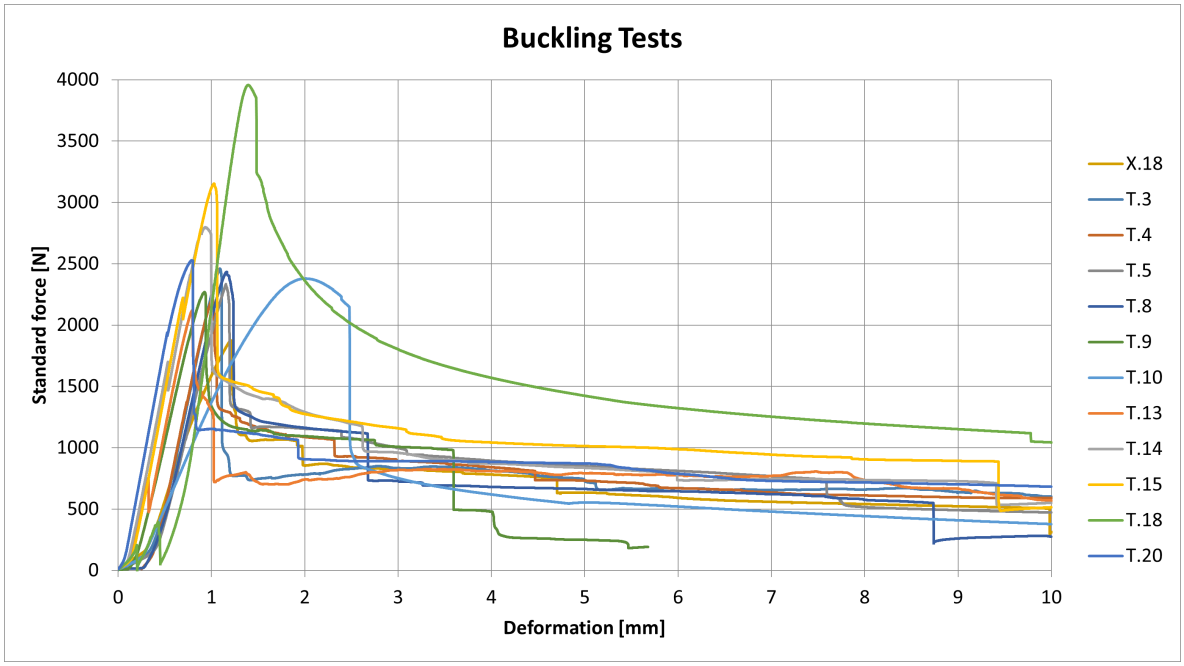

Figure C.9: Overview of all different buckling tests

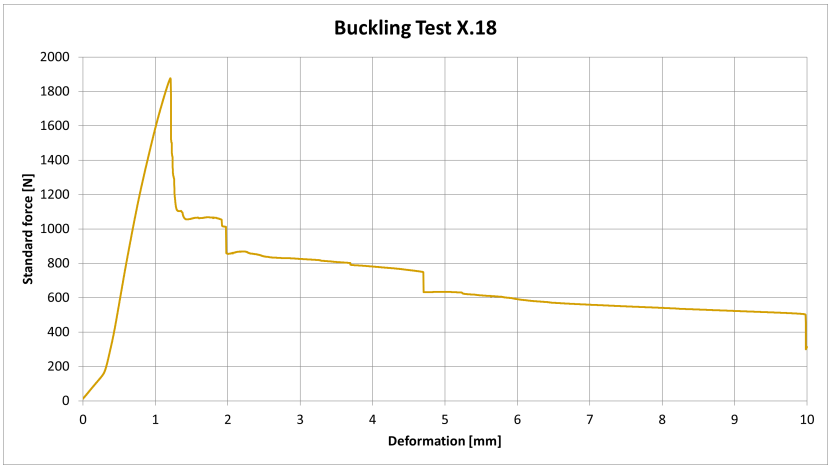

Figure C.10: Load-displacement graph for buckling test sample X.18

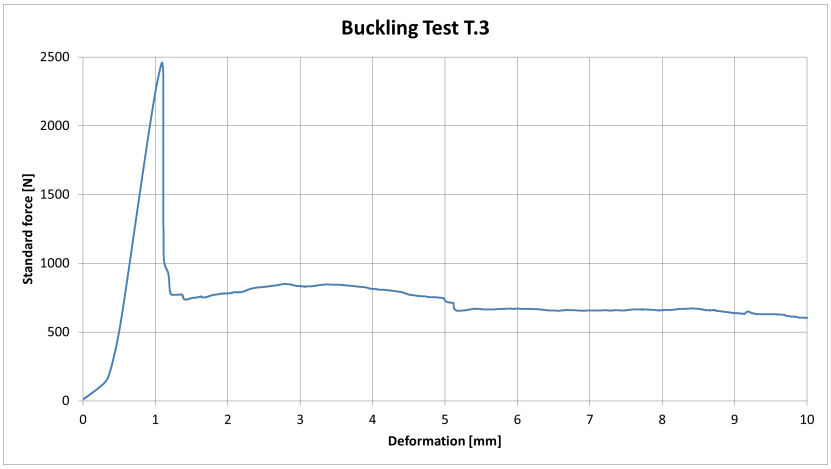

Figure C.11: Load-displacement graph for buckling test sample 3

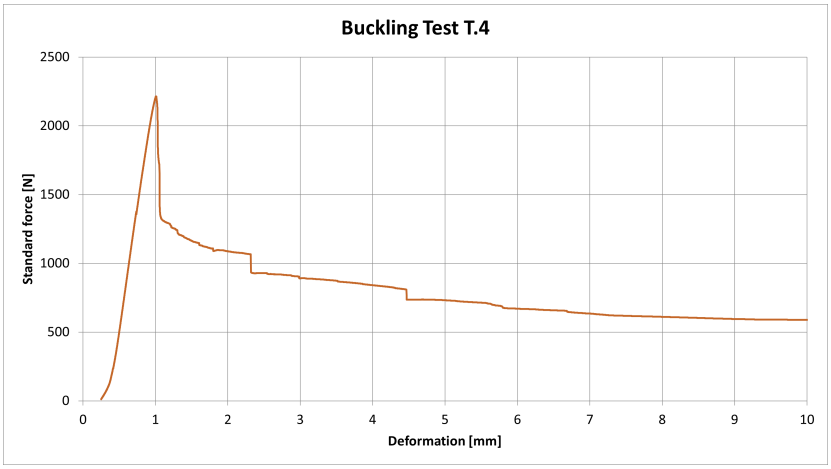

Figure C.12: Load-displacement graph for buckling test sample 4

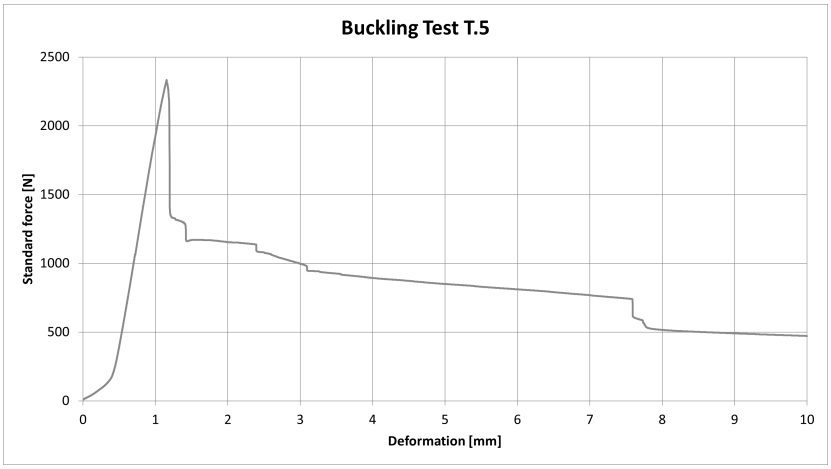

Figure C.13: Load-displacement graph for buckling test sample 5

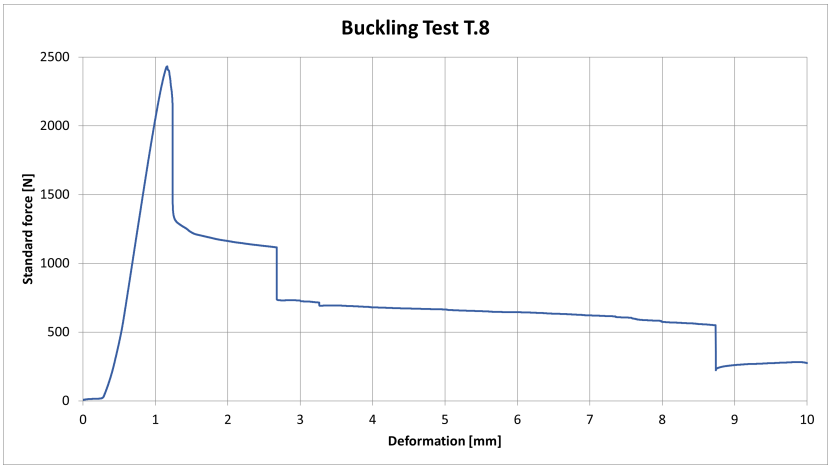

Figure C.14: Load-displacement graph for buckling test sample 8

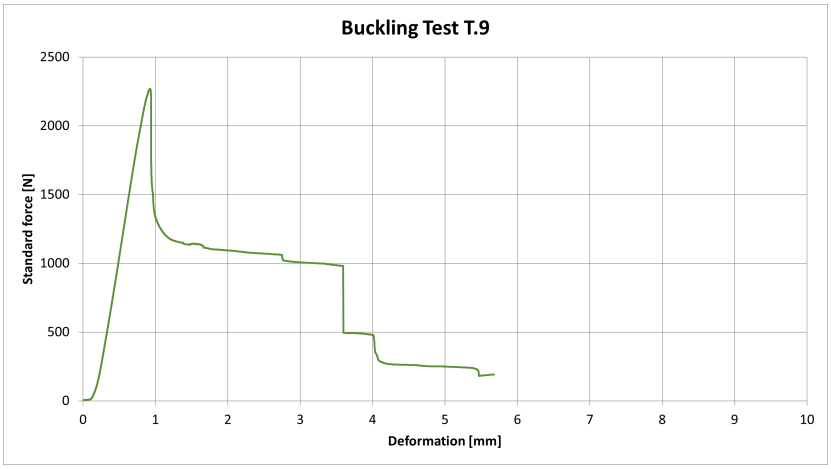

Figure C.15: Load-displacement graph for buckling test sample 9

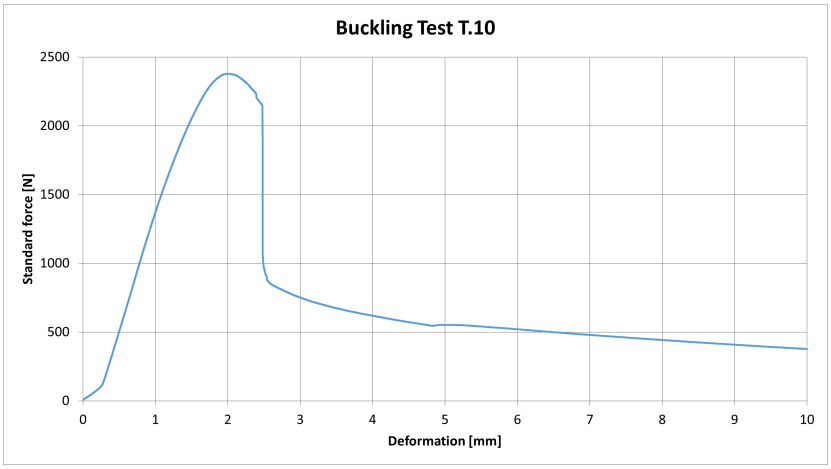

Figure C.16: Load-displacement graph for buckling test sample 10

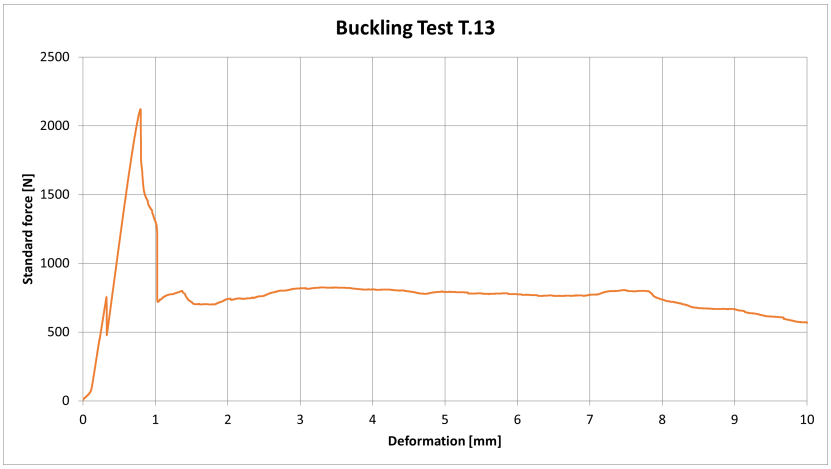

Figure C.17: Load-displacement graph for buckling test sample 13

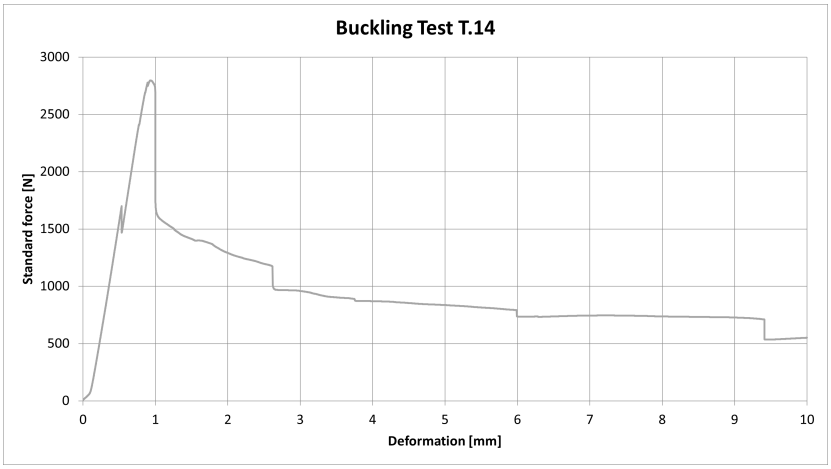

Figure C.18: Load-displacement graph for buckling test sample 14

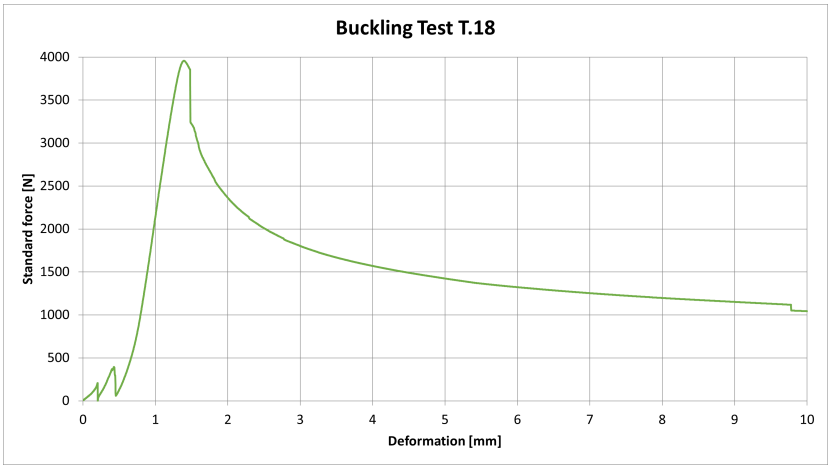

Figure C.19: Load-displacement graph for buckling test sample 18

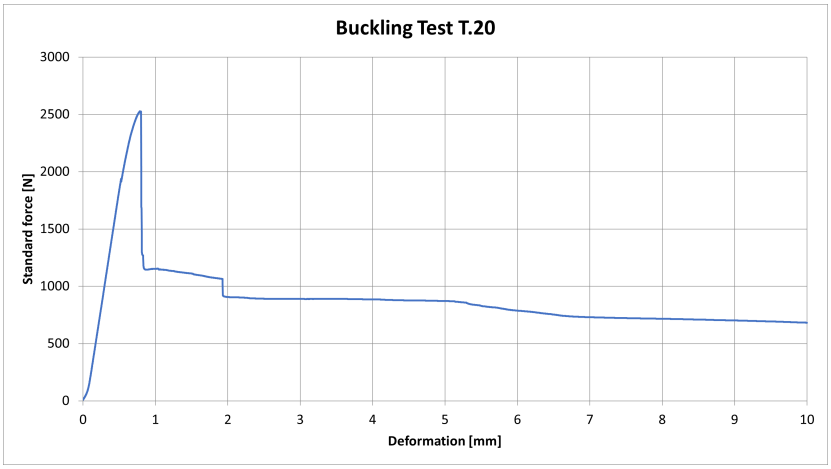

Figure C.20: Load-displacement graph for buckling test sample 20

Appendix D

Helical Winder Demonstrator Component Design

This Appendix presents the requirements and design details of all the different components of the Helical Winder Demonstrator, namely the external frame, the bottom fixture, the top fixture, central cylinder, crank support and drivetrain sub-assemblies.

D.1 Frame

The external frame of the structure has several functions to fulfill. First and foremost, it is the component in the assembly that is responsible for balancing all the loads generated in the structure, including the torsional load generated between top and bottom and the (not to be underestimated) weight of all the components. Additionally, the frame provides guidance for the translational motion of the upper fixture, imposing a tolerance on the straightness of the frame. Because it encases the entire setup, the frame should be large enough to accommodate all the components required for the largest envisioned helical configuration (a diameter of 300 mm and a helical pitch of 75 mm with 4 repetitions), while preferably allowing for larger configurations by swapping a few of the frame's components.

All of the above stated requirements could be fulfilled by use of standard aluminium 'Profile 8' options from the ITEM catalogue. High tolerances could be achieved by using solely perpendicular interfaces between frame members, as ITEM specialises in precisely cut standard profiles. By using their 'automatic fastening' option, strong interfaces could be created that could easily be assembled and disassembled. Due to their low stiffness requirements, the top and bottom of the frame used standard 40 mm × 40 mm profiles. Since the vertical members of the frame were much longer and had to support a torsional load over a large portion of this length, a 'heavy duty' 120 mm × 40 mm profile option was chosen. While a size of 80 mm × 40 mm would likely have sufficed as well, the 120 mm wide option provided the added benefit of a middle groove, making alignment of the bottom fixture to the external frame easier. These vertical frame members would also incorporate two double-sided guiding

shafts for the top fixture of the demonstrator. To accommodate a central cylinder of 300 mm in diameter and 1.2 m in length and all other components, the final frame formed a cuboid of 0.7 m × 0.7 m × 1.7 m. This final design is visualised in Figure D.1.

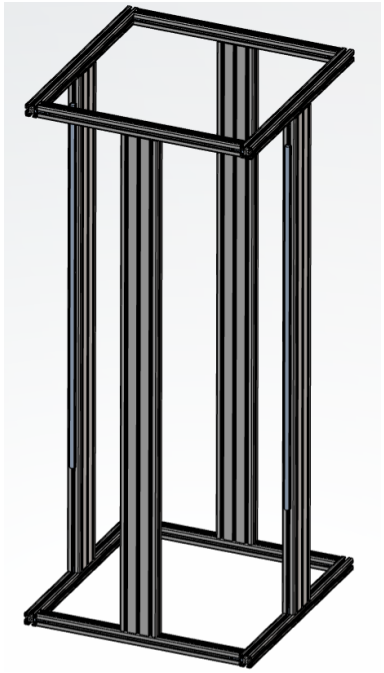

Figure D.1: Final design of the frame for the Helical Winder Demonstrator

D.2 Bottom Fixture

The bottom fixture could be considered an extension of the external frame for the Helical Winder Demonstrator. In terms of loads, it would carry the weight of the central cylinder above and the larger transmission wheel below, two of the heaviest components in the system, balanced by the interface with the external frame. Functionally, the bottom fixture would constrain all translational motion within the frame, while allowing one rotational degree of freedom for the cylinder around its central axis. As this rotation axis should be parallel to the vertical degree of freedom of the upper fixture, this imposed strict alignment tolerances on the bottom fixture. As an example, 1° of misalignment of the rotation axis would translate to an offset of 21 mm at the top of the cylinder.

To minimise misalignment of the central rotational axis, it was decided to incorporate a double bearing system in the bottom fixture. Spaced about 150 mm apart, these bearings would be housed inside a single hub. This hub was the first custom part of the design, housing both bearings while interfacing with four standard ITEM profiles to connect to the external frame. As most of the load reacted by the fixture would be in a vertical direction (being most of the weight of the structure), the four frame members were reinforced to accommodate this. For the same reason, angular contact ball bearings were selected for their higher resistance to axial loading when compared to deep groove ball bearings. The final design of this sub-assembly can be seen in Figure D.2

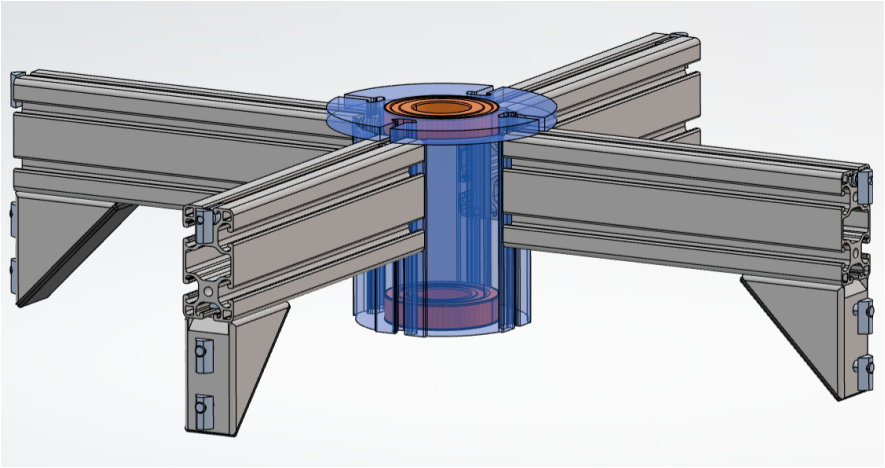

Figure D.2: Final design of the bottom fixture

D.3 Top Fixture

As already discussed, the main function of the top fixture is to hold one end of the composite samples, resisting the torsional load that will be introduced by these samples and allowing for vertical travel while the samples are twisted around the central cylinder. As a result, the fixture should be able to slide over the cylinder with minimal clearance, while still allowing for the winding of helices with different diameters. Preferably, it should be able to hold all samples wound in the same direction at once. With a total of ten helical members considered for the scope of this thesis, this implies five are wound clockwise and five are wound counter-clockwise.

The final design that satisfied these requirements was mostly constructed from standard ITEM profile options. A total of four bearing units would interface with the guide shafts of the external frame, two of which allowed for some horizontal adjustment. These bearing units were connected to a stiff outer shell for the top fixture, consisting of four 40 mm × 40 mm aluminium profiles. On top of this shell, a custom plate was placed to transition from the shell to the support for the composite samples. To make production for this plate as simple as possible, the plate was designed to be cut from a 10 mm thick sheet of aluminium using either laser or water jet cutting, depending on availability. The support for the composite samples was designed to be easily exchangeable for different sample helix diameters. This was done by designing two separate plates (one for a 200 mm helix and one for a 300 mm helix) that could both be bolted to the same mounting holes of the transition plate. The plates themselves featured slot supports for the composite samples, five of these slots allowing for the winding of clockwise members and five allowing for counter-clockwise members. As the fixture was initially designed to constrain the samples by a portion of its own weight, introducing a compressive load into the samples, separating the slots like this reduced the chance of the members slipping out during winding. With these decisions, the final design of the top fixture could be made, visualised in Figure D.3.

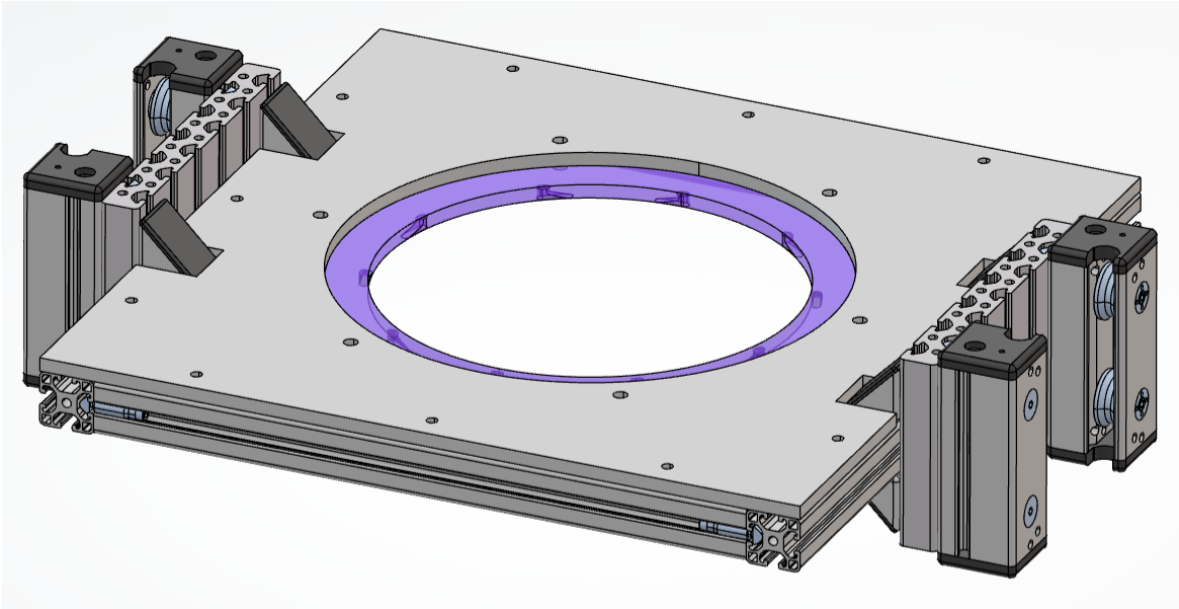

Figure D.3: Final design of the top fixture, with the support plate for 300 mm helices

D.4 Central Cylinder

One sub-assembly that could not be constructed from ITEM profiles was the central cylinder. This cylinder would be used to dictate the shape of the composite samples, providing a smooth surface for the samples to curve around. As such, it should be thick enough to resist indentation by the samples. Another requirement on the cylinder was the possibility to accommodate heating. With several heating options considered, the heat capacity of the cylinder should be maximised in order to be able to provide a stable temperature environment.

With these requirements in mind, two central cylinders were designed: a 200 mm and a 300 mm cylinder, both 10 mm thick. While for the final application of iso-trusses, this cylindrical structure should be made adaptable in diameter, for example by use of an expanding rubber tube, this is not considered within the scope of this thesis. In addition to these central cylinders, the cylinder assembly included the lower support plate for the samples, with slots similar to the ones in the top fixture. It was decided to connect the cylinder to the rotating lower support plate to couple their rotation. This implied that during the rotation of the samples, members would experience the least amount of friction near their lower support, while experiencing the most amount of friction near the upper support. If deemed necessary, this effect could be reversed by disconnecting the cylinder from the lower support plate and suspending it from the top of the assembly. To accommodate this, a lid on top of the cylinder was included to be able to connect the cylinder to an upper (bearing) structure, if deemed necessary. To complete the design, a threaded hole was included in the lower support plate to interface with a rotational central shaft in the drivetrain assembly. Of all these parts, only the lid could be partly machined through laser/water jet cutting. The lower support plate was added to the list of parts to be manufactured by DEMO, while the two central cylinders had to be outsourced due to their size and tolerance constraints on the outer surface. The final design of the central cylinder assembly can be seen in Figure D.4.

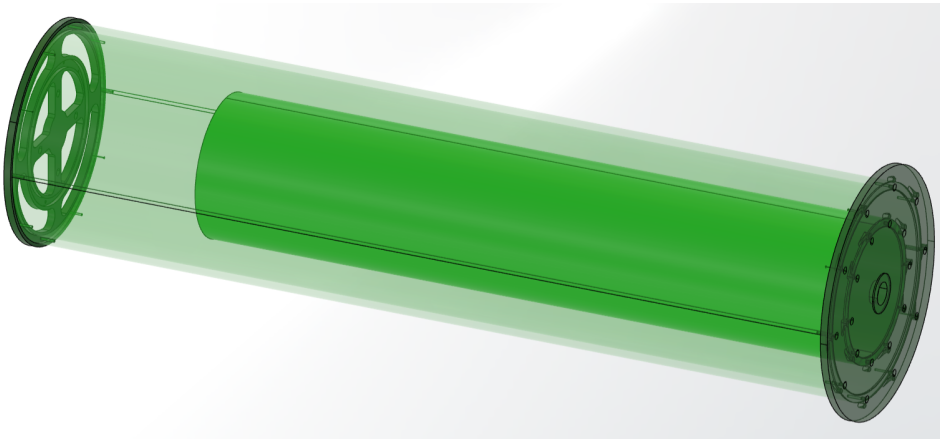

Figure D.4: Final design of the (rotated) central cylinder assembly, showing both cylinders

D.5 Crank Support

With the previously discussed components assembled, a freely rotating cylinder inside its support structure was obtained. To provide a controlled input to this structure, a crank was employed. The support for this crank should be able to house a crank arm and allow it to freely rotate while interfacing with the external frame. Additionally, it should accommodate a method for pre-tensioning the belt of the drivetrain in order to prevent it from slipping.

To meet these requirements, several different parts were needed. First, a crank hub was designed, similar to the central hub of the bottom fixture. This crank hub would be able to house another double bearing system. As the load experienced by these bearings would be mostly in their radial direction, deep groove ball bearings were selected for this purpose. Other features of this crank hub included a bolted connection to two support plates and a through-hole on the side to accommodate a lever for tensioning the belt of the drivertrain. Room for tensioning was accommodated in the two support plates, which both featured a slotted connection to the hub. These plates were also designed to be cut from a 10 mm thick sheet of aluminium through laser or water jet cutting. Finally, to interface with the external frame, two (reinforced) standard 40 mm × 40 mm aluminium ITEM profiles complemented the design, as visualised in Figure D.5.

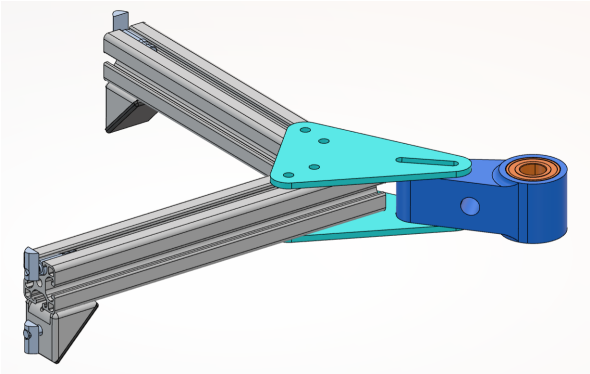

Figure D.5: Final design of the crank support

D.6 Drivetrain

Completing the design of the Helical Winder Demonstrator, the drivetrain translates a user's manual input to a rotational motion of the central cylinder and one end of the composite samples. To do this, a belt-driven geared system was used with a 10:1 gearing ratio. On one side, the user should introduce the input through use of a crank arm, while on the other side a system must be created to couple this input to the lower support for the composite samples. This system should be easily changeable and preferably be assembled from off-the-shelf components.

To fulfil these requirements, pulley components using a taper-bush system from Eriks were selected. This system allowed for a simple friction based connection to a driveshaft which could easily be disassembled. It consists of a cast iron pulley wheel which interfaces with a standard V-belt, and an iron taper-bush collar which tightens itself against both the pulley and an internal shaft through the tightening of several screws. Two driveshafts were designed for production by DEMO: One which interfaced with the lower support of the composite samples, and one which interfaced with an off-the-shelf large crank arm. The central driveshaft would be locked in place by threading on the lower support plate. For the crank shaft, a shaft collar was employed to lock the two bearings in the crank hub in between the top of the shaft and the collar. This final design can be seen in Figure D.6.

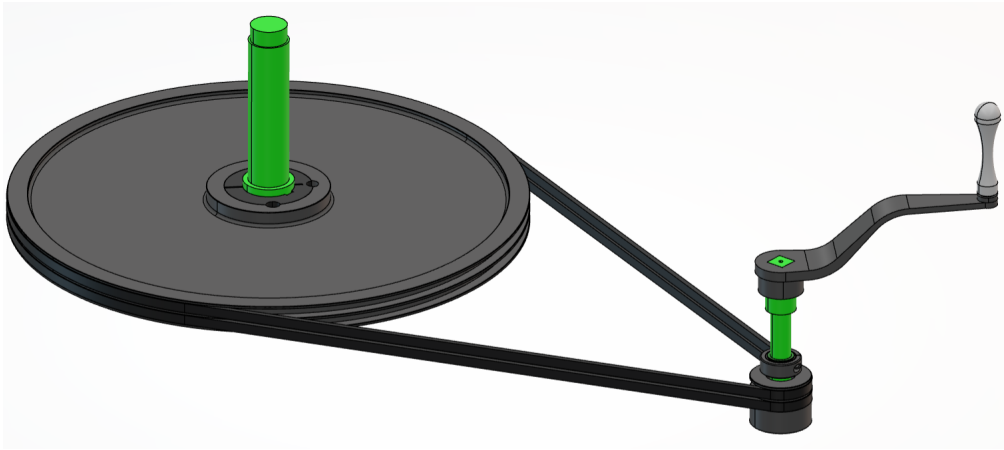

Figure D.6: Final design of the drivetrain assembly

D.7 Component Interfaces

Figures D.7 to D.9 show several key regions within the design with interfaces between different components: The top fixture and its guides, the central shaft hub and the crank hub.

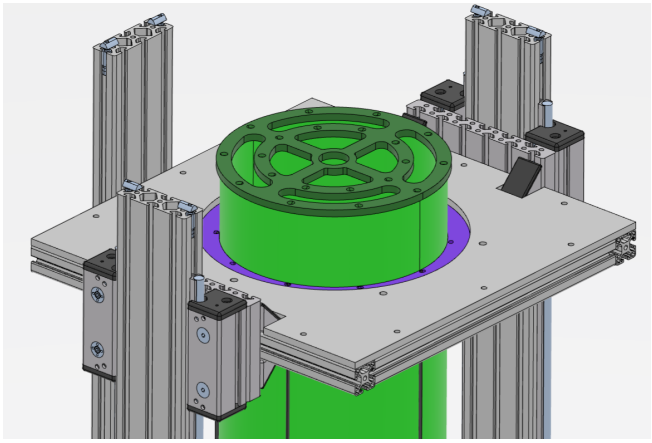

Figure D.7: Close-up of the top fixture with interface to the frame and central cylinder

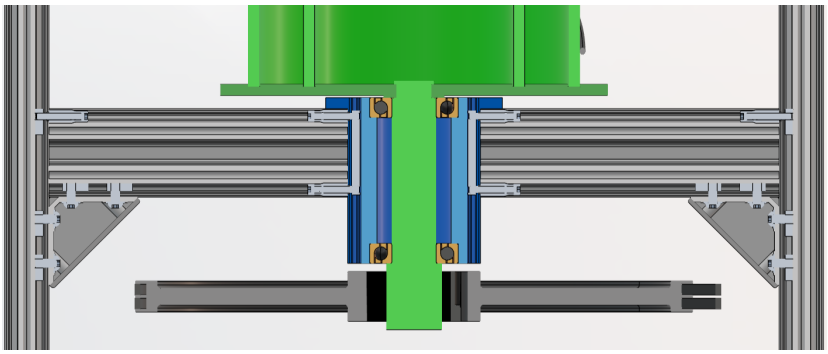

Figure D.8: Cutaway of the main driveshaft, showing interfaces between bottom fixture, central cylinder and drivetrain

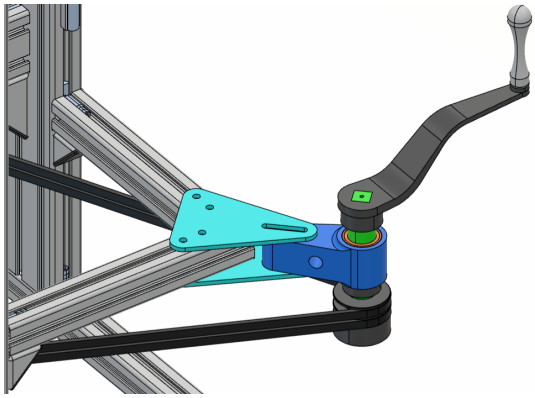

(a) Close-up of the crank

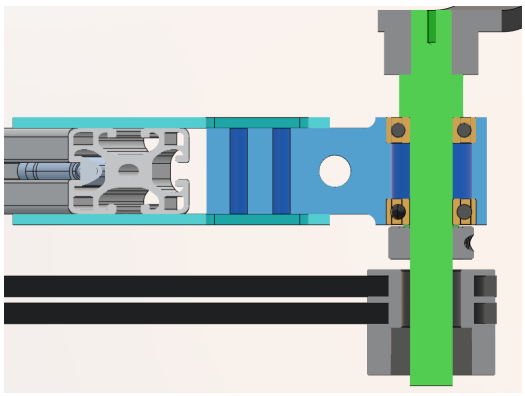

(b) Cutaway of the crank

Figure D.9: Details of the crank interfaces